공학박사학위논문

Optimal Design Procedure for Offshore Pipelines based on Computational Simulation of Pipe Forming Process

조관 공정의 수치시뮬레이션에 기반한 해저 파이프라인 최적 설계 절차

2017 년 2 월

서울대학교 대학원

건설환경공학부

이지운

Optimal Design Procedure for Offshore Pipelines based on Computational Simulation of Pipe Forming Process

지도교수 고 현 무

이 논문을 공학박사학위논문으로 제출함

2016년 12월

서울대학교 대학원

건설환경공학부

이 지 운

이지운의 공학박사학위논문을 인준함

2016년 12월

위 원 장 李海成 (인)

부 위 원 장 高銀武 (인)

위 원 金鎬卿 (인)

위 원 宋準鎬 (인)

위 원 姜秀昌 (인)

Abstract

A pipeline is made of segmented steel pipes connected to form a continuous pipe system for the transportation of oil or gas over a long distance. During the past several decades, *UOE and JCO* pipes have gained increasing application to produce at lower cost offshore pipelines with diameter larger than 16 inches instead of the conventional seamless pipe. In *UOE and JCO* pipe forming processes, the steel plate is subject to a series of plastic forming including pressing and spring back and a final welding stage to form the circular pipe. However, the complicated histories of the plastic forming processes executed in the *UOE and JCO* pipe forming methods involve the following problems.

First, the formed pipes develop material properties differing significantly from those of the raw plate. The repeated loading and unloading cycles conducted throughout the forming processes alter the yield strength and curved shape of the stress-strain response of the pipe due to the Bauschinger effect and work hardening. Apart from having critical effect on the structural performance of the steel pipes, these material properties are also representative indicators of their quality. Therefore, the accurate prediction of the material properties will result in non-negligible economy in terms of the cost and time spent for the repeated inspection, design and production performed to secure the strength and structural performance of the formed pipe.

The second problem relates to the geometric imperfection and residual stress inherent to the repetition of plastic forming and elastic spring back experienced throughout the *UOE and JCO* forming processes. Along with the material properties, the ovality and residual stress of the pipe are dominant parameters determining its collapse pressure or bending capacity but occur in such an unpredictable manner that they increase the design uncertainty.

The consideration of all these interrelated parameters by means of coefficients as well as the high material and geometrical nonlinearities in the design limits the accuracy of the prediction. This loss of accuracy itself results in excessively conservative design that does not guarantee the pipe to provide consistent quality

and satisfactory structural performance. Such situation stresses the pressing need for a method enabling to predict accurately the material properties and structural performance of *UOE and JCO* steel pipes.

This thesis presents an optimal design procedure for offshore pipelines manufactured by *UOE and JCO* forming processes. The proposed procedure involves (1) the computational simulation of *UOE and JCO* pipe forming processes by finite element analysis to provide accurate prediction of the parameters of the formed pipe including its material properties, geometrical imperfections, and residual stress; (2) the structural analysis of the steel pipe using the results of the simulation; and, (3) the maximization of the collapse pressure of the formed steel pipe known to be the main structural performance, while ensuring its producibility and quality.

To improve the accuracy of the simulation of the *UOE and JCO* pipe forming processes, nonlinear combined hardening model is applied to describe the plastic characteristics including yield plateau and evolution of Young's modulus as well as work hardening and Bauschinger effect. The strain-stress response is obtained by tension-compression cyclic test on the raw material, and the genetic algorithm and RMS method are combined to derive fifteen material parameters. Finite element simulation of the UOE, UOC, JCOE, and JCOC forming processes is performed and the corresponding configuration, material properties, geometric imperfections, and residual stresses are derived for each of the processes. From these results, the yield strength can be predicted directly and the producibility of the steel pipe can be checked by monitoring the shape change of the plate and the reaction force applied to the forming tools. The validity of the numerical simulation of the forming process as well as the derived results are verified by the tensile test conducted on a sample cut from a steel pipe produced by UOE forming.

Numerical analyses are then performed to estimate the collapse pressure and bending capacity of steel pipe based on the simulation outputs. Here also, the results are in good agreement with the experimental results of previous studies. Parametric analysis is performed to investigate the effect of the pipe expansion and compression on its material properties and structural performance. It is found that larger pipe expansion increases the tensile yield strength but degrades the collapse

performance. Therefore, executing compression instead of expansion can increase significantly the collapse performance but with some loss of the tensile yield strength. However, neither compression nor expression appears to affect relevantly the bending capacity.

Finally, the optimal design procedure for *UOE and JCO* pipes is proposed considering the trade-off effect of the design variables on the yield strength and collapse pressure. The proposed procedure is seen to improve the design consistency and efficiency compared to conventional methods and to achieve maximized collapse pressure while securing the producibility and quality of the *UOE and JCO* pipes.

Keywords : Offshore steel pipe, Material property, Collapse pressure, Computational simulation, Optimal design procedure

Student Number : 2012-30247

Table of Contents

List of Figures

List of Tables

1 Introduction

1.1 Background

Offshore steel pipe is today a major mean of oil and gas transportation owing to its reliable strength against harsh environments including extreme pressure and strong bending. As deep-water production of oil and gas is increasing with the ongoing growth of the energy industry, demand for stronger pipes with higher resistance has become larger than ever and brought the attention on thick-walled welded pipes. Among the pipe forming methods, the UOE, UOC, JCOE, and JCOC processes are known to be the most efficient for thick-walled pipes with diameter over 16 inches. In these processes, the steel plate is plastically deformed into circular shape through successive forming stages including crimping, U-forming and O-forming. Then both edges are joined by welding and the expansion (for UOE) or compression (for UOC) calibration is applied to improve the circularity and relieve the residual stress developed on the pipe wall. In JCOE and JCOC processes, the plate is formed into circular shape through stepwise punching involving dozens of plastic deformation and spring back and, followed by edge welding and calibration (see Section 2.1 for details on pipe forming processes). The designation of the processes mentioned above relates to the successive steps executed throughout the forming process (U for U-forming, O for O-forming, J for J-forming, E for Expansion, C for Compression). In this thesis, the term *UOE and JCO* is adopted to indicate generically UOE, UOC, JCOE and JCOC.

In spite of their production efficiency, *UOE and JCO* pipes present still concerns regarding their structural performance (Kyriakides et al., 1991; Herink et al., 2007). According to extensive experiments and related studies in early days, the collapse pressure of UOE pipe usually shows difference with that of seamless pipe. For the pipes calibrated by internal expansion during the forming process, the collapse pressure can be lower by 30% than that of the seamless pipe with nominal diameter and thickness. On the other hand, Reichel et al. (2011) reported significant enhancement of the collapse pressure when external compression of the UO pipe is executed instead of expansion calibration at the finishing stage.

The factors influencing the collapse pressure of offshore pipes have been examined in numerous studies (Yeh and Kyriakides, 1986; Murphey and Langner, 1985). In the case of thick-walled pipes experiencing buckling in the plastic range, the material properties, diameter-to-thickness ratio ($\boldsymbol{D/t}$), geometric imperfections, and residual stress were found to be the most important parameters influencing the structural performance. Except for the $\boldsymbol{D/t}$ ratio, those factors are essentially affected by the plastic deformations performed in the pipe forming process (Qiang et al, 2015; Tianxia et al, 2016). Namely, the stress-strain response of the *UOE and JCO* pipes differs significantly from that of raw plate because of the work hardening and Bauschinger effect related to the complicated plastic strain hysteresis (Kostryzhev et al., 2011). The material properties of steel pipes are not only variables that have a sensitive effect on the structural performance of steel pipes, but also are representative indices of steel pipe quality evaluation (API, 2012). Therefore, inaccurate prediction of the material properties will result in

lower strength and structural performance of the pipe and will lead to tremendous cost and time spent for the repeated inspection, design, and production tasks. Furthermore, the plastic deformation at each forming stage exerts direct influence on the subsequent forming stage. However, the geometric imperfections and residual stress occur with such high degree of uncertainty that their assessment at the design stage has become a challenging task due to their critical effect on the structural performance of the pipe like the collapse pressure (Aiman et al., 2008; Moen et al., 2008). The excessively conservative material production and cross-sectional design resulting from these uncertain factors lead not only to increased cost and time consumption time and cost, but also mean that the steel pipe design cannot guarantee consistency and satisfactory level of quality. Besides, the producibility is often not guaranteed due to limits in the plate wall thickness that can be worked by the pipe mills.

In absence of straightforward ways to derive these key design parameters analytically, conventional pipe design had no choice but to rely on trial-and-error based upon experience. However such subjective approach is far from being consistent in securing the desired yield strength, structural performance and producibility of the pipe. There is thus a pressing need for a standard design method based on the accurate prediction of the yield strength and structural performance of the formed steel pipes.

1.2 Literature Review

The pioneering work of Kyriakides et al. (1991) evaluated numerically the effect of UOE forming process on the collapse performance of pipes. This work was followed by numerous studies intending to assess the geometric imperfection, the residual stress, the change in the material properties and the resulting structural performance of *UOE and JCO* pipes.

Numerical approach was mainly adopted until recent days to quantify the key factors from the complex *UOE and JCO* forming processes. Huang and Leu (1995) analyzed the deformation of the plate during UOE forming process to identify the effect of the design variables on the geometry of the skelp using an elasto-plastic finite element program. Palumbo and Tricarico (2005) performed 2D finite element analysis to investigate the stress-strain state and residual stresses on pipe wall through calibration stage of UOE pipe forming, and 3D finite element analysis to obtain the whole profile of the finished formed pipe. Kyriakides et al. (2007) established a 2D finite element model assuming plane strain condition to simulate the UOE and UOC forming and assessed the influence of the parameters of each forming stage of the process on the geometrical shape and mechanical properties of the pipe. Herynk et al. (2007) also contributed to UOE forming simulation using finite element analysis and suggested that the optimum structural performance requires a tradeoff between geometric imperfection and material property due to expansion ratio or compression ratio at calibration stage. Qiang et al. (2015) and Tianxia et al. (2015) proposed a numerical method for predicting geometric configuration and O-forming gap of the plate after UOE manufacturing. To that

goal, Tianxia et al. (2015) developed a combined hardening model to characterize the plastic behaviors of the steel pipe. Thereafter, Tianxia et al. (2016) investigated the development of the yield strength from raw plate to UOE pipe by finite element simulation and concluded that the expansion ratio and $\boldsymbol{D/t}$ ratio are the two main factors determining the yield strength in UOE manufacturing. These authors also described specifically how yield strength is developed at each forming step in terms of work hardening and Bauschinger effect. Meanwhile, Gao et al. (2009) and Thome et al. (2011) predicted theoretically the final geometry of JCO pipes considering the punching depth as a most important design variable in view of the large amount of elastic spring back. Chandel et al. (2011) formulated the design variables of JCOE forming process and verified them experimentally. They stressed the importance of the correct assessment of the spring back as an indispensable factor for the decision of the radius of tools and dies used at the various stages of the pipe forming.

Since high level of degradation in collapse pressure was first reported in the series of tests performed for the Oman-India pipeline (Peter et al., 1995), significant efforts have been devoted to identify the variables influencing the collapse pressure along with bending capacity due to the similarity of their local buckling failure modes. Gresnigt et al. (2000) examined the effect of the manufacturing process on the collapse and local buckling behavior by full-scale test on UOE X65 pipes and finite element simulations under external pressure and bending. The Bauschinger effect was appeared to be the cause of the lower collapse pressure of the UOE pipes compared to that of the seamless pipe. On the other

hand, Gresnigt and Van Foeken (2001) found out that UOE forming process provided improved the bending capacity with respect to seamless pipes. Giannoula et al. (2016) examined the effect of UOE pipe manufacturing process on the structural response and resistance of the pipes using finite element analysis. They conducted a parametric study for clarifying the effects of pipe expansion on the structural capacity under bending, axial force, and external pressure at the installation phase.

1.3 Research Objective and Scope

This thesis intends to propose an optimal design procedure for *UOE and JCO* pipes maximizing the structural performance. The proposed procedure involves the computational simulation of the pipe forming process and the structural analysis of the pipes using the results from simulation to predict the structural performance of the pipes with high accuracy and to meet producibility condition and yield strength quality level.

As a first step, *UOE and JCO* forming processes are simulated using finite element method to track the development of the yield strength of the pipes throughout the multi-stage pipe forming process. The cross-sectional ovality and residual stress of the pipe derived from the simulation are then used in subsequent structural analyses such as collapse and bending analysis. For the simulation, combined nonlinear hardening model representing the work hardening, the Bauschinger effect, the yield plateau and the evolution of Young's modulus is adopted to describe the complicated plastic behaviors of steel due to repeated loading and unloading of the process.

The UOE, UOC, JCOE, and JCOC pipe forming processes are simulated by the virtual factory program formulated with 2 dimensional finite element model and applying the numerical material model. The simulation can track the development of the yield strength at each forming stage and investigate the geometric imperfections and residual stress of the pipe after manufacturing. An experiment on UOE pipe forming and uniaxial tension test on a sample cut from the pipe are

performed to validate the virtual factory program by comparing the analytic and experimental geometric configurations of the skelp at each forming stage and the tensile yield strength. In the following step, the collapse pressure and bending capacity known to be the principal structural performance indicators for offshore pipes are evaluated with refined 3-dimensional finite element model together with the results of forming simulation.

This study conducts extensive parametric analysis to examine the effect of three major design variables that are 1) $\boldsymbol{D/t}$ ratio, 2) expansion ratio and 3) compression ratio on the yield strength and structural performance of the pipe.

An optimal design procedure of the *UOE and JCO* pipes is proposed considering these key design variables so as to achieve maximized collapse pressure while securing the production possibility and quality of the pipe. The proposed design procedure is applied to the UOE pipe to show its feasibility.

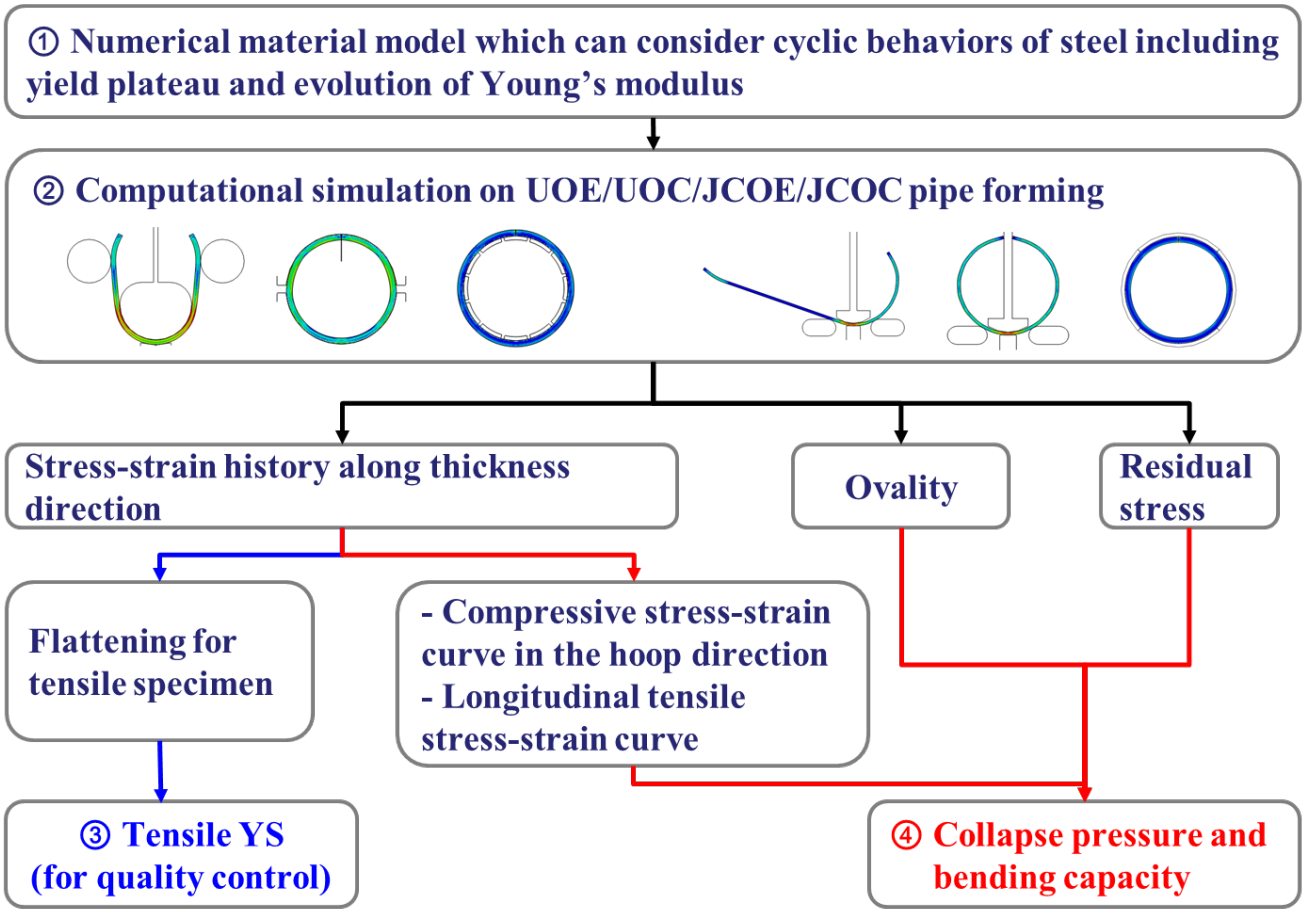

Figure 1.1 Flow chart for prediction of yield strength and structural performance of the pipe

1.4 Outline of thesis

Following this introductory chapter, Chapter 2 presents in details the pipe forming processes for offshore steel pipes including every stage of the UOE, UOC, JCOE and JCOC pipe forming processes. The change in the material property from the plate to the pipe due to plastic mechanism is investigated, and the ovality of the cross section and residual stress developed in the pipe wall are also reviewed.

Chapter 3 introduces the prediction of the yield strength and structural performance of the pipe using the finite element method. The establishment and specifications of the numerical material model based on combined hardening model for the computational simulation of pipe forming process are described. Then, this chapter addresses how the yield strength is calculated for quality control of the pipe and how ovality and residual stress are acquired as key outputs. Based on the results of forming simulation, collapse and bending analysis are conducted using refined 3-dimensional finite element method. Ordinary response of the pipe under external pressure and bending, definition of collapse and bending strength and design equations are provided here as well. Finally, both forming simulation and structural analysis are verified by comparing the results with experimental data and previous studies.

Chapter 4 investigates the influence of key design variables on the yield strength through parametric study with practical and feasible values and ranges of the parameters. The key design variables are identified and their influence on the collapse pressure and bending capacity is discussed.

Chapter 5 suggests an optimal design procedure for offshore pipes. The optimization problem is defined with the maximization of the collapse pressure as objective and the production possibility and yield strength quality of the pipe as constraints. The schematic flowchart is provided in order to introduce how a designer can adjust the key variables by monitoring the constraint and optimality condition. Finally, an illustrative example of UOE pipe is presented through to show the feasibility of the procedure.

Chapter 6 presents a summary of the major findings of this study and describes areas where further study is needed.

2 Pipe Forming Processes for Offshore Steel Pipe

2.1 Description of the Forming Processes

Generally there are two types of steel pipe production methods; welded pipe and seamless pipe. Again welded pipes can be classified according to their specific manufacturing method as spiral pipe, electric resistance welded (ERW) pipe, and *UOE and JCO* pipes. Among welded pipes, *UOE and JCO* pipes have been exclusively used for offshore application along with seamless pipe, thanks to the thick wall and small cross sectional imperfection. So the scope of this thesis covers only UOE, UOC, JCOE, and JCOC pipes and deals collapse and bending behaviors as they are fundamental limit states for offshore pipelines. First of all, this section introduces those four kinds of pipe forming process and their subordinate forming stages.

2.1.1 UOE and UOC Forming

As a representative pipe manufacturing method, UOE forming process is one of the efficient manufacturing methods for energy pipes with thick wall. During the process, a steel plate is plastically deformed into circular pipe through successive forming step including crimping, U-ing, O-ing and expansion or compression as shown schematically in Figure 2.1. In first crimping stage, both edges of the plate are bent to form an arc shape. The plates is bent by moving lower crimping tool

gradually upwards while keeping the upper tool stationary. The objective of this stage is forming edges to have a curvature radius close to that of O-formed skelp at third O-forming stage. Here an engineer has to determine the crimping length and the radius of upper and lower crimping tool considering expected deformed shape after elastic spring back.

The plate is set for the next U-forming stage where the plate is initially supported by a pair of supports as seen in first in Figure 2.2. While the U-forming punch is pressing the central part of the plate, anvil holds beneath the plate and moves downwards along with the punch to prevent a slip at a contact between the punch and the plate. U-forming punch stops when it travels by predetermined distance, afterwards the both supports move inwards keeping the punch in place, which forces the plate to have an incurved U-shape. This pair of tools is called side pushers. All the travel distance of the punch and side pushers, the initial center span and outer diameter of the tools should be selected adequately such that the final geometric configuration of the skelp after spring back is close to U-shape with vertical arms as seen in ④ of Figure 2.2.

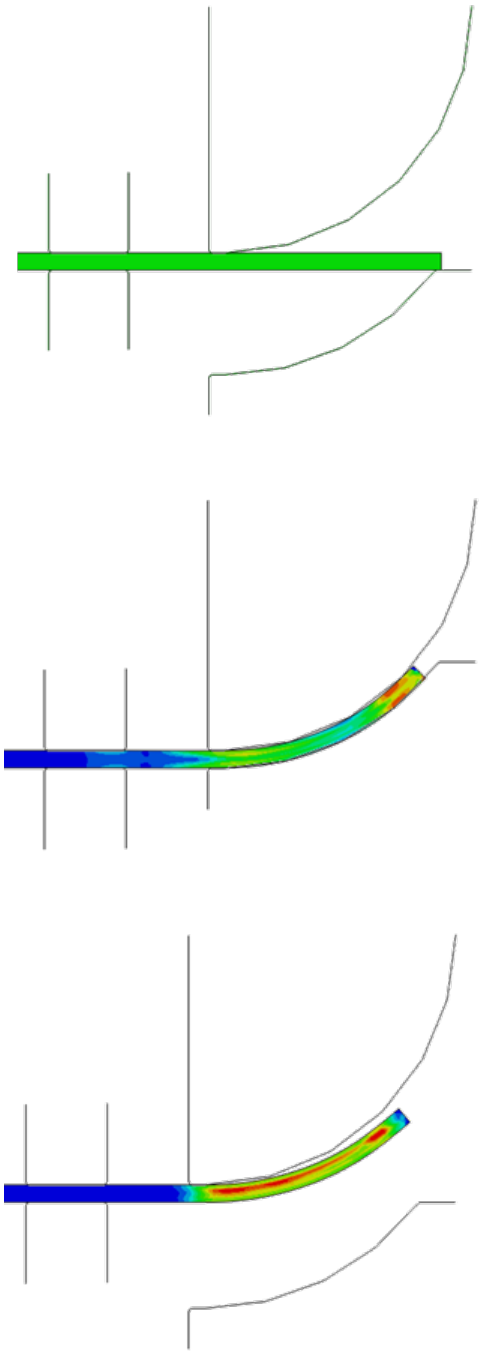

Figure 2.1 Schematics of the crimping stage

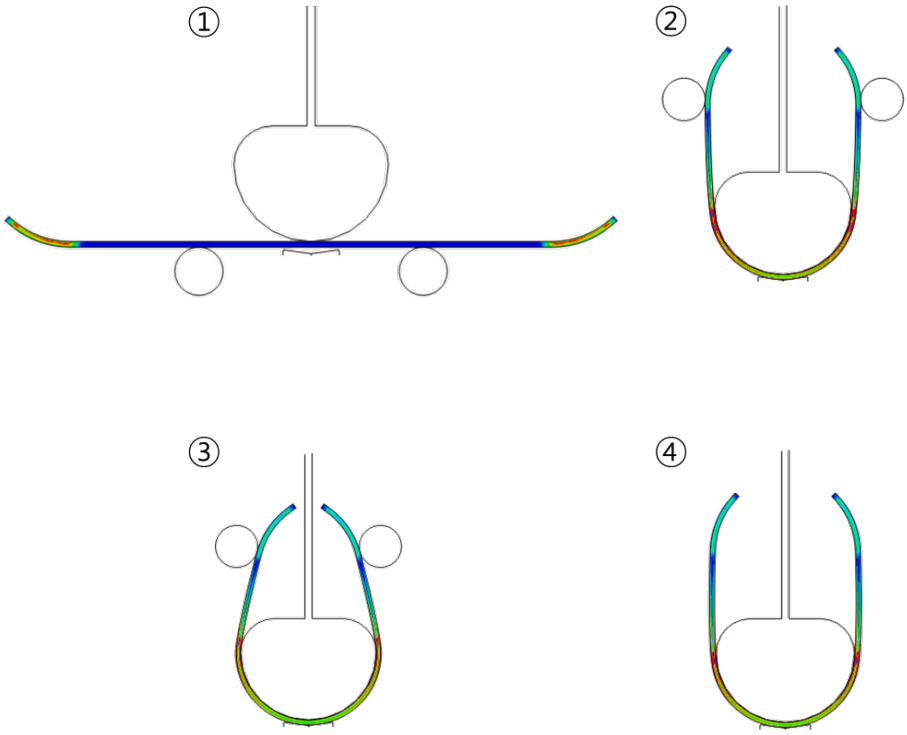

Figure 2.2 Schematics of the U-forming stage

Figure 2.3 shows how the skelp is formed into nearly O-shape at next stage. Upper O-forming tool is actuated downwards to bend straight arms while forcing slight reverse bending to central part of the skelp. To prevent excessive friction between the skelp and forming tool, lubricant is applied inside the O-forming tools. Achieving complete contact of the skelp and tools, O-shaped skelp is pressed slightly more leading to circumferential compression with net compressive strain of 0.1-0.4% to alleviate poorly formed part of straight arms, so called shoulder. This compression should be adjusted with care in that it has a great impact on the distance of welding gap. The gap is one of key process parameters in UOE pipes manufacturing which affects a possibility of pipe production. If the gap is too large, it causes a much difficulty in joining and welding. Those requires much forces on tool and they result in an excessive residual stress on pipe wall. On the other hand, too narrow gap makes it hard to clean both ends before welding, that leads to poor welding quality with reduced structural strengths of the pipe. According to previous researches and experiences, about 2-3% of the nominal outer diameter of pipe is regarded to be appropriate. At the same time, peak capacity of the actuating machine should be considered as the required force on forming tool increases sharply once it starts to apply circumferential compression.

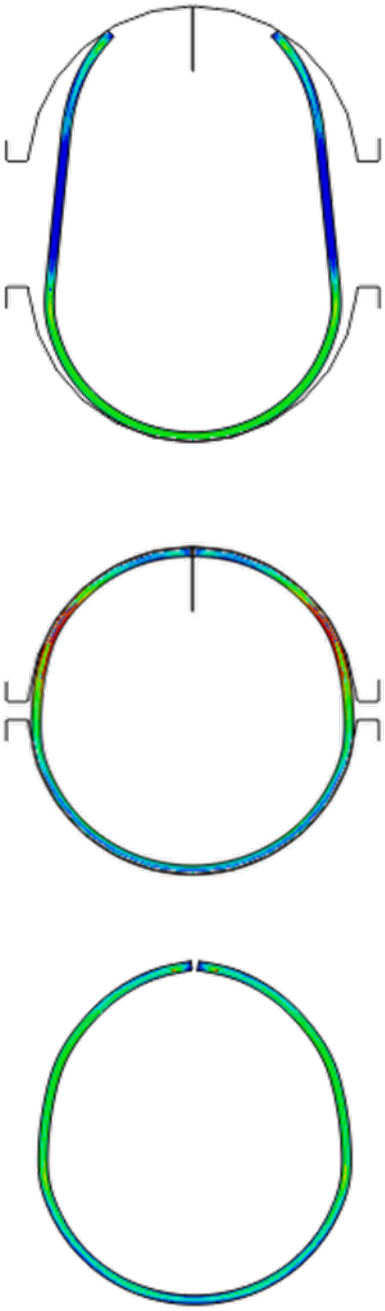

Figure 2.3 Schematics of the O-forming stage

After taking away upper O-forming tool, the pipe is prepared for next edge welding stage as washed and dried. Figure 2.4 describes the way pipe is fixed by side rollers and the edges are welded. Prior to welding, both edges have to be tack welded along its entire length while being aligned by a number of side rollers as seen in a second picture of Figure 2.4. Unless this tack welding is applied properly, there could be a severe damage such as a leakage of melted welding rod during the submerged arc welding. If inspection on tack weld is found to be superior, the pipe is then conveyed to submerged arc welding machines. Likewise tack welding, a scrutinize examination using ultrasonic shall be performed on the welded zone. Inspection for detecting defects commonly includes evaluation by hardness and Charpy V-notch impact tests. As is well known fact with offshore pipes, the strength of welding and heat affected zone does not have much decisive effect on collapse and longitudinal bending capacity of the pipe while it becomes essential factor when it comes to fatigue limit state or ultimate limit state of bursting and others. Therefore the edge welding of the pipe would not be dealt or modeled specifically in this study.

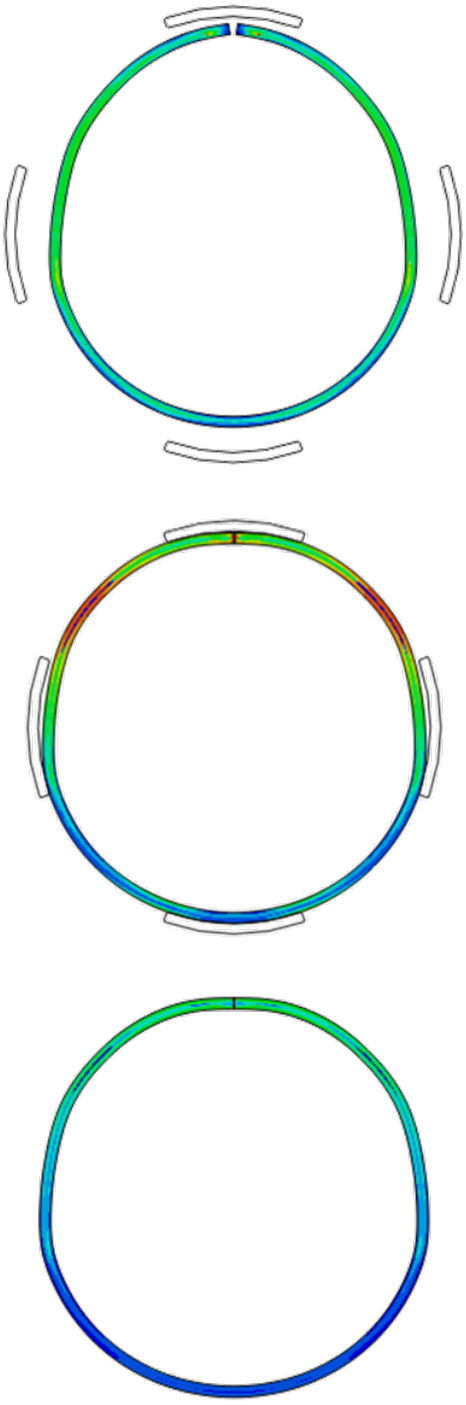

Figure 2.4 Schematics of the welding stage

Next expansion calibration can be applied to improve cross sectional ovality and relieve residual stress on pipe wall. Expansion calibration is carried out by a series of expandable mandrels moving outward from inside the pipe shown in Figure 2.5. Lubricant is applied again to reduce the friction at surface which will be in contact with the expanding device. A hydraulic piston is used to actuate the mandrels. After expanding a length of 1 to 1.5 diameter at once, it is contracted and moves toward unexpanded section to repeat same operation. Though the main purpose of this expansion stage is simply making the tube section circular and relieving residual stress on wall, it has been revealed in early works that material properties such as yield stress and tensile strength can be shifted considerably. Also it brings identical tensile strain to every fiber through thickness direction only if it is applied ideally. This indicates it has more powerful effect than other bending operation which brings opposite strains to inner and outer fiber of the wall. Meanwhile it has much flexibility in pipe design, in other words, changing this parameter is most convenient way for pipe designer to adjust yield strength quality or structural strengths. Therefore the extent (ratio) of expansion is regarded as the most influential factor in pipe design. For that reason, applying expansion to welded pipe and the extent are the demanding matter in UOE pipe design. Section 2.2 and 2.3 will discuss on this phenomenon in detail. Sometimes it can be even skipped, i.e. unexpanded pipe would be dispatched, especially when ovality is not required to be quite small or tensile yield strength is strong enough as welded. The pipe as welded here is called ‘UO’ pipe. Since the pipe is stretched in hoop direction at this stage, the width of the initial steel plate should be determined considering not only nominal diameter of the pipe but also expansion ratio and its spring back.

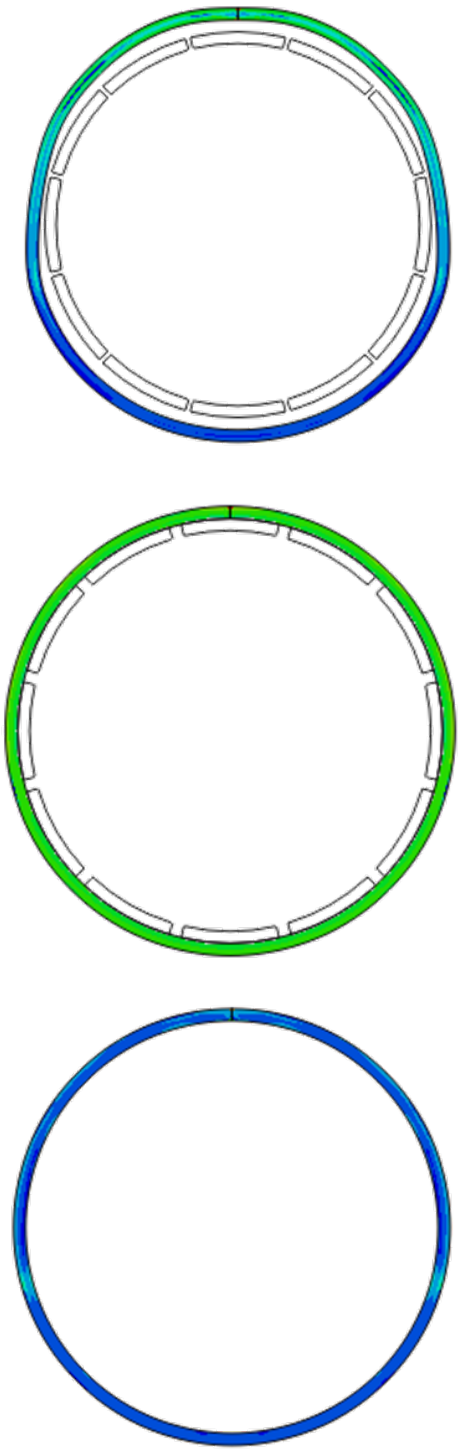

Figure 2.5 Schematics of the expansion stage

If an expansion phase is altered by compression as illustrated in Figure 2.6, the whole procedure is called UOC forming process. As Kyriakides et al. had pointed out in the early 1990, expansion could be replaced by compression because it also can reduce an ovality and residual stress to an acceptable level. This proposition had been validated by full-scale test as well as finite element analysis (Kyriakides et al. 2006; Herynk et al. 2007; Pavlyk et al. 2009). Compression can be applied using four compression tools as shown in Figure 2.6. Each of four compressing tools covers a circumferential sector of $\pi/2$ preventing local buckling at gap between the tools. This compression calibration is known to be capable of diameter tolerances of less than 0.5 mm and ovality smaller than 0.3% as fine as expansion calibration. Noticeable feature is that this stage clearly tends to enhance the compressive yield strength in hoop direction, in contrast with what expansion calibration does. This strengthening effect also will be dealt specifically in Section 2.2.

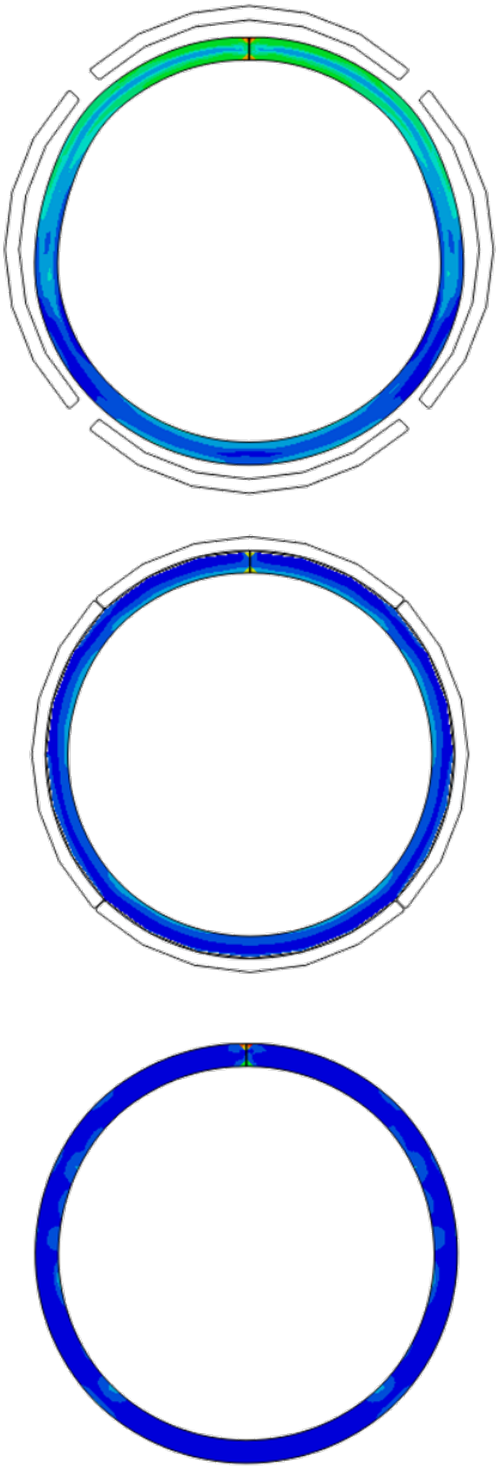

Figure 2.6 Schematics of the compression stage

Throughout the whole UOE and UOC process, the plate experiences complicated plastic deformation. Because all the forming stages except for expansion stage forms the plate partially, each fiber located along circumferential direction has the unique strain hysteresis. For example, fibers located opposite to welding zone would have most complex history, whereas those near 2 O'clock position would undergo simpler strain path not being formed at U-forming stage. Furthermore, those forming stages apply different strains to fibers through thickness direction due to bending forming. Figure 2.7 show consecutive forming procedures of UOE process, and Table 2.1 summarizes history of deformations of outer and inner fibers located at 6 O'clock position where the deformation phase changes most frequently. Naturally 'T' of expansion stage should be replaced with 'C' for compression stage of UOC pipe.

Table 2.1 Deformation history of the fibers located at 6 O'clock position of UOE pipe

Locations through the thickness at six o'clock position	**U**-forming	**O**-forming		**E**xpansion
	Bending	Bending	Compressing	Tension
Outside (Outer layer)	T (Tension)	C	C	T
Inside (Inner layer)	C (Compression)	T	C	T

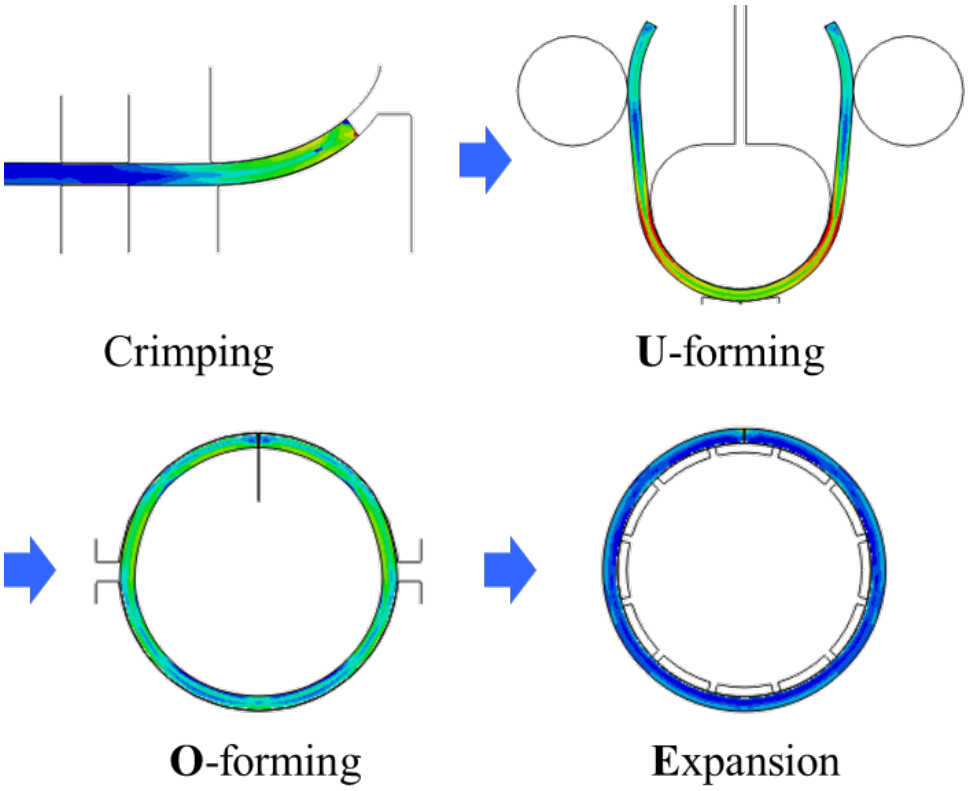

Figure 2.7 Stepwise procedure of UOE forming process

2.1.2 JCOE and JCOC Forming

JCOE forming process is one of typical pipe forming method along with UOE process. In this process, the U and O forming stages of UOE process are replaced by a series of J-C-O forming stages. As its name indicates, a flat plate is to be formed into circular shape through successive J-C-O forming. Then it is welded and undergoes expansion or compression calibration as UOE and UOC pipes are finalized.

First of all, JCOE process adopts crimping stage as previously introduced for UOE process. Half of remaining central part of the plate is then pressed N-times by punching tool at planned intervals until J-shape is developed as described in first picture of Figure 2.8. The other straight section is piecewise stroked by N-times as well, to form full C-shape. Lastly the punch presses the center of skelp to form O-shape with small gap. This forming stage develops desired geometric configuration of the pipe by adjusting forming parameters such as punching depth, die spacing and punching number N. This mean JCO forming process has a merit of flexibility in pipe production because it does not replace the forming tools even when the diameter of ordered pipe changes. Therefore it is evaluated to be economic and suitable for moderate scale of production.

Supported by the machine which forces to put both edges together, the welding gap is closed using submerged arc welding. Ovality and distortions due to forming and welding process can be improved in the next calibration operation as UOE pipe. Surely in the same manner with UOC, pipe can be manufactured by JCOC process by replacing expansion calibration stage to compressive one.

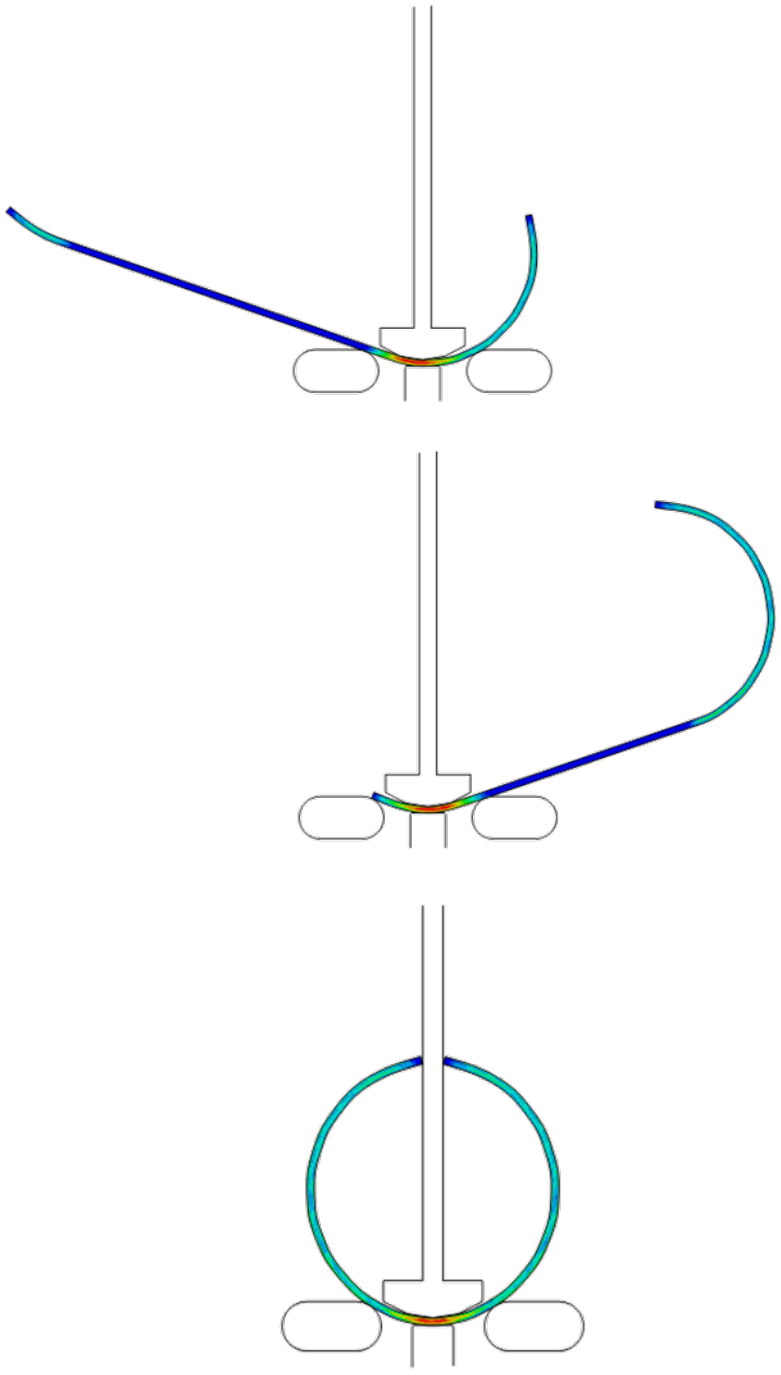

Figure 2.8 Schematics of the J-C-O-forming stage

An advantage of JCOE and JCOC process is that thicker walls can be accommodated more easily, as a step-by-step forming does not requires much force capacity of the forming tools, compared with the O-forming tool of UOE or UOC pipe. And required investments to cope with new pipe with different geometric specification is much cheaper than UOE process due to its good adaptability. However, expansion or compression calibration at the level of 1% is essential for good circularity. Besides the production rates of the JCO process are about eighteen pipes per hour, which is significantly lower than thirty-five pipes per hour of UOE process.

Likewise UOE process, each part of the plate deforms undergoing tension and compression as illustrated in Figure 2.9. Deformation history of fibers located at 6 O'clock position is summarized in Table 2.2. Though it is simpler than that of UOE, those kind of complicated plastic deformations combined with their spring back effect cause irregular ovality and residual stress as well as considerable amount of change in material properties, which are not observed for seamless pipe. For this reason, there have been numerous experiments which demonstrate the ultimate collapse pressure and bending capacity of the pipe can be significantly different with those of corresponding seamless pipes. Therefore how and why they are developed during the forming process should be investigated for precise prediction on structural performance of *UOE and JCO* pipes.

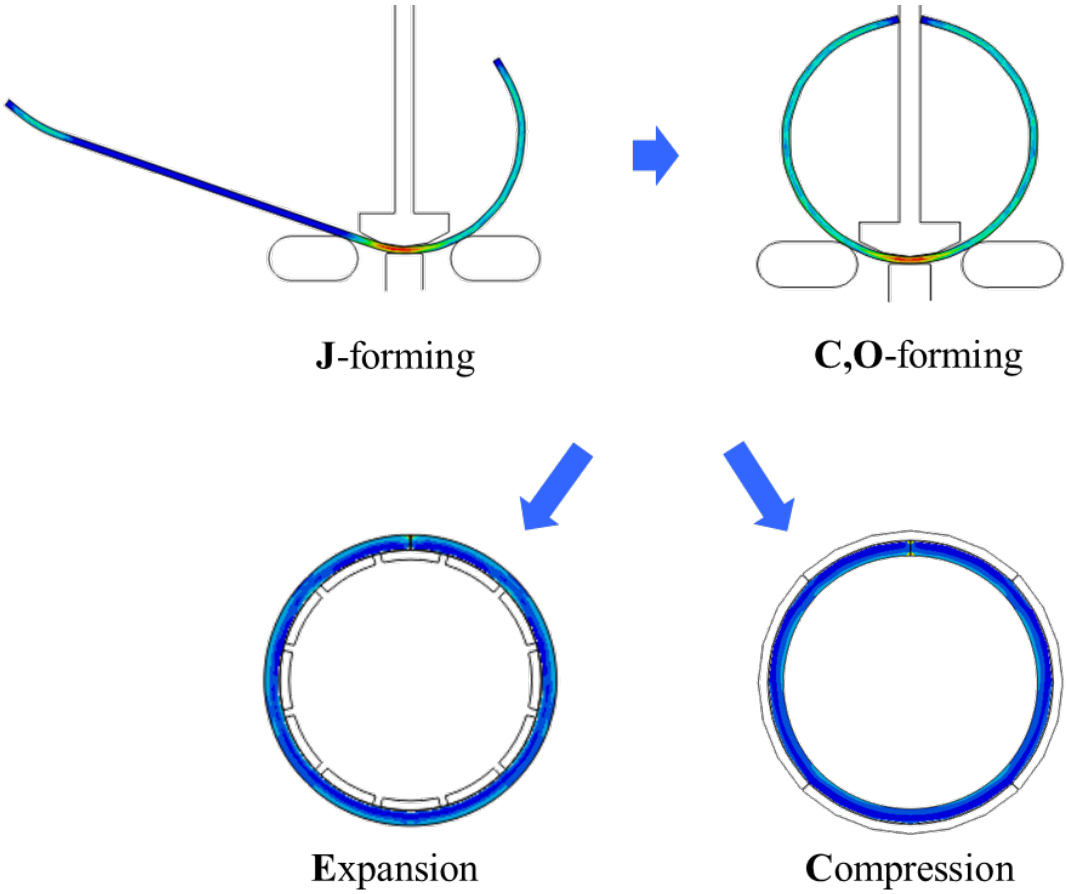

Figure 2.9 Procedures of JCOE and JCOC process

Table 2.2 Deformation history of the fibers located at 6 O'clock position of JCO pipes

Locations through the thickness at six o'clock position	**J-C-O**-forming	**E**xpansion	**C**ompression
	Bending	Tension	Compression
Outside (Outer layer)	T (Tension)	T	C
Inside (Inner layer)	C (Compression)	T	C

2.2 Change in Material Properties during the Forming Process

As mentioned before, material properties of *UOE and JCO* pipes are usually significantly different from those of the steel plate before pipe forming. This includes a hardening or weakening of the yield strength of the pipe. According to previous researches on the influence of pipe forming (Kyriakides et al, 1991; Yoshida et al, 2002), it had been figured out that the changes of material properties are caused mainly by work hardening and Bauschinger effect due to plastic deformation of complicated history. In consequence of repetition of loading, unloading and reloading during the forming process, these two antithetic effects both can exert influences on mechanical properties in different way. This section introduces fundamental concept of work hardening and Bauschinger effect form the view point of pipe forming.

2.2.1 Work Hardening

Working hardening, also called strain hardening is the strengthening effect of a steel when it deforms plastically. Let us consider a uniaxial tension test on a steel coupon made of API X70 as an example. Figure 2.10 shows stress-strain response of the steel when it is stretched by 1.5%, unloaded, and tensioned again by 3%.

The response exhibits a linear relation from the start of stretching to elastic limit point A. Here the slope of line OA is defined as Young's modulus, *E*. As material loses its stiffness slowly beyond A, the declination of slope decreases gradually. This region is called elastic-plastic regime. Steel has a yield stress where elastic-plastic regime finishes and full plastic behavior turns out, say, point B. Now suppose that this material is loaded to a higher level so that point C is reached. Unloading from point C follows line CD parallel to tangential line to the curve at the origin. When fully unloaded to point D, the material returns to its original shape partially by ε_e but residual strain of ε_p remains uncovered. This residual elongation of the material is called the residual strain. If the steel is reloaded from point D, the trajectory follows almost exactly same curve with what was drawn for unloading stage. Then it continues going upward to the point C where unloading began during the previous tensile loading. There it just follows the original curve as if nothing happened, say reloading. What is interesting is that this seems like new material curve with an origin point D. From that point of view, the proportional limit is increased to point C from point A. Besides the yield stress is expected to be higher than original one, which can be interpreted that material properties are changed. Such a response is called strain hardening or work hardening, as the

apparent stress level at which plastic action takes place increases with strain or plastic work.

Typical example of advantageous using of the work hardening effect is UOE and JCOE pipe forming for on-land use. Work hardening has a beneficial effect on pipes destined for internal pressure loading, because an expansion calibration has a strengthening effect on the tensile response of the pipe. On the contrary, UOC and JCOC pipes show higher compressive yield strength compared with virgin plate. So those processes are well-suited for offshore pipelines under high hydrostatic pressure.

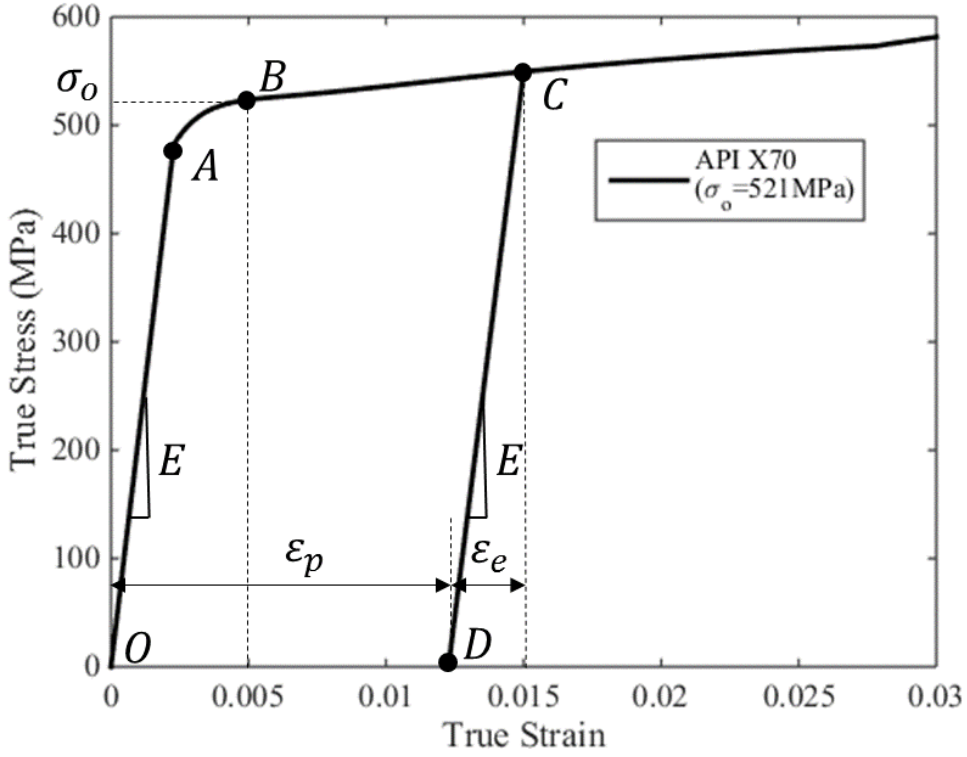

Figure 2.10 Stress-strain curve of X70 steel

2.2.2 Bauschinger Effect

The Bauschinger effect refers to the phenomenon that the stress-strain response of the metal changes as a result of microscopic stress distribution. Actually it represents reduction in compression yield strength of the steel after tensile plastic strain is applied, as shown in Figure 2.11. It illustrates the material's stress-strain characteristics following unloading from a certain point A beyond yielding and reverse compressive loading along $\overline{ABC}$. Point B is seen as a new elastic proportional limit which stress is much lower than A of initial tension. Indeed, the strain hardening to point A from tension leads to a considerable reduction in compressive strength, which is called Bauschinger effect. It can be easily found that compressive yield stress at 0.5% strain, $|\boldsymbol{\sigma_c}|$ is pretty lower than initial tensile yield stress, σ_o. Another interesting point is that elastic-plastic response of reverse loading $(\overline{ABC})$ has a significantly different shape compared with that of initial tensile loading $(\overline{OA})$. The latter exhibits a clearer transition from elastic to elastic–plastic behavior than the former. This difference should be taken into account for the problems involving reverse loading.

UOE and JCO forming processes imply that steel fiber experiences intensive tensile and compressive strain in hoop direction, which leads to a reduction of the yield strength due to Bauschinger effect. It was reported that compressive yield strength of the steel can be reduced by as large as 30% compared with that of raw plate. (Stark and McKeehan, 1995) Thus it is recommended that the actual compressive yield strength in hoop direction is to be evaluated when the pipe is designed to sustain external pressure load.

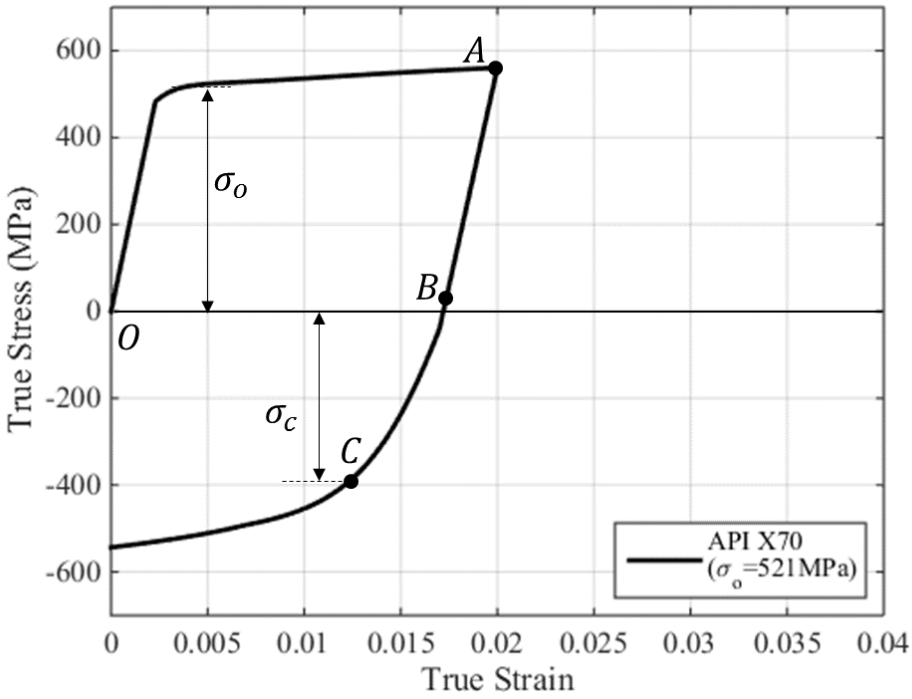

Figure 2.11 Early yielding on strain reversal due to Baushinger effect

2.3 Ovality and Residual Stress after Forming Process

2.3.1 Ovality of the Cross Section

Failure of the pipe under uniform external pressure depends much upon the geometric imperfection (Timoshenko and Gere, 1989; Fraldi and Guarracino, 2013). The most common imperfection of the pipe structure is cross-sectional ellipticity, so called ovality. To take the effect of ovality into account for design criteria, it is necessary to represent an ovality with an intuitive and simplified way. For example, DNV-OS-F101 defines the ovality parameter as Eq. (2.1) paying attention to the first buckling mode of the externally pressurized pipe.

$$f_0 = \frac{D_{max} - D_{min}}{D_{avg}} \tag{2.1}$$

where D_{max}, D_{min} and D_{avg} are maximum, minimum and averaged outer diameters of the manufactured pipe as shown in Figure 2.12. In practice, the diameter is measured at least at the angular positions shown in Figure 2.13 for convenience. Ordinarily the geometric imperfection is regarded suitable if f_0 is less than 1% at the end section of pipe. Wide-ranging experiment by Yeh and Kyriakides (1986) covered that the collapse pressure of the pipe is strongly sensitive to initial ovality for all diameter-thickness ratios of interests. The results in Figure 2.14 show the ovality has a negative effect on the collapse pressure evidently.

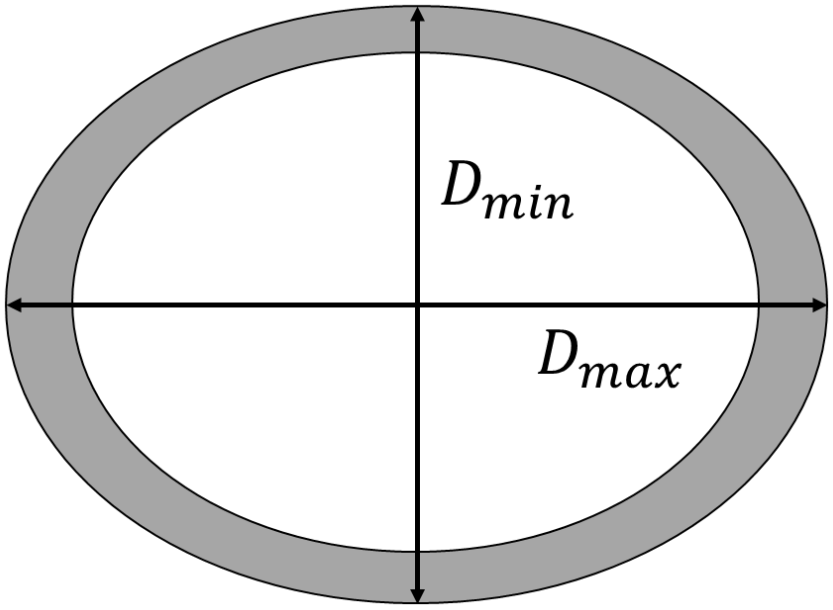

Figure 2.12 Parameters used for define cross sectional ovality of the pipe

According to the analyses conducted in some previous works, it is important to quantify the ovality of the pipes if the structural strength should be estimated accurately. (Fraldi and Guarracino, 2011) *UOE and JCO* forming processes tend to bring larger ovality with many classes of shape than seamless pipe, due to its complicated plastic deformation as introduced. Hence the evaluation of roundness is considerably of interest in the *UOE and JCO* pipe manufacturing field. Because it is still challenging to assess the ovality with its complex shape by analytic method, finite element analysis of *UOE and JCO* forming processes can be used as an efficient tool for implementing ovality to structural performance assessment.

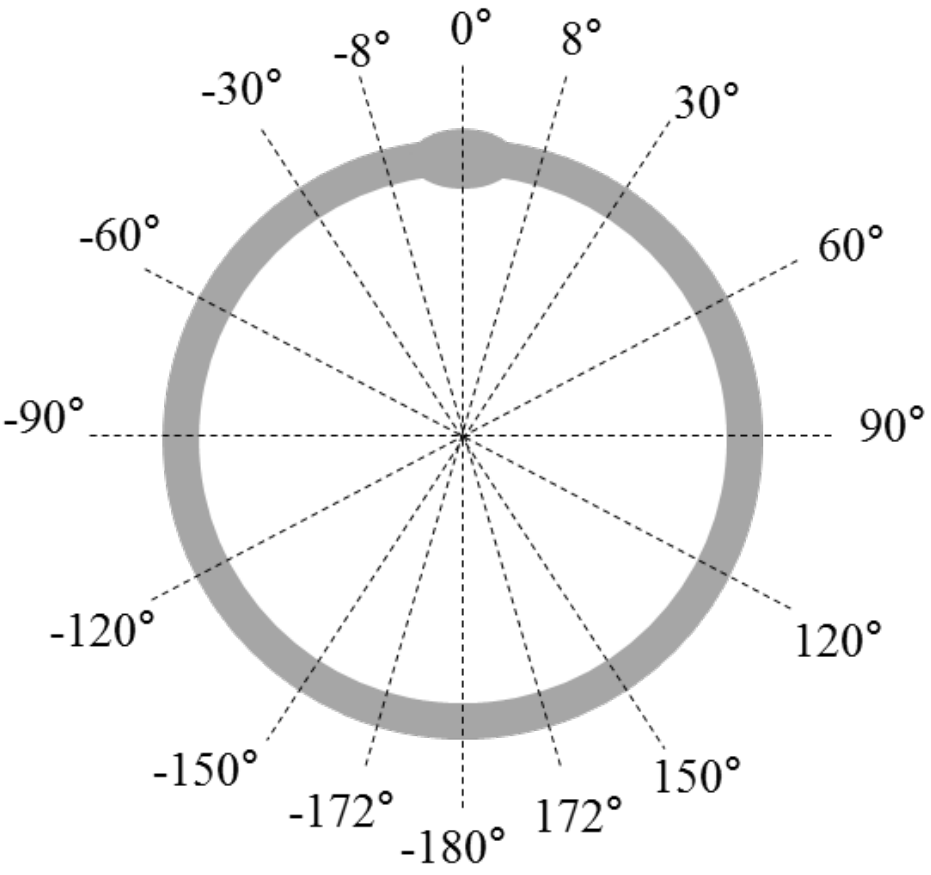

Figure 2.13 Angular positions at which diameter measurements are taken for calculation of the ovality

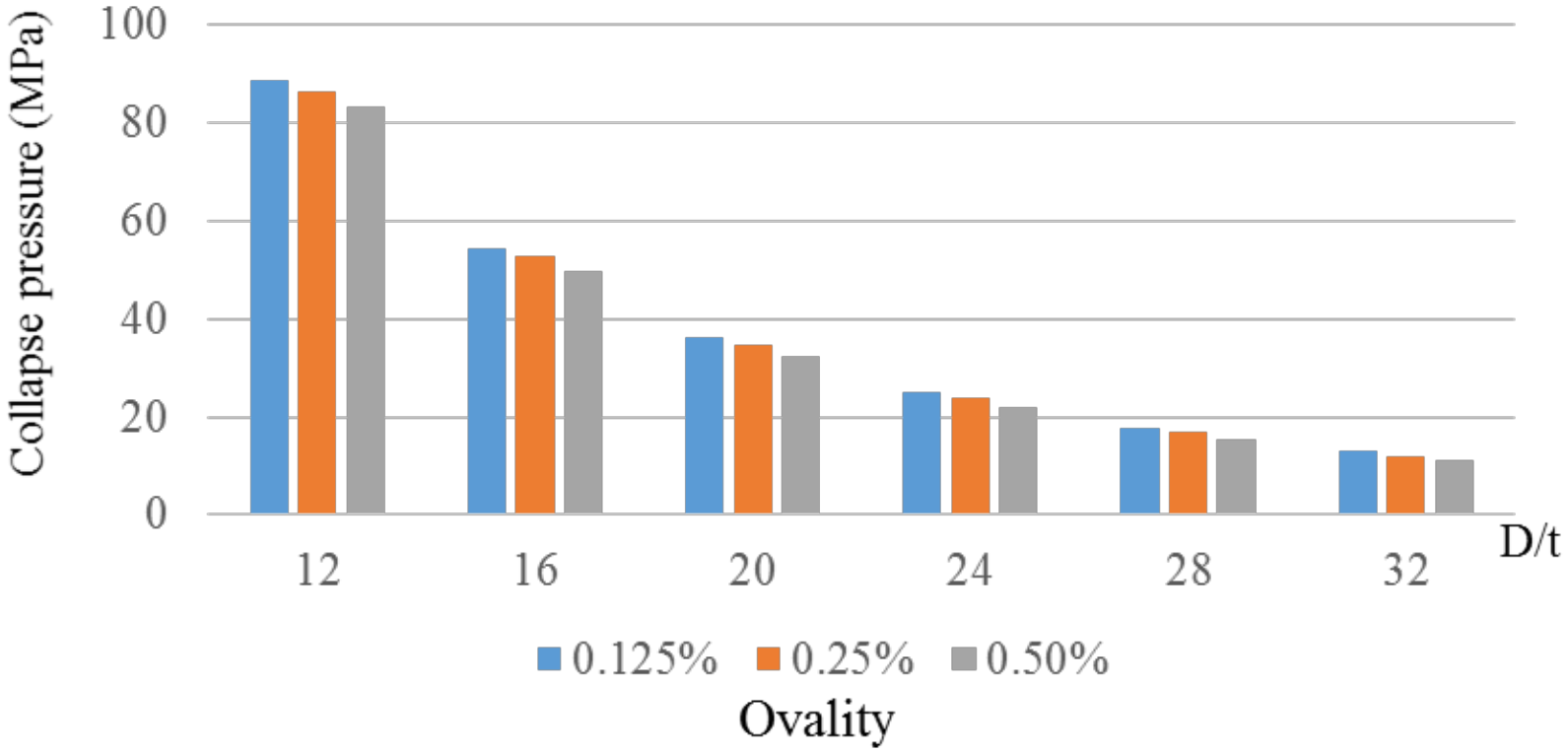

Figure 2.14 Collapse pressure for imperfect pipes with various diameter to thickness ratios ($\boldsymbol{D/t}$) (API X70)

2.3.2 Residual Stress on Pipe Wall

UOE and JCO forming processes basically consist of plastic bending and its elastic spring back. This series of manufacturing process imparts residual stresses as well as plastic strains with complex aspect. Let's take a look on the fiber which is located at 6 O'clock position of UO pipe. The stress distribution of the fiber through thickness direction depicted in Figure 2.15. Circumferential compression at O-forming stage is neglected because it has only minor effect compared with other forming stages.

This kind of residual plastic strain and stress can affect to not only yield strength but also structural performance of the pipe (Yu WW., 2000). The influence of this type of residual stress on collapse pressure of the API X70 pipe has been represented by experiment as in Figure 2.16 (Bastola *et al*, 2014). Calculated collapse pressures in the presence of residual stress were normalized by the corresponding values with zero residual stress. For low $\boldsymbol{D/t}$ pipes, the effect of residual stress on the collapse pressure seems to be minor. But the effect grows with $\boldsymbol{D/t}$, so that for $\boldsymbol{D/t}$ = 25 a residual stress with amplitude of 80% of yield stress reduces the collapse pressure by about 15%. Thus residual stress should be considered appropriately when the pipe is manufactured by plastic forming process. However it is challenging to predict the manufacturing-induced residual stress quantitatively in detail (Wang, J. *el al*, 2013). Hence the finite element analysis technique is required to take it into consideration for design of *UOE and JCO* pipes.

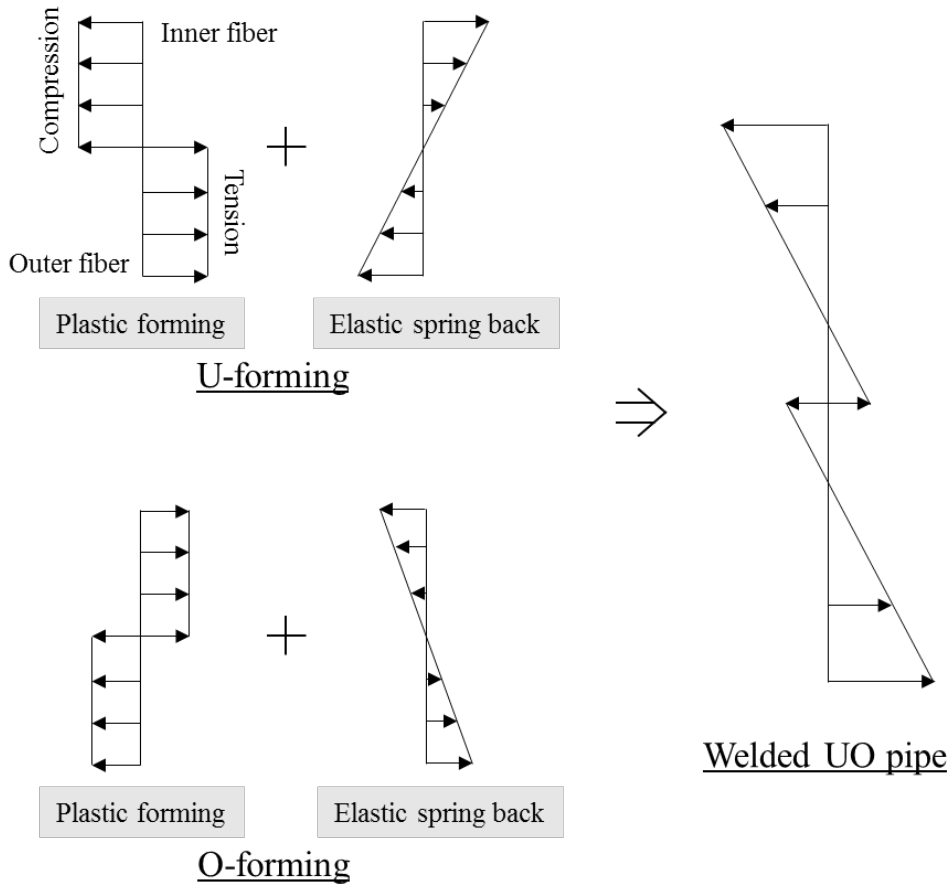

Figure 2.15 Residual stress of 6 O'clock position of UO forming process through thickness direction

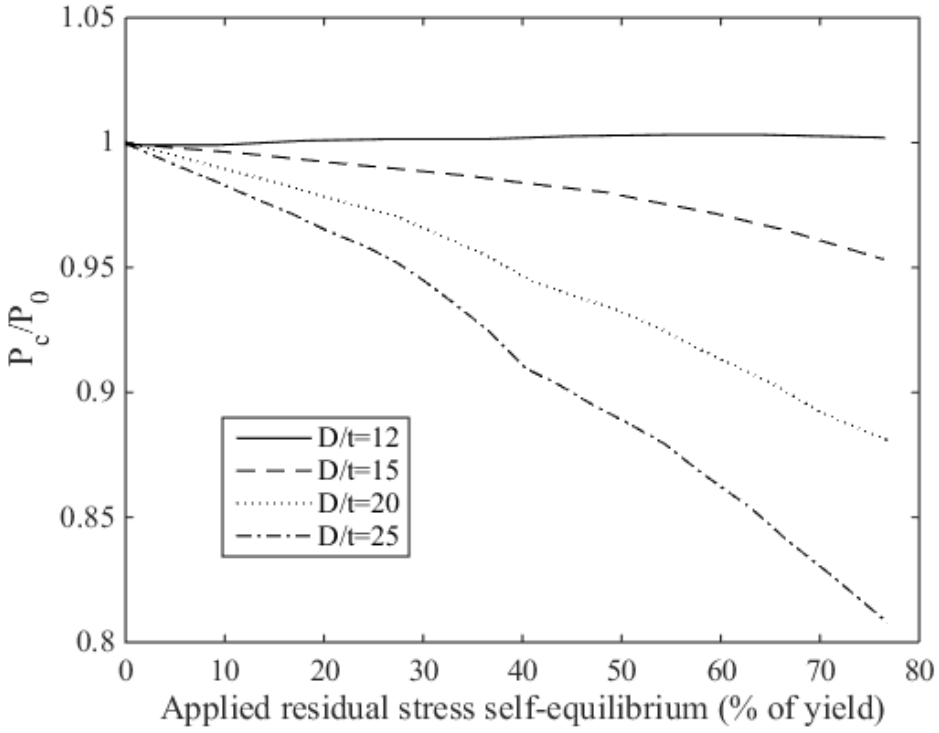

Figure 2.16 Effects of residual stress in hoop direction (Bastola *et al*, 2014)

3 Prediction of Yield Strength and Structural Performance of the Pipe

3.1 Numerical Material Model for the Simulation

During the whole pipe forming process, the material undergoes elastic-plastic deformations including repeated load reversals. Therefore the accurate material modeling is of major importance for the reliable prediction of yield strength of the pipe. For that, refined numerical material model which describes the elastic-plastic behaviors including work hardening and Bauschinger effect is required. In this thesis, the modified Chaboche model (Zou et al, 2016) is adopted as a constitutive model. It modified original Chaboche model to have flexibility for wide range of material characteristics. Apart from work hardening and Bauschinger effect, it is capable of representing clear yield plateau and evolution of Young's modulus. On the other hand, uniaxial tension test was performed to calibrate material parameters of the model.

3.1.1 Constitutive model

When it comes to numerical approach to plastic behavior of the material, one of most concerning problem is the material modeling. In this study, constitutive model by Chaboche and Rosselier (1983) based on Mises yield function with combined isotropic-kinematic hardening theory is adopted. By describing hardening event

with cumulated and present plastic strain, Chaboche model offers better descriptive possibilities despite its simple formulation. Fundamental Mises yield surface function for isotropic hardening has the form of :

$$\boldsymbol{f(\sigma, K) = f_o(\sigma) - K = 0} \qquad \textbf{(3.1)}$$

where $\boldsymbol{K}$ is isotropic hardening term. The shape of the yield function is specified by the initial yield function, and its size grows up as $\boldsymbol{K}$ changes. This indicates also that the yield surface preserves its shape but expands with increasing stress as Figure 3.1 shows.

Above isotropic hardening implies that the yield surface always remains symmetric about the stress axis. In other words, even if the yield surface develops with larger plastic strain, the material has always same yield strengths to tension and compression direction. However in practice, a hardening in certain direction leads to softening in opposite direction due to Bauschinger effect. This phenomenon can be described by Kinematic hardening model that has general form of:

$$\boldsymbol{f_0(\sigma - \alpha) = 0} \qquad \textbf{(3.2)}$$

where $\boldsymbol{\alpha}$ indicates back-stress tensor. Kinematic hardening rule assumes the yield surface remains the same shape and size but translates in stress space by back-stress which is a function of plastic strain. This can be also illustrated as Figure 3.2.

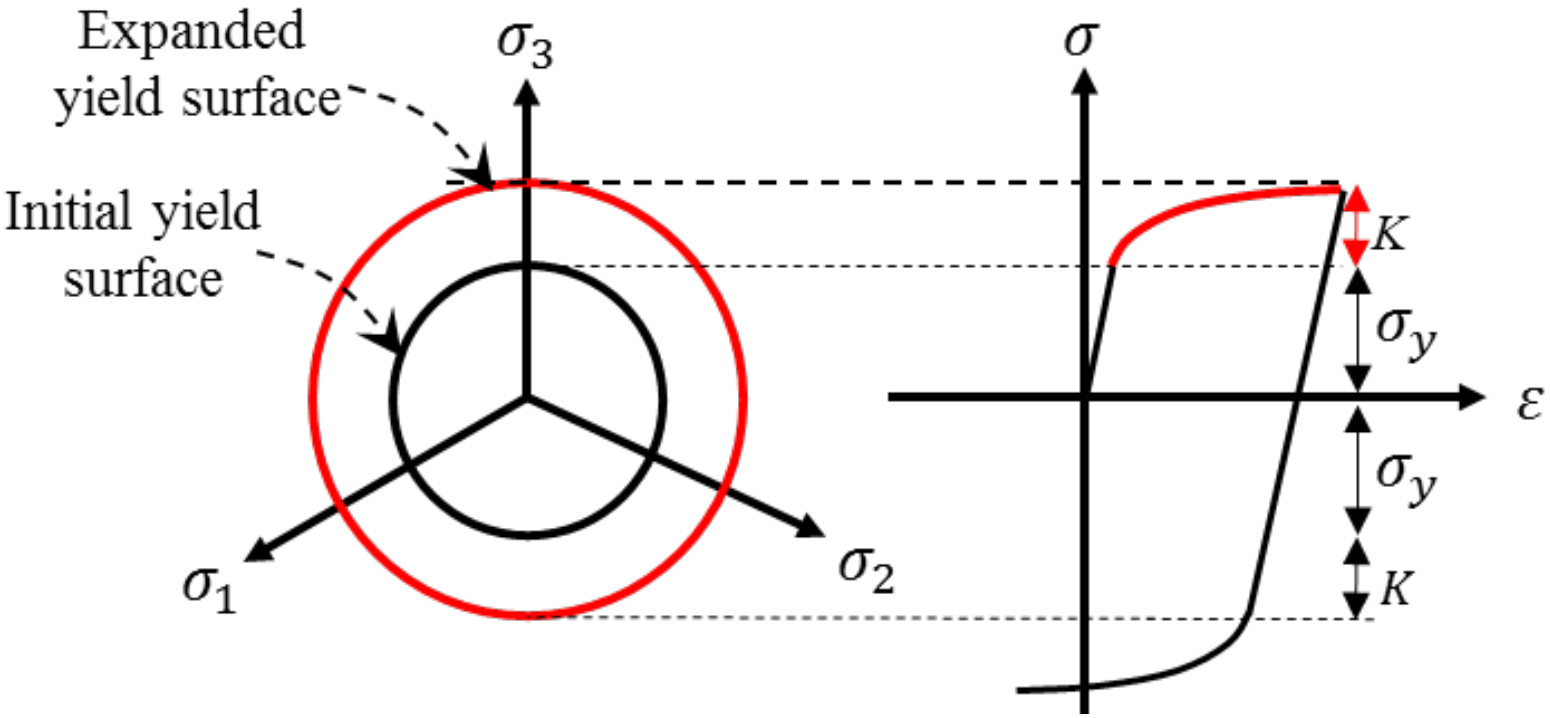

Figure 3.1 Concept of isotropic hardening model

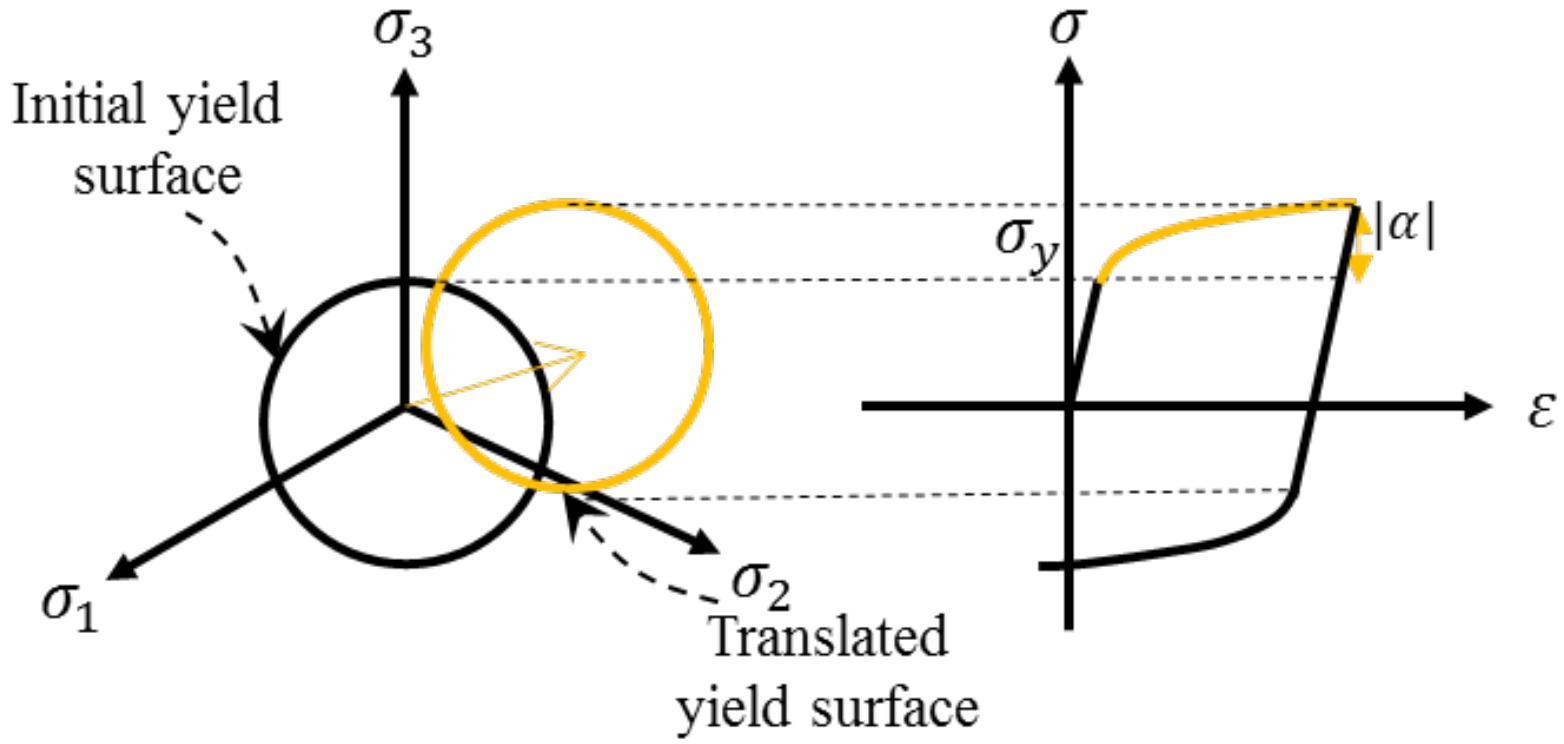

Figure 3.2 Concept of kinematic hardening model

The combination of these two hardening models facilitates the representation of more complicated hardening behaviors that could not be modeled easily by either of isotropic or kinematic hardening rule. According to Von Mises yield function, the combined hardening model has a form of:

$$\boldsymbol{f(\sigma, K) = \sqrt{\frac{3}{2}(\sigma' - \alpha'):(\sigma' - \alpha')} - K = 0} \qquad \textbf{(3.3)}$$

where $\boldsymbol{\sigma'}$ and $\boldsymbol{\alpha'}$ are deviatoric parts of stress and back-stress respectively. Here back-stress term $\boldsymbol{\alpha}$ was suggested as a summation of multiple components of the back-stress components by Chaboche and Rosselier (1983) :

$$\begin{cases} \boldsymbol{\alpha = \sum_{i=1}^{n} \alpha_i} \\ \boldsymbol{\dot{\alpha}_i = \frac{2}{3} A_i \dot{\varepsilon_p} - C_i \dot{p}} \end{cases} \qquad \textbf{(3.4)}$$

where $\boldsymbol{\alpha_i}$ is back-stress component; $\boldsymbol{A_i}$ and $\boldsymbol{C_i}$ are material hardening parameter; $\boldsymbol{\dot{\varepsilon_p}}$ is present plastic strain rate and $\boldsymbol{\dot{p}}$ is accumulated plastic strain rate. Here subscript $\boldsymbol{i}$ is index of back-stress component and $\boldsymbol{n}$ is total number of back-stress components. Theoretically the larger $\boldsymbol{n}$ is, the more it can implement the stress-strain curve precisely. In this thesis, 3 components were determined to be sufficient for describing the response of material undergoing *UOE and JCO* forming processes ($\boldsymbol{n}$ = 3). By integrating both sides of Eq. (3.4) in terms of $\boldsymbol{\varepsilon_p}$, $\boldsymbol{i}$-th back-stress component under uniaxial cyclic loading can be represented as:

$$\alpha_i = \pm\frac{A_i}{C_i} + \left(\alpha_{i0} \mp \frac{A_i}{C_i}\right)\exp(-C_i|\varepsilon_p - \varepsilon_{p0}|) \quad \textbf{(3.5)}$$

where subscript '**0**' indicates the corresponding values at the last change of plastic strain rate. Plus-minus and minus-plus signs is determined depending on the direction of plastic flow.

One simple formulation to express the isotropic hardening term $\boldsymbol{K}$ with respect to plastic strain is:

$$K = Q(1 - \exp(-bp)) \quad \textbf{(3.6)}$$

where $\boldsymbol{Q}$ and $\boldsymbol{b}$ are material parameters to be calibrated by test. Physically $\boldsymbol{Q}$ means saturated value of isotropic hardening stress when the plastic strain is infinite.

Although above model is powerful for describing shifted yield strength as well as rounded curve shape due to work hardening and Bauschinger effect, it has limitation when it comes to represent the yield plateau. Size of yield surface defined by the above model monotonically increases right after initial yielding, as a plastic strain gets larger. It is because both isotropic hardening and kinematic hardening contribute to the outward expansion of yield surface. During the yield plateau range, however, the stress stays almost stationary even plastic strain goes larger. Therefore special treatment should be applied to deal steel materials with distinct yield plateau. This study splits the plastic section of isotropic hardening

term by accumulated plastic strain (p) to implement different equations within yield plateau range as:

$$K = \begin{cases} \sigma_0 + (\sigma_1 - \sigma_0)\big(1 - exp(-\beta p)\big) & p \le l_{pl} \\ \phi + Q(1 - exp(-bp)) & p \ge l_{pl} \end{cases} \quad \textbf{(3.7)}$$

where $\sigma_1,\ \beta, \sigma_0,\ Q$ are material parameters to be calibrated based on coupon loading test. Another material parameter ϕ should be determined thereby to satisfy continuity condition at $p = l_{pl}$. Eq. (3.7) shows that isotropic hardening term decreases with larger plastic strain for counterbalancing with increased kinematic hardening term to model nearly constant size of yield surface.

On the other hand, unloading stress-strain path is found to be slightly curved, which means Young's modulus is not constant but varies depending on accumulated plastic strain. Yoshida *et al*. (2002) investigated that such a strain dependency of Young's modulus would much influence the spring back behavior especially when the steel sheets are subjected to a large deformation. They concluded that the effect of accumulated plastic strain on Young's modulus can be expressed as a simple function as:

$$E = E_0 - (E_0 - E_a)[1 - exp(-\xi p)] \quad \textbf{(3.8)}$$

where E_0 and E_a are initial Young's modulus and saturated Young's modulus at

infinitely large accumulated plastic strain, respectively; ξ is a material parameter.

Consequently, 15 relevant parameters should be fitted to implement the adopted numerical material model. In following section, the cyclic loading test on the specimen and parameter fitting procedure using the test results will be introduced. Meanwhile a significant necessity of modification on original Chaboche model will be examined as well.

3.1.2 Calibration of material parameters using test result

The pipe material used for this thesis is API X70 steel which is widely applied high strength steel in pipe industry. Firstly, the specimen from the steel sheet was prepared for cyclic tension-compression-tension test. The shape of the specimen is illustrated in Figure 3.3. The test was conducted as in Figure 3.4 to get a stress-strain response involving work hardening, Bauschinger effect, yield plateau and evolution of Young's modulus. The specimen is tensioned to 3% strain and then compressed to -3% strain after unloading, and then tensile loading is applied again to 3% strain such that the response curve draws loop as blue line in Figure 3.5. One can figure out that Bauschinger effect exhibits rather rounded curve shape around compressive yielding point and tensile yielding point thereafter. Also the other plastic behaviors seem to be characterized quite well.

To calibrate material parameters of the numerical model, least-square method was taken combined with genetic algorithm. The standard error of the fitting calibration was defined as:

$$G(\underline{x}) = \sqrt{\frac{\sum_{i=1}^{n}\left(\sigma(\underline{x}) - \sigma_{exp}\right)^2}{n}} \quad \textbf{(3.9)}$$

where $\sigma(\underline{x})$ and σ_{exp} are the fitted stress using calibrated parameters and experimental result, respectively. n is the number of available stress-strain data derived from the experiment. Total 15 best-fit parameters were drawn through genetic algorithm and they are listed in Table 3.1. There were good agreements of fitted curve with experimental data as shown for red and blue solid lines in Figure 3.5.

Fitted curve with original Chaboche model is also illustrated with dotted line for comparison. Though it follows similar trajectory with test result after first unloading, it shows a large error for initial monotonic tension before unloading. If original Chaboche model is used as it is, it cannot help resulting in serious error grown from beginning of the analysis. Table 3.2 shows tensile yield strength in hoop direction and collapse pressure of the UOE pipe finalized by expansion of 1.25%. Those results were predicted from the numerical analysis on identical pipes except for the numerical material model; one with modified Chaboche model and the other with original Chaboche model. Original Chaboche model overestimates not only yield strength but collapse pressure by large amount; 17% in case of collapse pressure. This clear difference explains why modification considering yield plateau and evolution of Young's modulus is required for better calibration as expressed in Section 3.1.1.

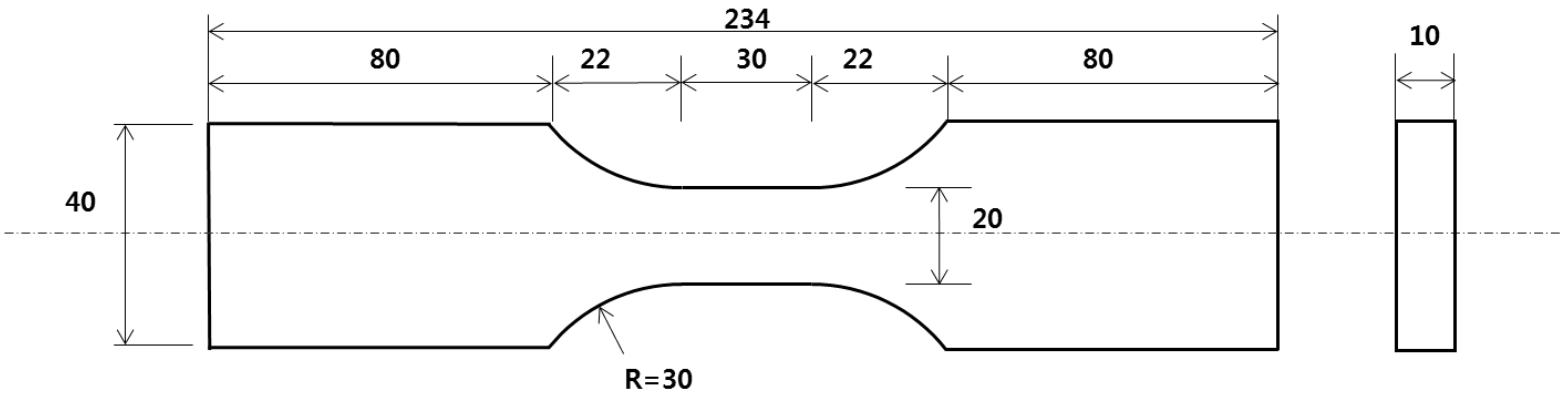

Figure 3.3 Shape of specimen for cyclic tension-compression test

Figure 3.4 Uniaxial cyclic loading test on X70 specimen

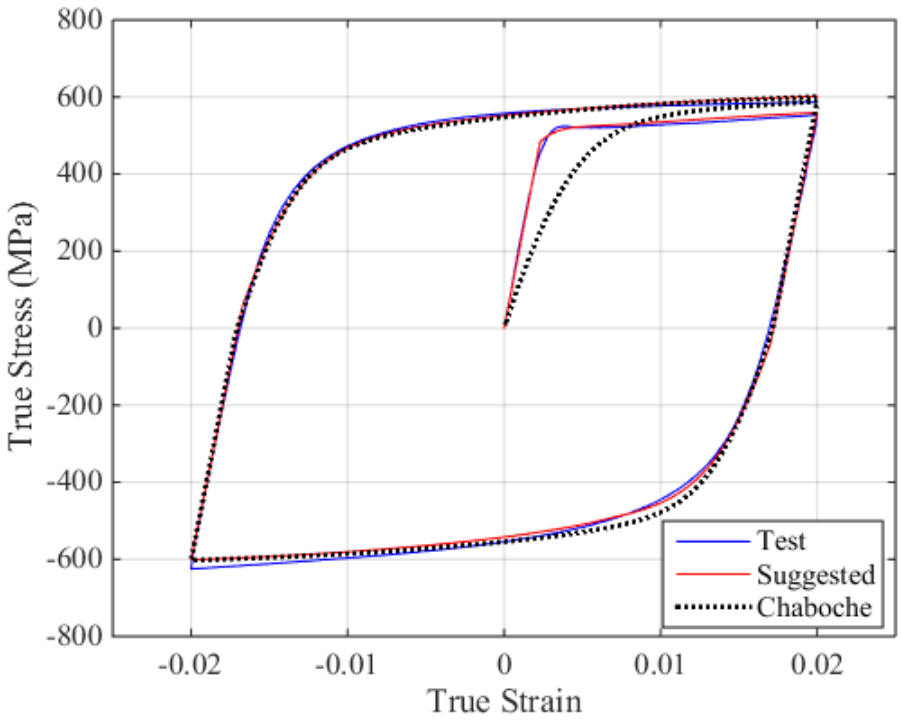

Figure 3.5 Result of cyclic loading test and fitted stress-strain curves of X70 steel

Table 3.1 Fitted values of loading test for API X70 steel

Parameter	Lower bound	Upper bound	Fitted value
E_0 (MPa)	2000000	22000000	210697.1
σ_0 (MPa)	500	600	482.6
l_{pl}	0.015	0.025	0.0249
E_a (MPa)	180000	200000	200000
ξ	70	200	183.8
Q (MPa)	100	300	299
σ_1 (MPa)	300	450	300
A_1	20000	100000	4892
A_2	20000	100000	63866
A_3	20000	100000	67109
C_1	200	2000	52.6
C_2	200	2000	459.0
C_3	200	2000	1016.2
b	10	100	88.8
β	100	500	470.4

Table 3.2 Predicted yield strength and collapse pressure using different material model

	Modified Chaboche model	Original Chaboche model
Yield strength in hoop direction of the pipe (MPa)	526.4	543.7
Collapse pressure (MPa)	5.8	6.6

3.2 Computational Simulation of Pipe Forming Process

Numerical analysis on forming process has been regarded as an efficient way to estimate pipe's quality such as yield strength or structural performance with accurate calculation of ovality and residual stress. Furthermore, geometrical configuration of the skelp at each stage of forming process also can be estimated. It is essential to guarantee the satisfactory producibility of the pipe. For example, the width of gap between both plate edges after O-forming should be adequate for good weldability. In this section, *UOE and JCO* forming processes are numerically modeled with 2-dimensional finite element model using modified Chaboche model. There would be described three key outputs; yield strengths, ovality and residual stress. This section introduces how those outputs are treated and processed for assessing the quality and structural performance of the pipe. Then developed model is verified with pipe forming test and tensile loading test on the specimen cut from the formed pipe. The model would be used to develop an understanding of how each forming step influences the pipe shape and material properties as well as the collapse pressure or bending capacity.

3.2.1 Finite Element Modeling Description

The problem is solved within the nonlinear finite element code ABAQUS using a UMAT subroutine that implements the combined hardening model successfully. Practically a length of *UOE and JCO* pipe is usually over 10 meter, much larger

than a diameter. And deformation through longitudinal direction is negligible compared with severe deformation in cross sectional plane. So the plate is formed under plane strain conditions in the 2D finite element model. The plate is discretized into 7 elements along thickness direction while mesh seed is set moderately to horizontal axis through comprehensive convergence study as shown in Figure 3.6. Though the forming process operates dynamically, the simulation is performed as a quasi-static analysis since dynamic term such as inertia effect and damping can be neglected considering rather slow motion of the tools.

In spite of complicated series of plastic deformation, every single forming stage brings only bending or axial loading to the plate that can be modeled simply with ordinary element. Thus 4-node bilinear quadrilateral, reduced integration plane strain continuum elements (CPEG4R) was used for mesh. One element has totally 12 degree of freedom; translation along x and y-axis and rotational deflection about z-axis are allowed at each node. Every forming tools and dies are modeled as a non-deformable analytical rigid surface. For updating stress in plastic region, a classical radial return mapping algorithm is used.

The plate undergoes maximum plastic strain of the analysis is much larger than yield strain, which means large deformation analysis. In this problem, geometric nonlinearity and boundary nonlinearity as well as material nonlinearity are implemented. As is well known for large deformation problem, unique stress for a certain strain value does not exist due to path dependency. Therefore we should note that the solution in this study has a limit of lack of guarantee since this is ill-posed problem with high nonlinearity. Surely for this problem, experimental

verification should be accompanied. The updated Lagrangian approach is chosen for this analysis. All the static and kinematic variables are referred to the last calculated configuration. For path-dependent elastoplastic materials, the constitutive relations are readily incorporated in the updated Lagrangian formulation. Generally for the updated Largrangian formulation with time increments, nonlinear response of the body is replaced by a sequence of piecewise linear increments which form:

$$\int_{\Omega^t} \Delta T_{Ji} \overline{u_i}_{,J} d\Omega^t = \int_{\Omega^t} \rho \Delta b \overline{u_i} d\Omega^t + \int_{\Gamma_F^r} \Delta t_i \overline{u_i} d\Gamma^t \qquad \textbf{(3.10)}$$

at time t with $\Delta t \ll 1$. For this simulation, the term t simply converts to displacement of the forming tools in that the whole analysis is control by them.

Node-to-surface contact condition between the plate and tools or dies is accomplished by a master-slave algorithm, in which rigid surfaces plays a role as the master surface. This means that the plate cannot penetrate into the forming tool during the whole analysis. Friction between contact pairs is modeled as Coulomb friction coefficient of 0.1. By using ‘no separation’ condition between the blank and U-forming punch, any node pair involved to them is not allowed detach in normal direction once they contact each other. Only small sliding to tangential direction is considered with Lagrange multipliers.

UOE and JCO forming processes require multiple design parameters to form the plate into intended shape at each stage as in Figure 3.7, Table 3.3 (UOE) and Table

3.4 (JCOE). Since forming processes dealt in this dissertation consist of successive forming stages, the deformed shape in a previous phase can exert great effect on the subsequent stages. Thus design parameters should be determined considering their close interrelation, not to mention size of the pipe and material properties. For the sake of accuracy and time efficiency for design parameter setting, a prevalidation program for forming parameters was developed in this study. It automatically generates ABAQUS input file with whole design parameters only if it is equipped some fundamental variables such as size of the pipe, material properties and how much the pipe shall be expanded (or compressed) at calibration stage. Developed program can substitute a conventional design method based on trial-and-error approach, resulting in consistent design parameter set at once.

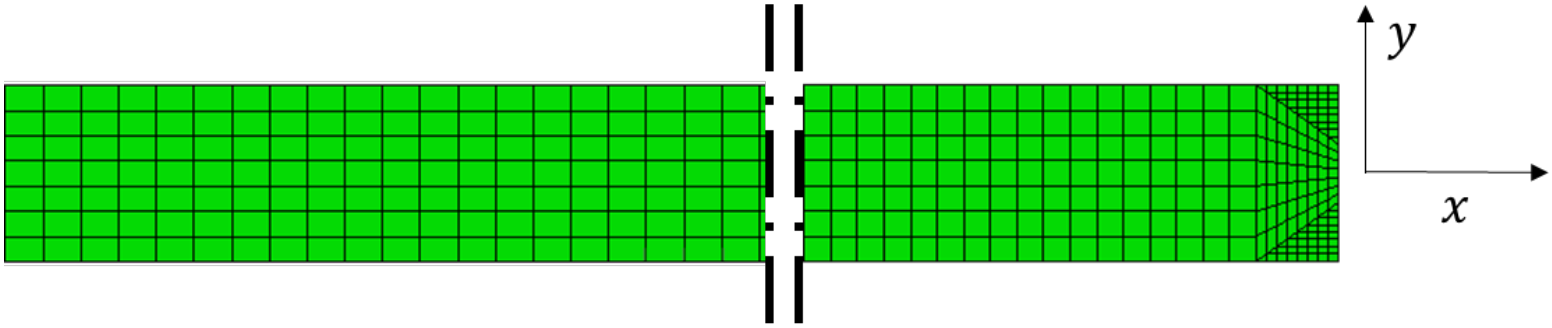

Figure 3.6 Shape of specimen for cyclic tension-compression test

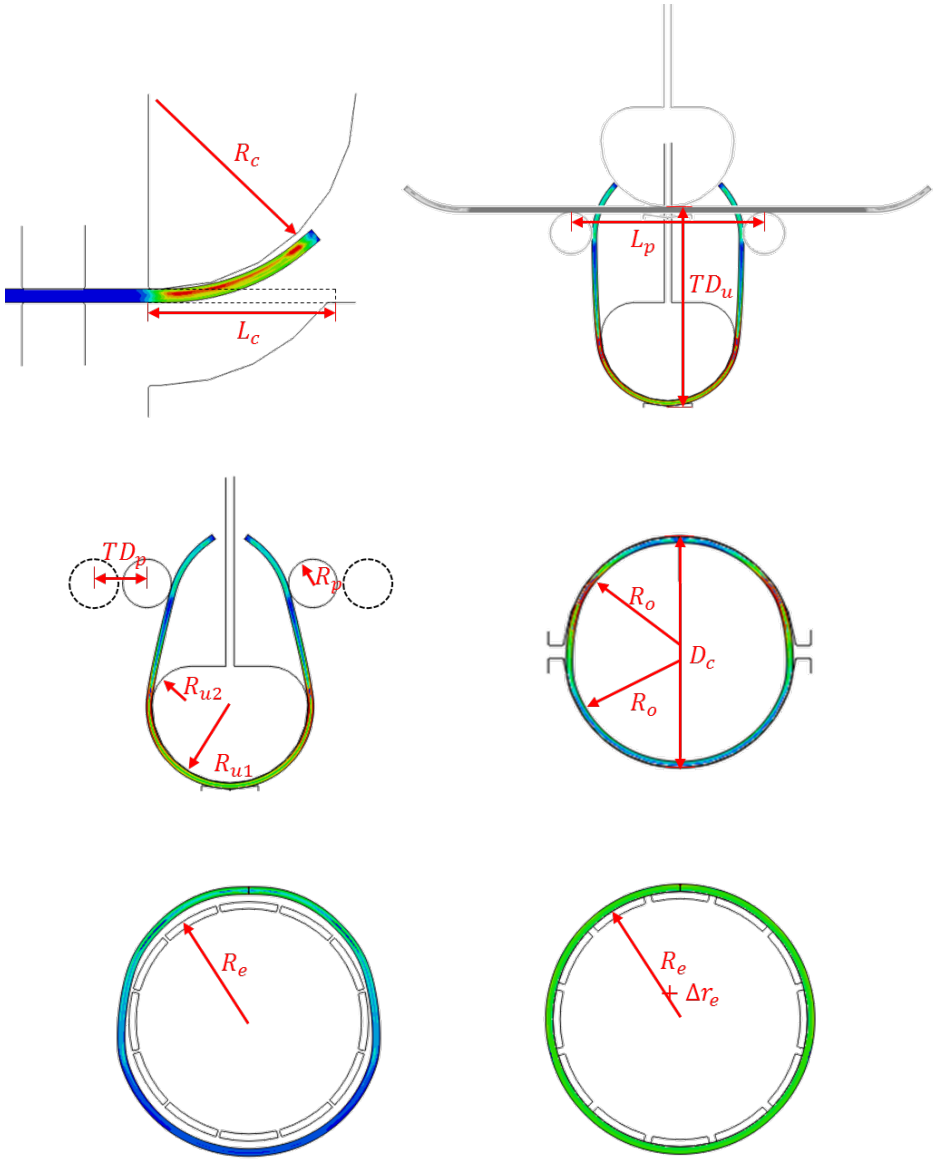

Figure 3.7 Schematic diagram of forming parameters in UOE pipe manufacturing

Table 3.3 Design parameters required for UOE pipe forming

(Ex : $\boldsymbol{D}$ = 30 in, $\boldsymbol{t}$ = 12.7 mm, expansion ratio = 1%)

	Symbol	Description	Value
OD	OD	Target outer diameter (in)	30
Plate	t	Thickness (mm)	12.7
	W	Initial width (mm)	2339.8
	σ_o	Yield stress at 0.5% (MPa)	521
Crimping	R_c	Crimp tool radius (mm)	290
	L_c	Length of crimped part (mm)	270
U-forming	R_{u1}	U-forming tool radius (mm)	288
	R_{u2}	U-forming tool small radius (mm)	144
	L_p	Pusher horizontal position (mm)	1100
	TD_u	U-forming tool travel distance (mm)	900
	TD_p	Pusher travel distance (mm)	260
	R_p	Pusher radius (mm)	150
O-forming	R_o	O-forming tool radius (mm)	373.38
	D_c	Maximum distance between upper and lower O-forming tool (mm)	758.9
	δ_{oc}	Compression ratio at O-ing stage (mm)	0.004
Expansion	δ_e	Expansion ratio before spring back (mm)	0.0125
	R_e	Expansion tool outer radius (mm)	365.5
	δ_{pe}	Permanent expansion ratio (mm)	0.0100
	Δr_e	Expansion value (mm)	4.6
	OD_o	Outer diameter before expansion (in)	29.78
	OD_f	Final outer diameter (in)	30.0

Table 3.4 Design parameters required for JCOE pipe forming

(Ex : $\boldsymbol{D}$ = 28 in, $\boldsymbol{t}$ = 18.5 mm, expansion ratio = 1%)

	Symbol	Description	Value
OD	OD	Target outer diameter (in)	28
Plate	t	Thickness (mm)	18.5
	W	Initial width (mm)	1857
	σ_o	Yield stress at 0.5% (MPa)	521
Crimping	R_c	Crimp tool radius (mm)	250
	L_c	Length of crimped part (mm)	240
J-C-O-forming	D_{p1}	Ordinary punching depth (mm)	47
	D_{p2}	Final punching depth (mm)	58
Expansion	δ_e	Expansion ratio before spring back (mm)	0.0125
	R_e	Expansion tool outer radius (mm)	341.5
	δ_{pe}	Permanent expansion ratio (mm)	0.0100
	Δr_e	Expansion value (mm)	4.2
	OD_o	Outer diameter before expansion (in)	27.78
	OD_f	Final outer diameter (in)	28.0

Figure 3.8 and Figure 3.9 demonstrate UOE and UOC processes simulated by finite element analysis, respectively. JCOE and JCOC processes were also analyzed numerically in similar way as illustrated in Figure 3.10 and Figure 3.11.

Actually after O-forming, the pipe has to be welded longitudinally using double submerged arc welding (DSAW) method that welds the seam first on the inside and then on the outside. It is important step because it brings much heat and geometric deformation around heat affected zone. Though it is, it is well known that longitudinal welding does not disturb collapse pressure or bending capacity of the pipe interested in this thesis. Therefore welding is simply described here by compatibility condition of both welding edges.

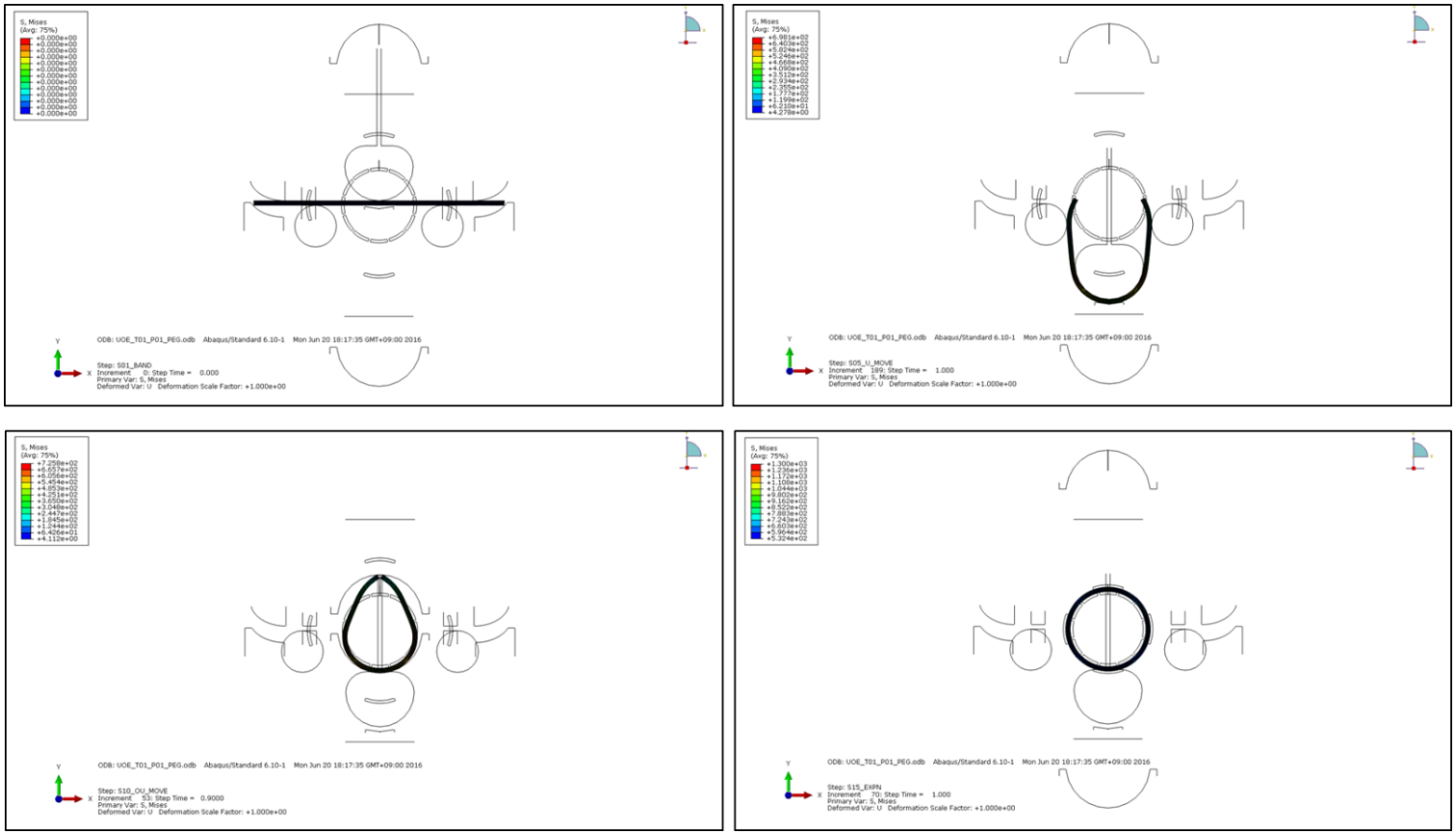

Figure 3.8 Finite element analysis on UOE forming process

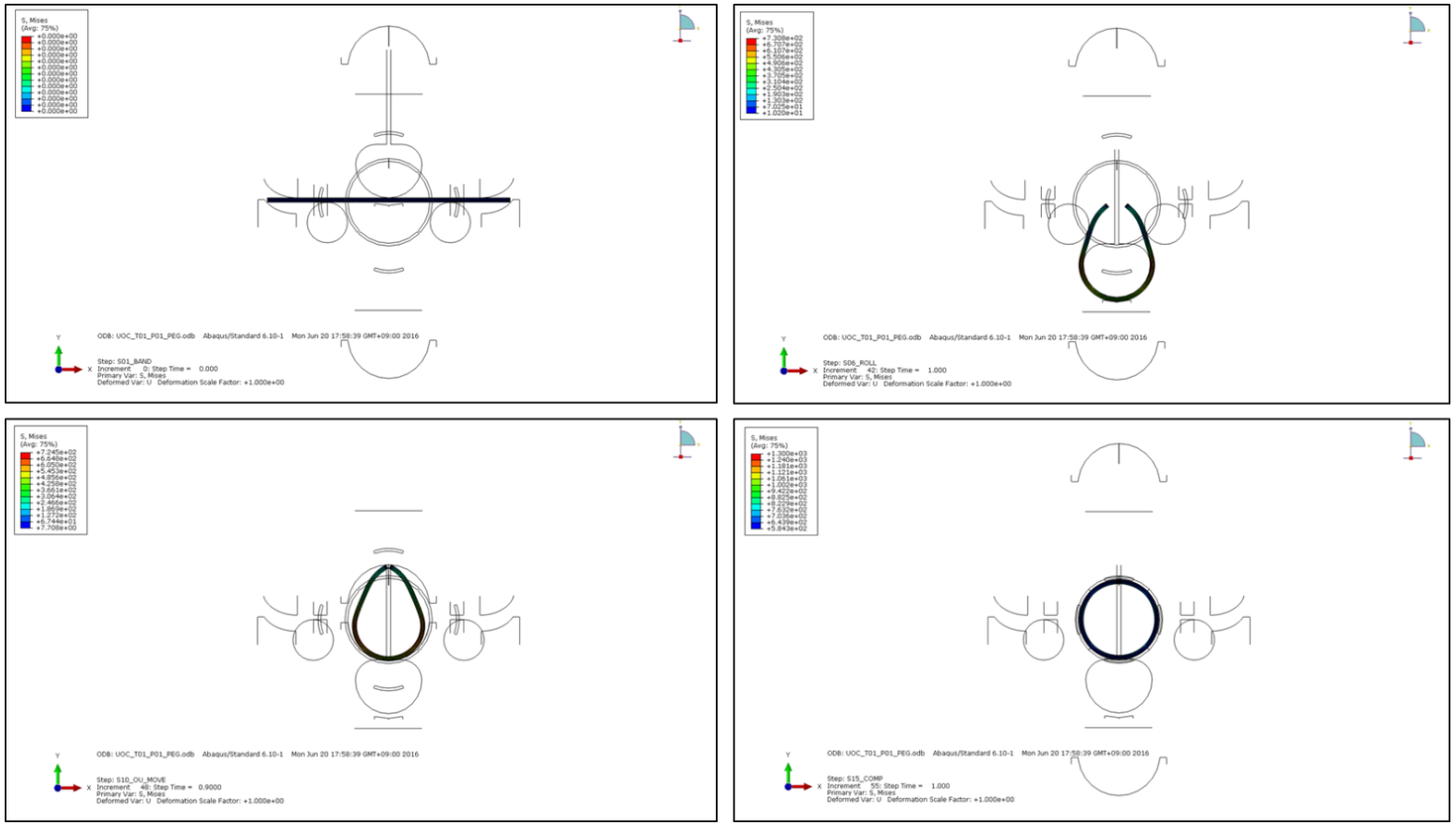

Figure 3.9 Finite element analysis on UOC forming process

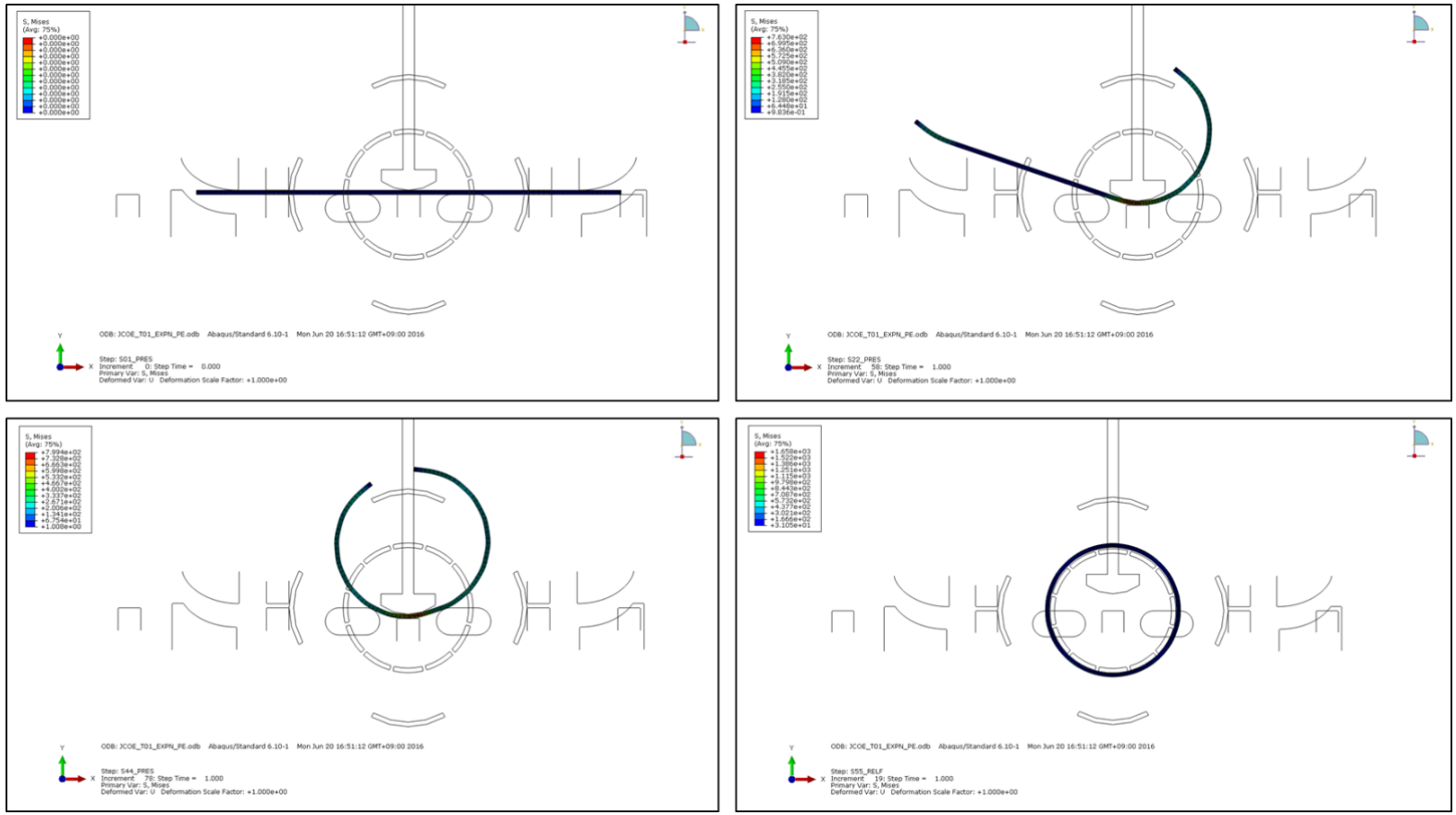

Figure 3.10 Finite element analysis on JCOE forming process

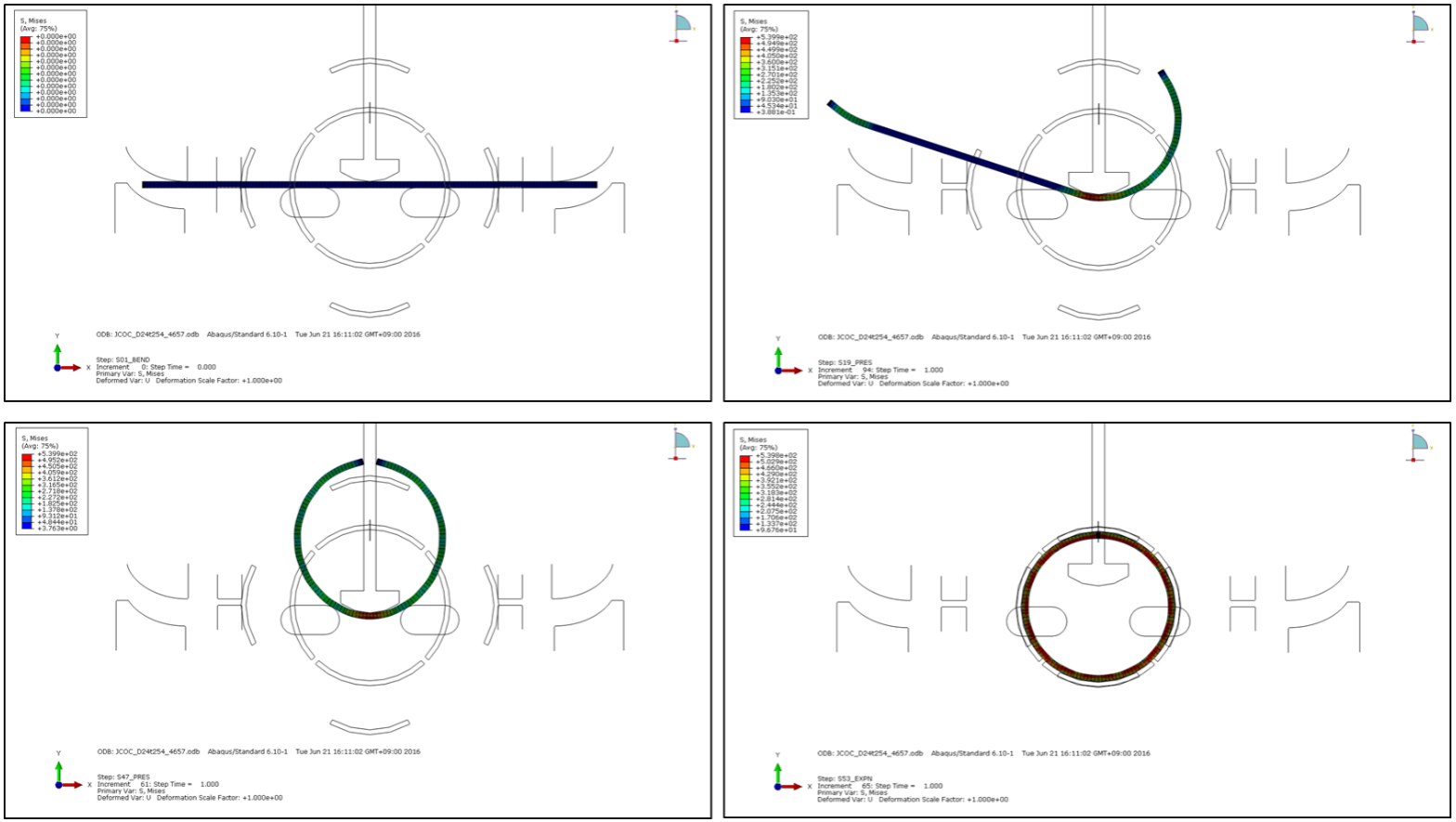

Figure 3.11 Finite element analysis on JCOC forming process

3.2.2 Calculation of Yield Strengths

As the most dominant factor for structural performance of the pipe, yield strengths should be predicted as following; 1) compressive yield strength in hoop direction for collapse capacity and 2) tensile yield strength in longitudinal direction for bending capacity. Also recalling that 3) tensile yield strength in hoop direction is an index of pipe quality in API specification, it is also required estimated at design stage.

First compressive yield strength in hoop direction should be predicted since it is used as an initial material property for the collapse analysis. Figure 3.12 (a) and (b) illustrate stress-strain histories of outside and inside layers of the 6 O'clock section of the pipe undergoing UOE process. Compressive yield strength of each fiber, $\boldsymbol{\sigma_{c,i}}$ $(\boldsymbol{i} = 1,2, \dots, n)$ is defined as the stress at the point where negative straining of 0.5% is applied additionally to current accumulated strain as shown in Figure 3.12. Here $\boldsymbol{i}$ is layer index where 1 indicates outermost layer and n is for innermost layer. Then compressive yield strength of the corresponding section can be regarded as an averaged value for whole layers as (Zhang *et al*, 2012):

$$\boldsymbol{YS_{compressive}} = \frac{\sum_{i=1}^{n} \boldsymbol{\sigma_{c,i}}}{\boldsymbol{n}} \qquad \textbf{(3.11)}$$

To acquire a range of compressive stress-strain curve to be embedded as an input in following collapse analysis, totally 2% of negative strain is applied further as illustrated with red lines in Figure 3.12.

Because the plate experiences different strain hysteresis along circumferential and longitudinal direction, yield strength shifting occurs independently to each direction. This is illustrated in Figure 3.13. Longitudinal tensile yield strength and stress-strain curve can be derived in the almost same manner except for loading direction. Since the element should be stretched in longitudinal direction after calibration stage (or welding stage in case of UO and JCO pipes), that is not feasible with current 2D model, another method is needed. In this particular study, a unit-cube finite element model is used. Material parameters including back-stress term and equivalent plastic strain from each element are brought to corresponding unit-cube as an initial condition. Naturally the plastic deformations from the forming process are maintained in this way. Then the cube is loaded under uniaxial tension in the direction parallel to the pipe axis. The way yield strength is defined and the stress-strain response is predicted are same as those for hoop compressive yield strength prediction.

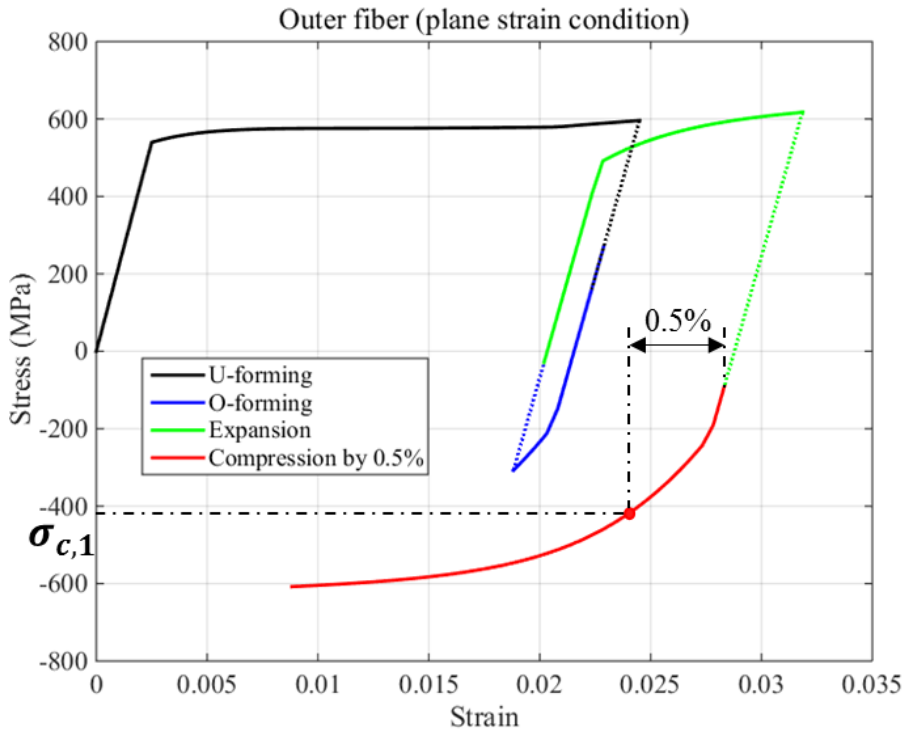
Outer fiber (plane strain condition)
Stress (MPa)
Strain
800
600
400
200
0
-200
-400
-600
-800
0
0.005
0.01
0.015
0.02
0.025
0.03
0.035
U-forming
O-forming
Expansion
Compression by 0.5%
0.5%
$\sigma_{c,1}$

(a)

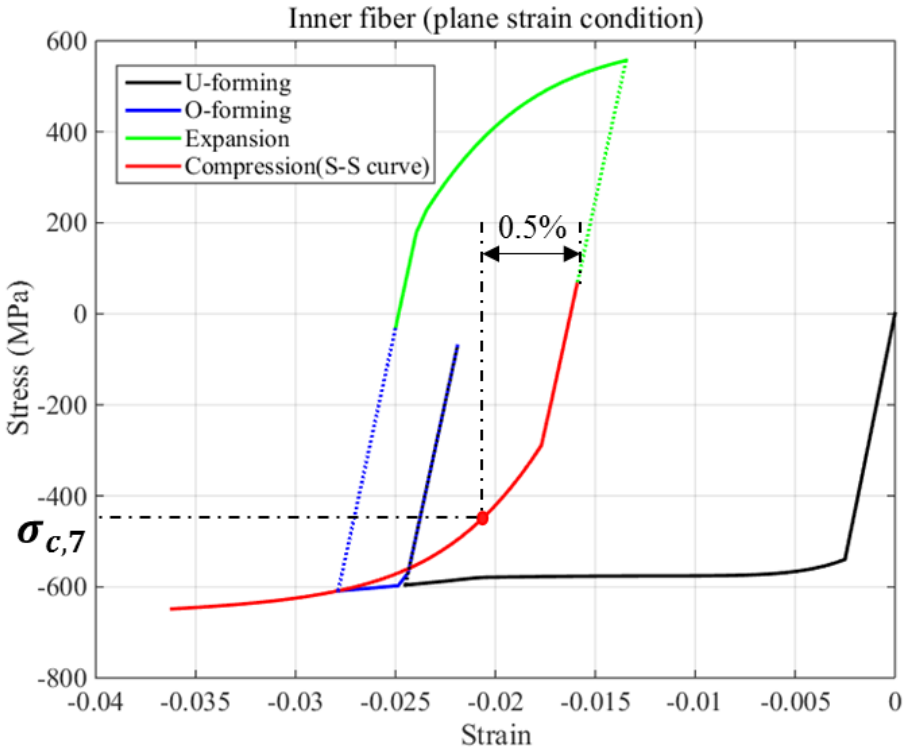

(b)

Figure 3.12 Stress-Strain history (a) Outer layer (b) Inner layer of the UOE pipe

(Dotted line indicates spring back response of same-colored forming)

(Ex : $\boldsymbol{D}$ = 30 in, $\boldsymbol{t}$ = 16 mm, expansion ratio = 1%)

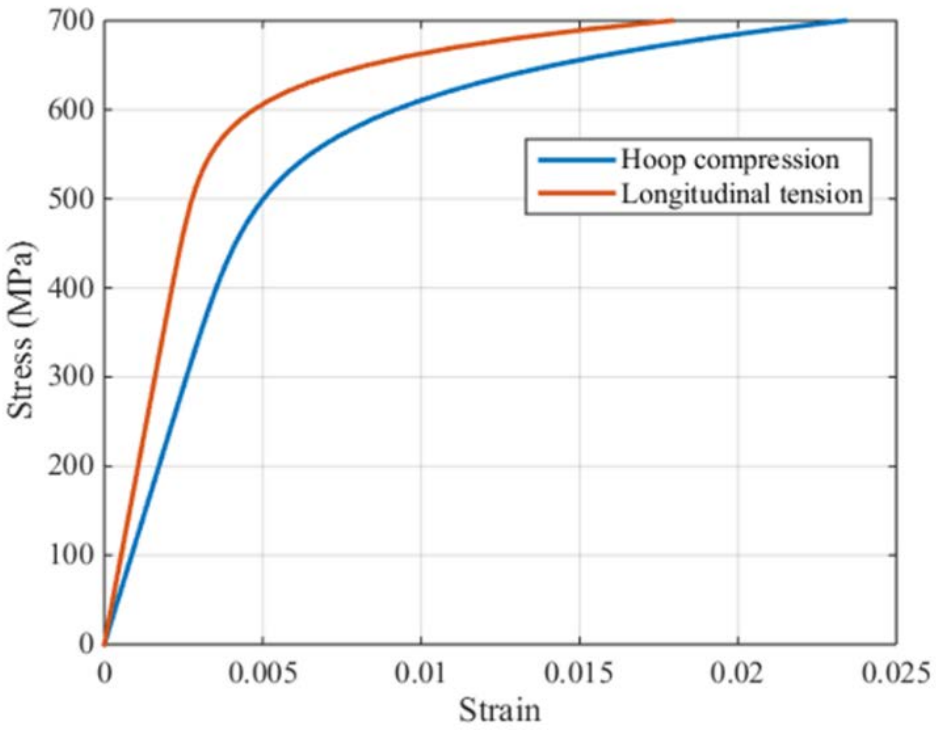

Figure 3.13 Comparison of stress-strain responses from UOE pipe

(Ex : $\boldsymbol{D}$ = 30 in, $\boldsymbol{t}$ = 22 mm, expansion ratio = 1%)

On the other hand, the yield strength of the manufactured pipe under tension is regarded as one of the most important characteristics required for quality control of industrial plant. According to API specification, specimen should be taken from the manufactured pipe to be tensioned after flattening. The location of the samples shall be a minimum of 90° from the weld to avoid heat affected zone which brings local improvement of strength. In practice, specimen is taken from 6 o'clock position since it has most complicated loading hysteresis. To represent realistic test condition, a specimen tension is also simulated after calibration stage as shown in Figure 3.14. Being extracted from the pipe, dummy step with no external loading is performed to relieve residual stress to zero. From this stage, whole boundary conditions are modified to express plane stress condition, not plane strain condition any more. After flattening and its spring back, the specimen is circumferentially tensioned by 0.5% strain. Consequently, tensile yield strength of the pipe for quality control can be calculated from final reaction force and cross sectional area of the specimen.

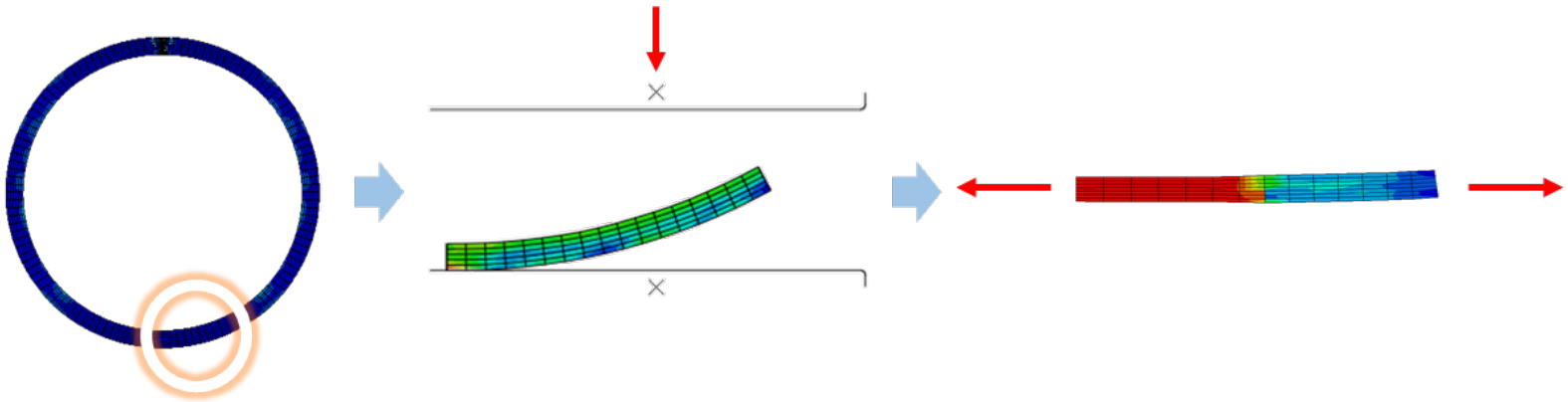

Figure 3.14 Flattening and tension test on specimen from the pipe for quality control

3.2.3 Results for Ovality and Residual Stress

Along with tensile yield strength in hoop direction, ovality of manufactured pipe would be assessed to guarantee moderate quality of the product. Ordinarily in practice, the cross sectional ovality is inspected to be less than 1% for offshore application. Numerical simulation on forming process enables to examine the radius variation along circumferential direction at interested forming stages as illustrated in Figure 3.15. These results are helpful in respect of ensuring production possibility and quality of the pipe. Unwanted severe misalignment of the skelp at O-forming or welding stage can be treated adequately with a reference to radius variation. Meanwhile, ovality before and after calibration operation is recorded that sufficient extent of calibration and other related design variables are obtained for satisfactory level of out-of-roundness.

Also, developed simulation program is equipped to survey on residual stress on pipe wall after the forming process. Figure 3.16 depicts how distribution and magnitude of the residual stress on pipe wall changes in accordance with expansion calibration. As it was expected, distribution of residual stresses along thickness direction turned to be linear with a gentle slope demonstrating considerable decrease in their magnitude after the calibration. So the forming simulation can be regarded as to be quite advantageous for determining extent of calibration and other related design variables.

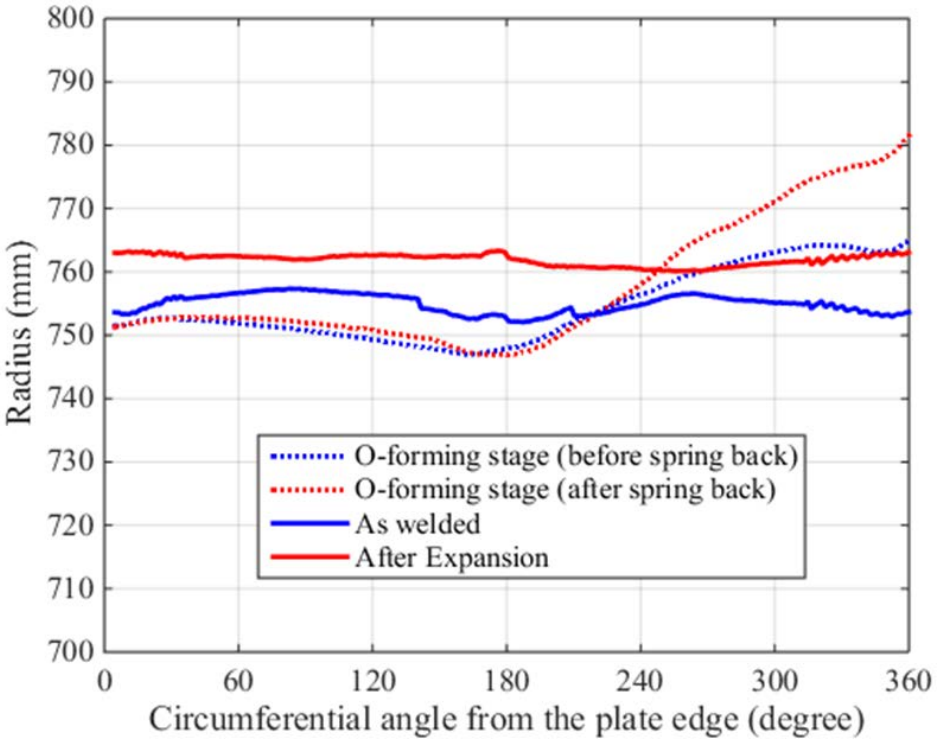

Figure 3.15 Radius variation of the UOE pipe at several forming stages

(Ex : $\boldsymbol{D}$ = 30 in, $\boldsymbol{t}$ = 22 mm, expansion ratio = 1%)

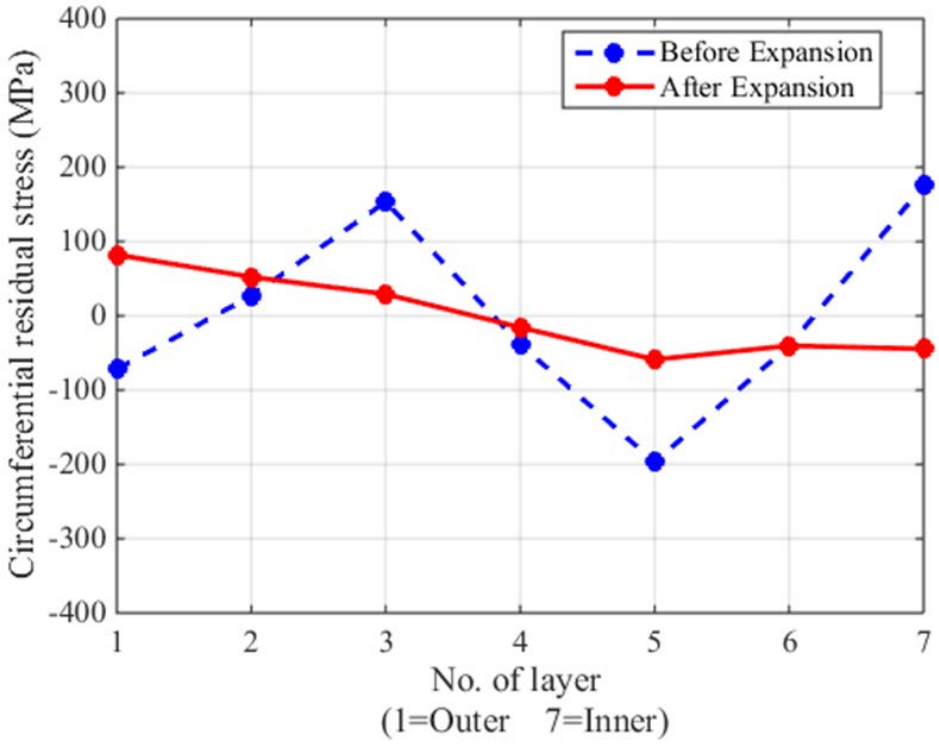

Figure 3.16 Residual stress distribution through thickness of UOE pipe

(Ex : $\boldsymbol{D}$ = 30 in, $\boldsymbol{t}$ = 22 mm, expansion ratio = 1%)

3.2.4 Experimental Verification of the Model

The UOE forming process with the specification listed in Table 3.5 is taken as an example to verify the forming simulation program. The design parameters used in the forming analysis are also listed in the table. Figure 3.17 shows each forming stages of the experiment and manufactured pipe sample. The geometric configuration of the skelp and demanding force on forming tool at each stage are computed to be compared with measured data. For the purpose of in-depth verification, pressing at O-forming stage was performed twice with step-by-step approach. After first O-forming pressing and spring back occurs, the O-shaped plate is pressed again 0.6 mm more than previous pressing to vertical direction.

U-shaped plate, O-shaped plate, as-welded pipe and expanded pipe are illustrated in Figure 3.18 to Figure 3.20 with their geometric parameters used for verification. And corresponding calculated results are compared with measured ones in Table 3.6 to Table 3.8. Results from numerical analysis seem to be pretty close to tested data with slight error. Though there appears relatively large error by percentage for O-forming gap, it can be regarded to be insignificant since the difference in absolute value is less than scalable unit, 1 mm.

Table 3.5 Specification of the X70 pipe and design parameters used for model verification

	Symbol	Description	Value
OD	OD	Target outer diameter (in)	30
Plate	t	Thickness (mm)	21.5
	W	Initial width (mm)	2318
	σ_o	Yield stress at 0.5% (MPa)	553
U-forming	R_{u1}	U-forming tool radius (mm)	288
	R_{u2}	U-forming tool small radius (mm)	144
	L_p	Pusher horizontal position (mm)	987
	TD_u	U-forming tool travel distance (mm)	850
	TD_p	Pusher travel distance (mm)	140
O-forming	R_o	O-forming tool radius (mm)	379.4
	D_c	Maximum distance between upper and lower O-forming tool (mm)	1st : 760 2nd : 759.4
Expansion	δ_e	Expansion ratio before spring back (mm)	0.0145
	R_e	Expansion tool outer radius (mm)	359.1
	Δr_e	Expansion value (mm)	5.2

Figure 3.17 Experimental test of the UOE pipe forming

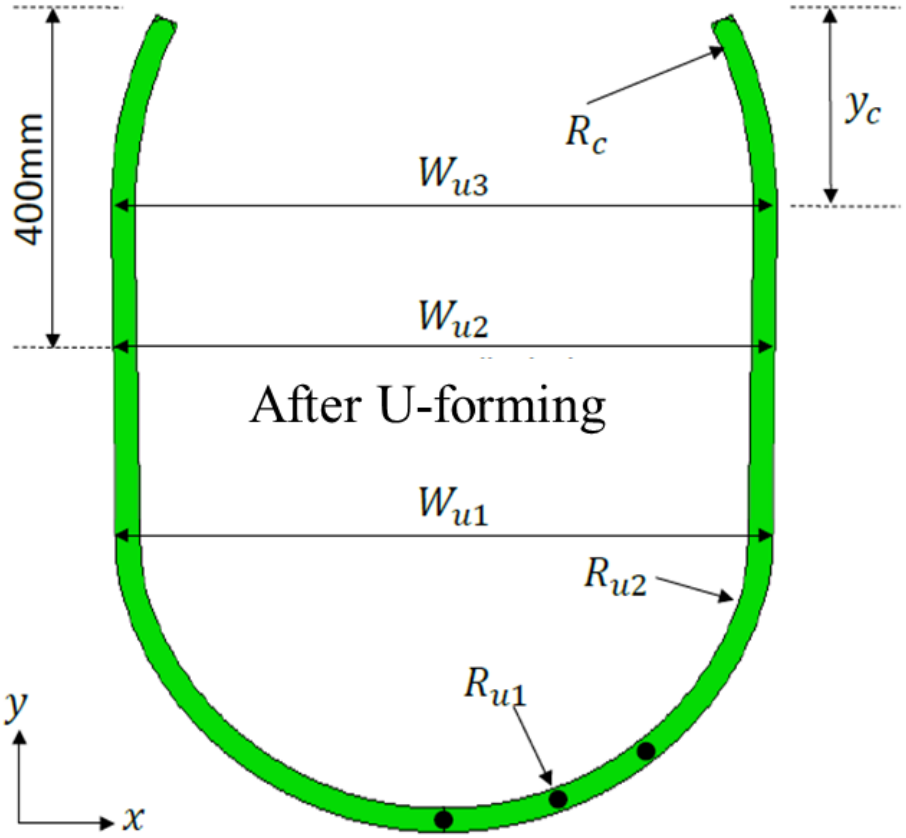

Figure 3.18 Geometric parameters of U-formed plate

Table 3.6 Calculated results and measured data for U-formed plate

(unit : mm)

	Experiment	**FEA**	**Error**
W_{u1}	700	709	1.3%
W_{u2}	693	696	0.4%
W_{u3}	683	685	0.3%
R_{u1}	340	340	0%
R_{u2}	274	266	2.9%
R_c	387	374	3.4%
y_c	243	244	0.4%

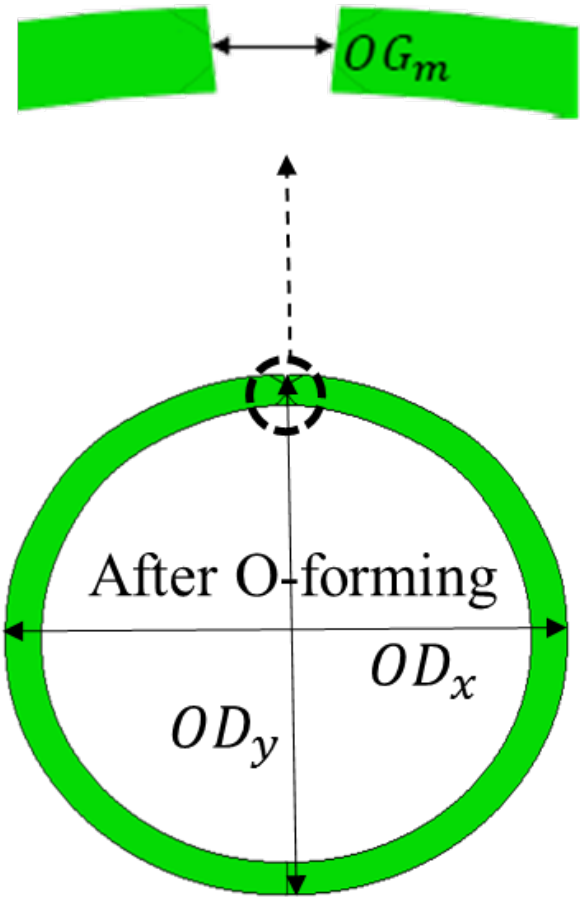

Figure 3.19 Geometric parameters of O-formed plate

Table 3.7 Calculated results and measured data for O-formed plate

(unit : mm)

		Experiment	**FEA**	**Error**
1st Pressing	OG_m	3	3.2	6.7%
	OD_x	758	760	0.3%
	OD_y	762	757	0.6%
2nd Pressing (1st + 0.6 mm)	OG_m	6.5	5.8	10.8%
	OD_x	761	764	0.4%
	OD_y	760	757	0.4%

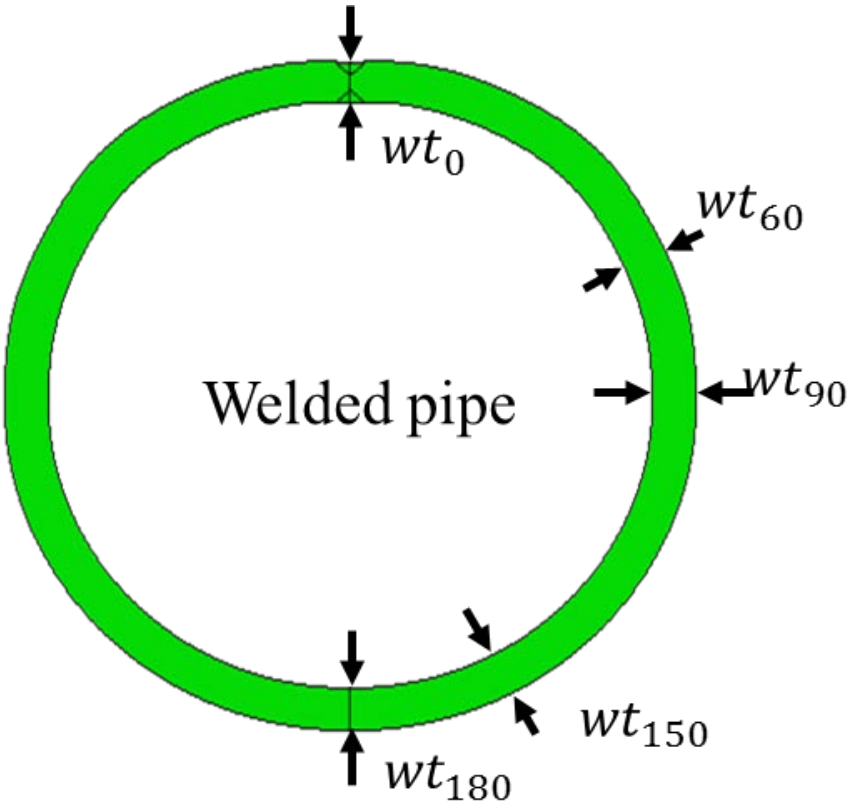

Figure 3.20 Geometric parameters of as-welded and expanded pipe

Table 3.8 Calculated results and measured data for as-welded and expanded pipes

(unit : mm)

		Experiment	**FEA**	**Error**
As-welded	wt_o	21.61	21.56	0.2%
	wt_{60}	21.64	21.66	0.1%
	wt_{90}	21.66	21.70	0.2%
	wt_{150}	21.61	21.61	0.0%
	wt_{180}	21.60	21.60	0.0%
Expanded (0.8%)	wt_o	21.48	21.22	1.2%
	wt_{60}	21.52	21.42	0.5%
	wt_{90}	21.52	21.44	0.4%
	wt_{150}	21.62	21.33	1.3%
	wt_{180}	21.60	21.40	0.9%

After the UOE pipe manufacturing, a testing specimen is cut from the pipe for model verification in terms of yield strength prediction as shown in Figure 3.21. The dimension of the specimen and specific cutting procedure comply with API specification to avoid an aging effect from welding heat. Uniaxial tension test on the specimen was carried out to obtain the stress-strain curve illustrated in Figure 3.22. The calculated result is comparable with the measured data with such a small difference, which indicates the current approach can be utilized for the prediction of yield strength of the pipe. On the basis of comparison between the experimental results and corresponding result from numerical analysis as listed in Table 3.9, it is found that developed model gives an excellent accuracy for the forming process simulation referring to prediction on geometrical configuration of the plate and tensile yield strength in hoop direction.

Figure 3.21 Cutting and flattening of the specimen for the tension test

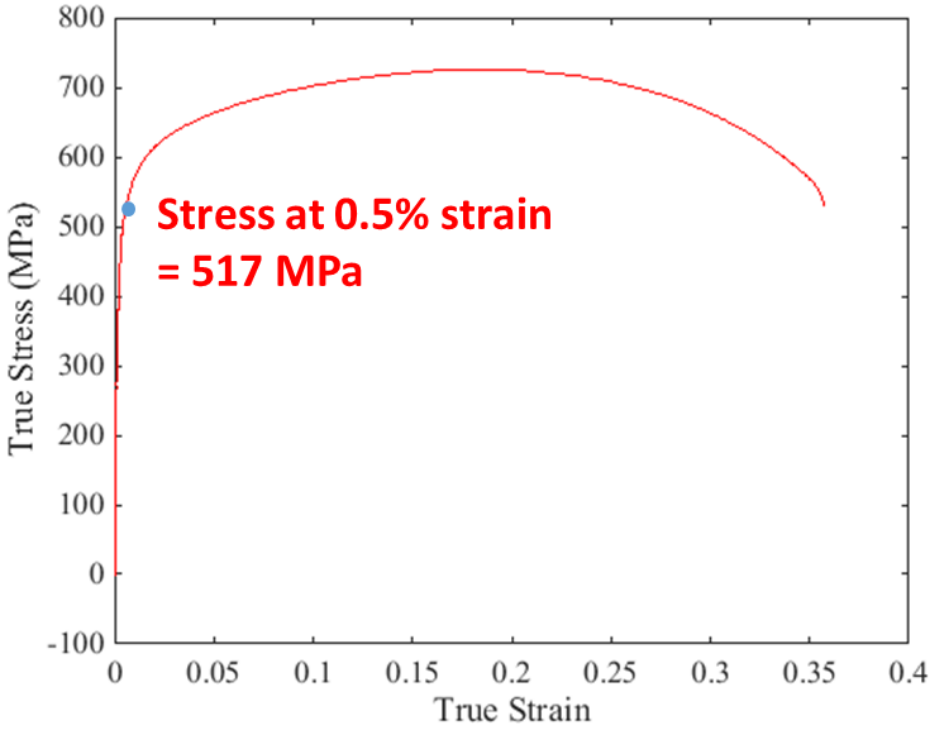

Figure 3.22 Stress-strain response of specimen under uniaxial tension test

Table 3.9 Predicted yield strength in hoop direction of the pipe

(unit : MPa)

Layer	1st	2nd	3rd	4th	5th	6th	7th	Avg.
YS	412.2	417.4	434.4	550.5	574.2	587.2	592.7	**513.9**

3.3 Prediction of Structural Performance of the Pipe

3.3.1 Collapse and Bending of the Steel Pipes

Collapse phenomena of the pipe have been the subject of a great deal from the 1980's up to now. According to a design code for offshore pipeline (DNV-OS-F101), collapse is a kind of local buckling in which gross deformation of the cross section confined to a short length of the pipe occurs. When the local buckling is triggered only by external over pressure, corresponding limit state is defined as *collapse*. Collapse of the pipe can be treated as a local buckling behavior of column structure as they show similar phase on load-displacement curve. An ideally straight column loaded within elastic regions carries axial compression with its axial stiffness. Reaching at certain critical load over stable condition, a straight column would be bent to be structurally useless, i.e. it becomes to be with little stiffness. The load that makes this abrupt switch is defined as a *critical buckling load*. This point on load-displacement curve is called *bifurcation* as two solutions become possible at this critical point; straight line extending initial elastic curve and curved line that represents reduced stiffness. Practical column, however, cannot help having moderate geometric imperfection from the early stage. In this case, the response curve does not show bifurcation. Instead, the column will be bent with buckling mode shape while progressively approaching the critical buckling load. As applied load gets closer to critical load, the column undergoes larger reduction in its stiffness and finally meets structural failure. Material nonlinearity can make this reducing effect more catastrophic and complicated when the material yields with a large strain.

Externally pressurized pipe experiences similar aspect structurally with above column case. The response of the API X70 (Yield strength = 521 MPa) pipe under external pressure is shown in Figure 3.23, where P and P_0 are uniform external pressure and yield pressure, respectively. Horizontal axis indicates the maximum radial deflection (w_{max}) of the pipe normalized by outer radius. Pipe with a diameter to thickness ratio ($\boldsymbol{D/t}$) of 20 was considered, which has relatively thick wall for deep water pipeline since it requires high strength against internal and external pressure. It should be noted that the response differs depending on geometry and material property of the pipe.

At a certain critical pressure followed by linearly increasing pressure, perfect pipe bifurcates into a fundamental buckling mode of uniform-ovality shape. Buckling usually takes place in plastic region beyond elastic limit for this kind of thick-walled pipe, so that it referred to as plastic buckling. Through a bifurcation point, the pressure increases monotonically to maximum value, P_{co} also defined as a *collapse pressure*. When the load reaches P_{co} beyond elastic region, the stress distribution of cross section of the pipe can be illustrated as Figure 3.24. After reaching the *collapse pressure*, the response follows decreasing trajectory as collapse gets localized. In other words, the pipe becomes useless structurally over *collapse pressure*.

Result for imperfect pipe is also involved in the Figure 3.23 with a solid line. As a most detrimental imperfection to external pressure, realistic ovality for UOE pipe (= 0.1%) was adopted. Its curve gets closer to that of perfect one from below. In the same manner, a maximum value was derived beyond the initial elastic region.

Pipe subjected to a bending moment also has a risk of failure by local buckling as well as fracture. Being distinct from the beam theory, the actual response of the pipe induces ovalization of the cross section. As grown with further bending, ovalization causes a progressive reduction in bending rigidity. Actually in that case, a pipe experiences analogous behavior to that of collapse failure above. Figure 3.25 illustrates moment-curvature relationship of the pipe subjected to pure bending keeping pressure and axial force constant. Initially the pipe shows almost linear behavior within the elastic range of material with global deformation. According to DNV-OS-F101, such a global deformation literally indicates a deformation formed uniformly over a range larger than 3 to 4 times the diameter of the pipe. After reaching the linear limit, bending stiffness of the pipe decreases but it still accompanies with global deformation. Further increase in loading can initiate the onset of local buckling (ovalization) due to material nonlinearity and geometric imperfection. Clearly the linear behavior is sustained longer leading late onset of local buckling as $\boldsymbol{D/t}$ ratio goes lower. For continuously increasing loading, the pipe absorbs more and more bending energy till the external moment is equal to bending capacity where the pipe cannot support any more bending. Right after this limit point, catastrophic capacity reduction starts with large deflection of pipe wall like as collapse by external pressure. Thus, this moment maximum can be defined to be the limit state of the pipe structure.

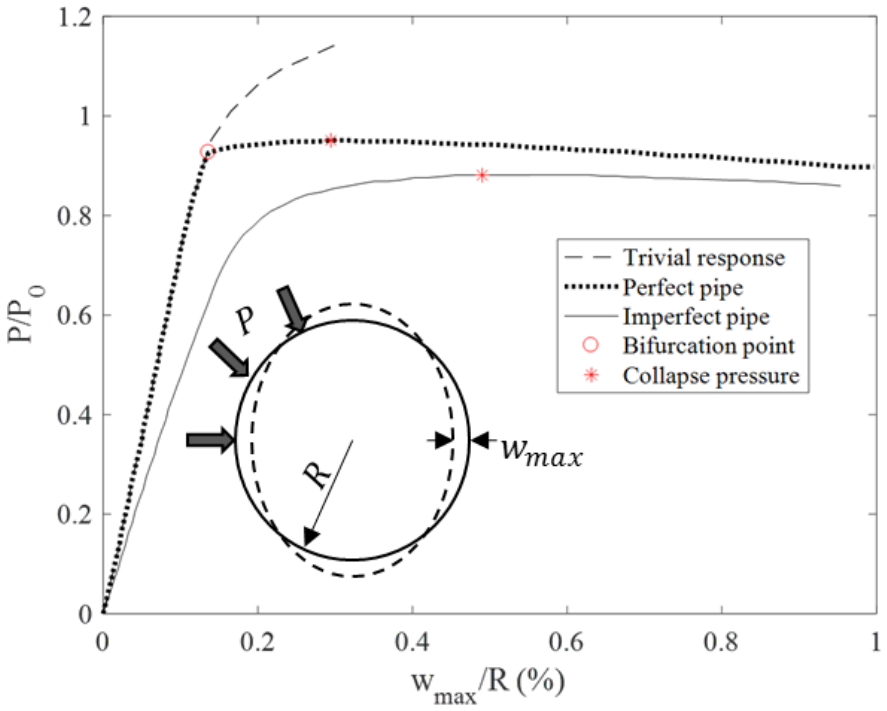

Figure 3.23 Nonlinear external pressure-maximum displacement response of the pipe

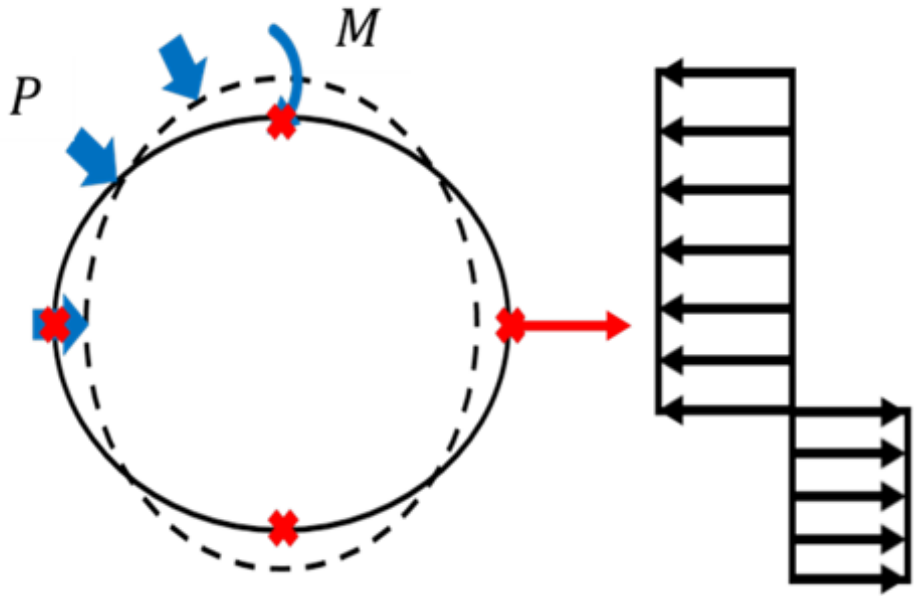

Figure 3.24 Stress distribution of cross section of the pipe which plastically collapses under external pressure

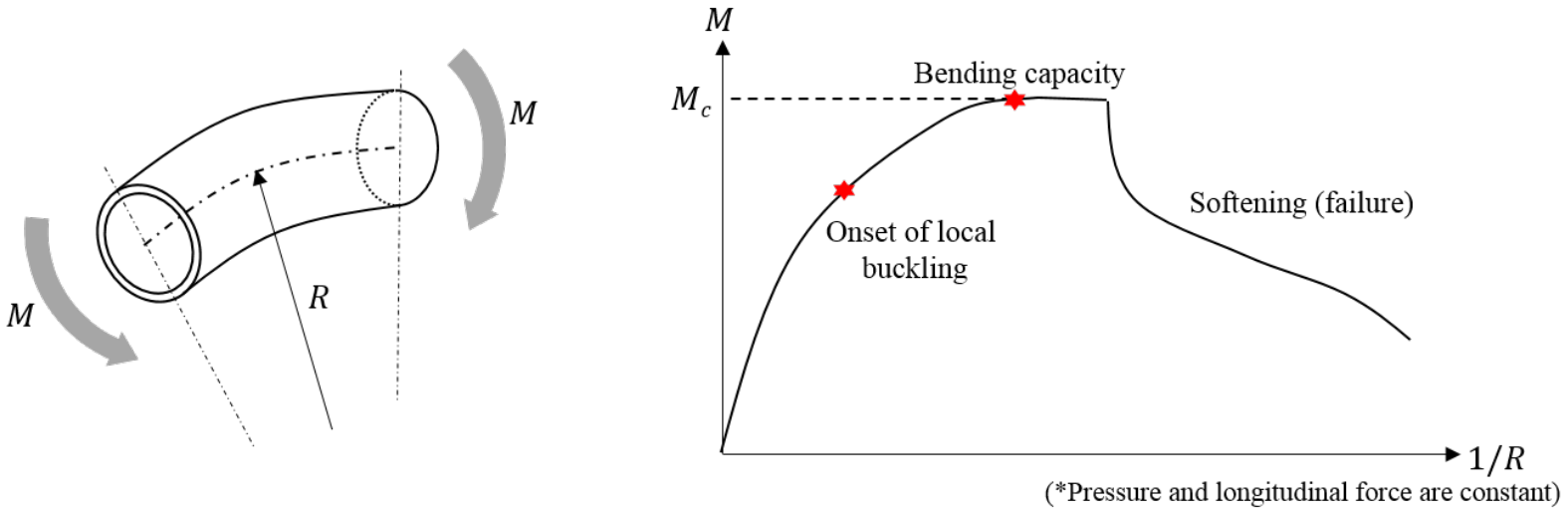

Figure 3.25 Nonlinear bending moment-curvature response of the pipe

3.3.2 Details of Finite Element Modeling

With the results from the developed pipe forming simulation program, structural performance of the formed pipes is assessed in this thesis. Apart from the 2D model aforementioned, refined 3-dimensional finite element analysis was conducted for representing the realistic behavior of the pipe. Here the model developed and analytically verified by Jin (2016) was used. The offshore steel pipe is modelled by half, i.e. the longitudinal symmetric boundary condition is applied at one end. In Figure 3.26, a dotted axis indicates fixed degree of freedom (DOF) while a solid axis means the free DOF. The 8-noded brick element with reduced integral (C3D8R) is used for the analysis as that typical element is fully capable of describing limit state due to ovalization. Each node has six DOFs and it is commonly used for large deformation analysis. Mesh sensitivity study was carried out and showed that 7 elements through thickness and 90 elements along circumferential direction are sufficient to ensure accuracy of the results.

Stress-strain responses to hoop compressive direction derived in Section 3.2.2 is implanted to whole element for collapse analysis, because monotonic compressive behavior is regarded to be dominant for collapse pressure calculation. Likewise, previously acquired material property in longitudinal direction was applied for bending analysis. To represent smoothly curved stress-strain response of the pipe, the Ramberg-Osgood model is determined to be adequate for material model. The model is configured as:

$$\varepsilon = \frac{\sigma}{E}[1 + \alpha\left(\frac{\sigma}{\sigma_o}\right)^{n-1}] \quad \textbf{(3.12)}$$

where ε, σ and E are strain, stress and Young's modulus and σ_o is the yield strength of the material. α and n are hardening parameters. Following the procedure presented in Section 3.2.2, acquired material curve is fitted with least square error method to find unknown parameters.

The ovality of manufactured pipe is mapped to 3D model to configure the cross section of one end where symmetric boundary condition is applied. (Right end in Figure 3.26) The cross sectional shape of the other end is assumed to be perfect circle so that collapse occurs only limited range near free end. Ovalities within the medium region were calculated by linear interpolation from the cross sectional shapes specified at the boundaries. Residual stress in hoop direction is directly mapped from pipe forming simulation without the variance in longitudinal direction.

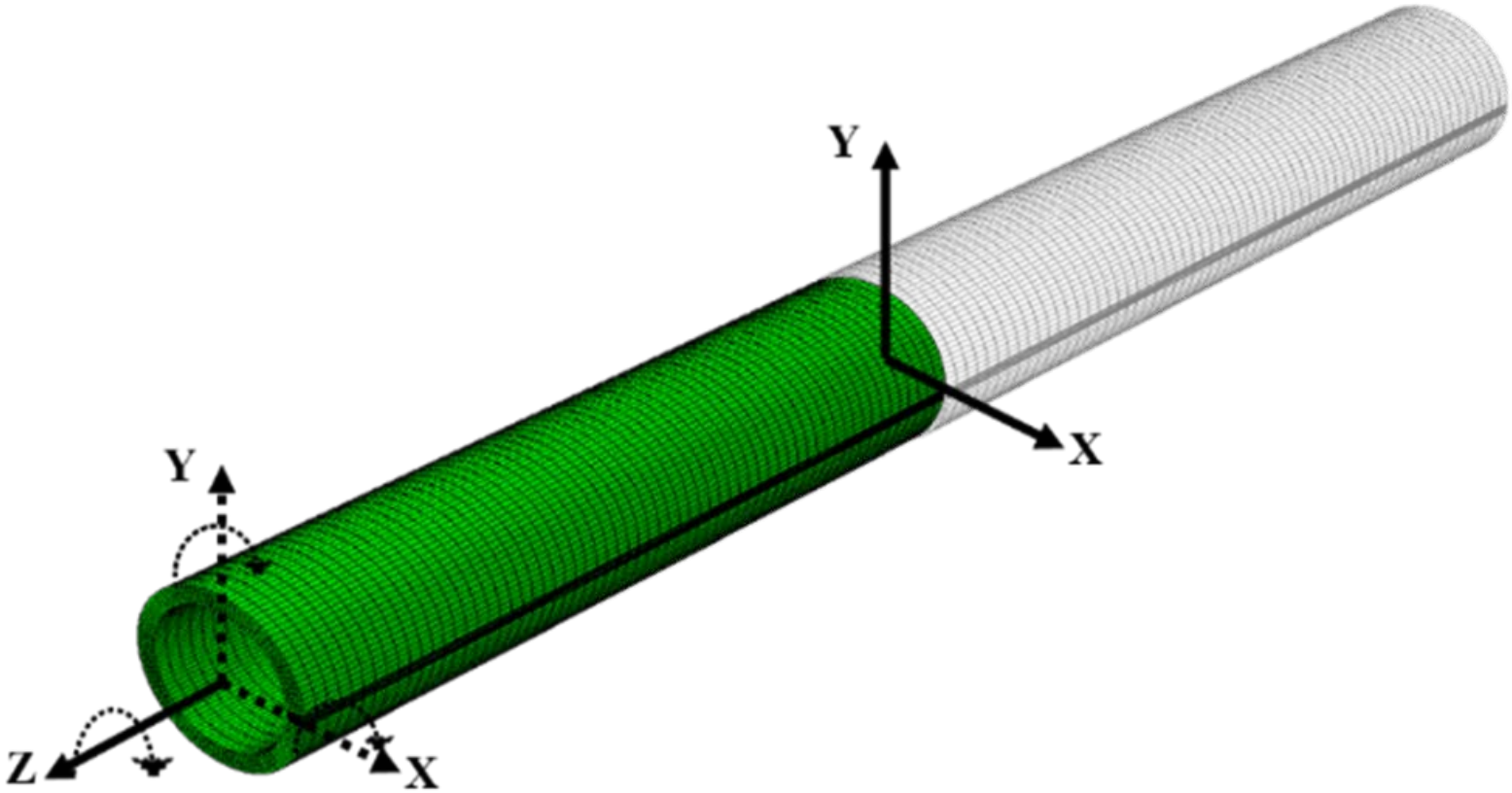

Figure 3.26 3D Finite element model of the pipe

3.3.3 Calculation of the Structural Performance

Collapse pressure of the pipe model under external pressure is calculated by the modified Riks method, which is common tool for the problems with severe nonlinearity. It was chosen considering that tangent stiffness changes sign and load magnitudes are governed by a single scalar parameter; uniform external pressure and pure bending. It finds a solution at an intersection point from an equilibrium curve and given arc-length as geometrically interpreted in Figure 3.27. Therefore it is generally used to predict unstable, geometrically nonlinear collapse of a structure. Figure 3.28 shows loading condition applied for collapse analysis of the pipe and consequent deformed shape. It uses load control method by increasing uniform external pressure. Figure 3.29 depicts the result for Riks analysis on the pipe under uniform external pressure. Horizontal axis indicates the displacement of the model pipe's zenith relative to its nadir. When the curve reaches maximum, corresponding pressure is defined as a collapse pressure of the pipe.

Bending capacity is assessed under pure moment loading. Applied loading condition and deformed configuration are shown in Figure 3.30. The cross sectional planes of the both pipe ends were constrained to remain plane during the analysis. Bending is applied by rotational displacement control of the reference node of pipe end. Figure 3.31 illustrates the response of pipe under pure bending. Red triangle mark on the moment-rotational angle response is the limit moment and the onset of local buckling failure. In this thesis, the point is defined as the status at which bending capacity is valued.

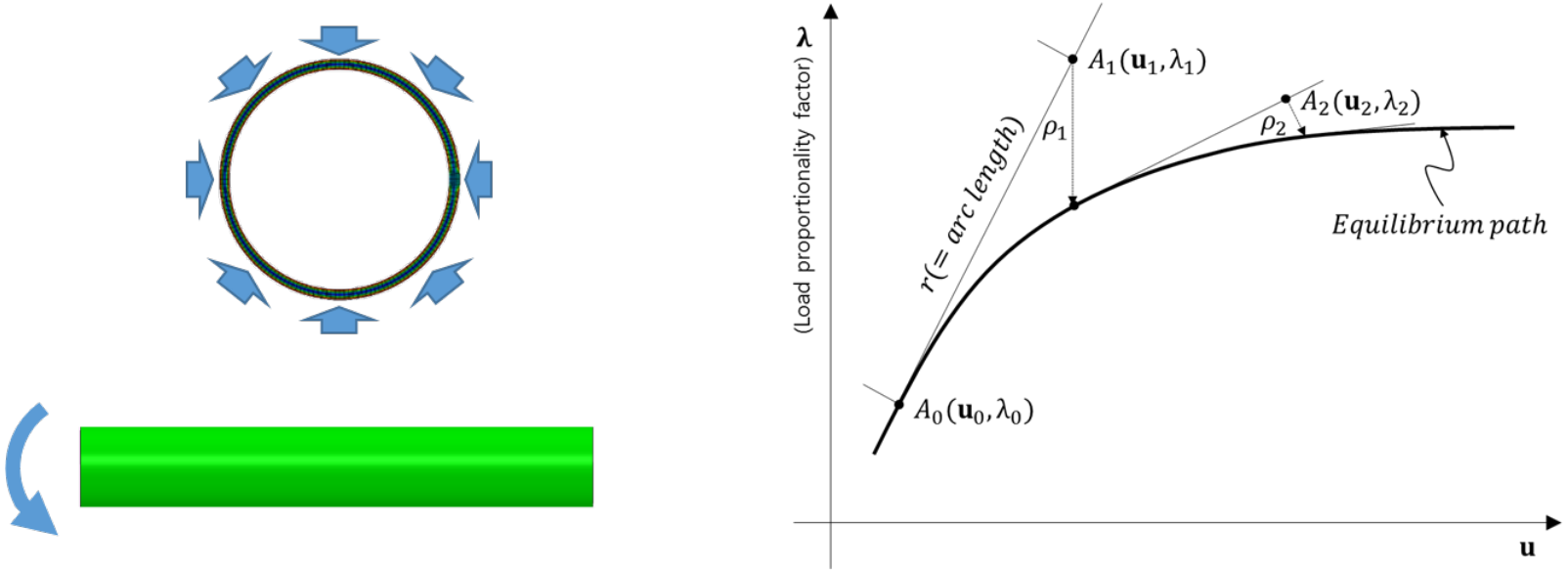

Figure 3.27 External loads with a single scalar of the problem (Left) and geometric interpretation of modified Riks method (Right)

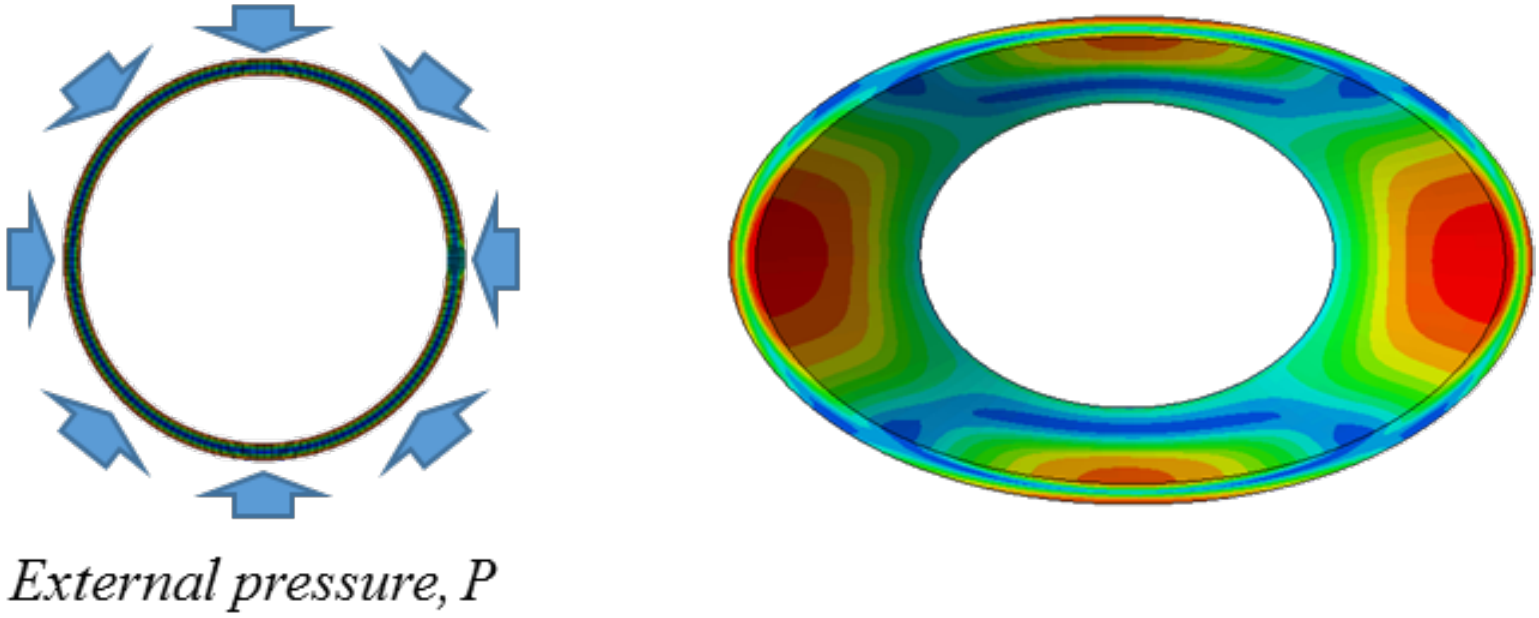

Figure 3.28 Loading condition and deformed shape of pipe collapse analysis

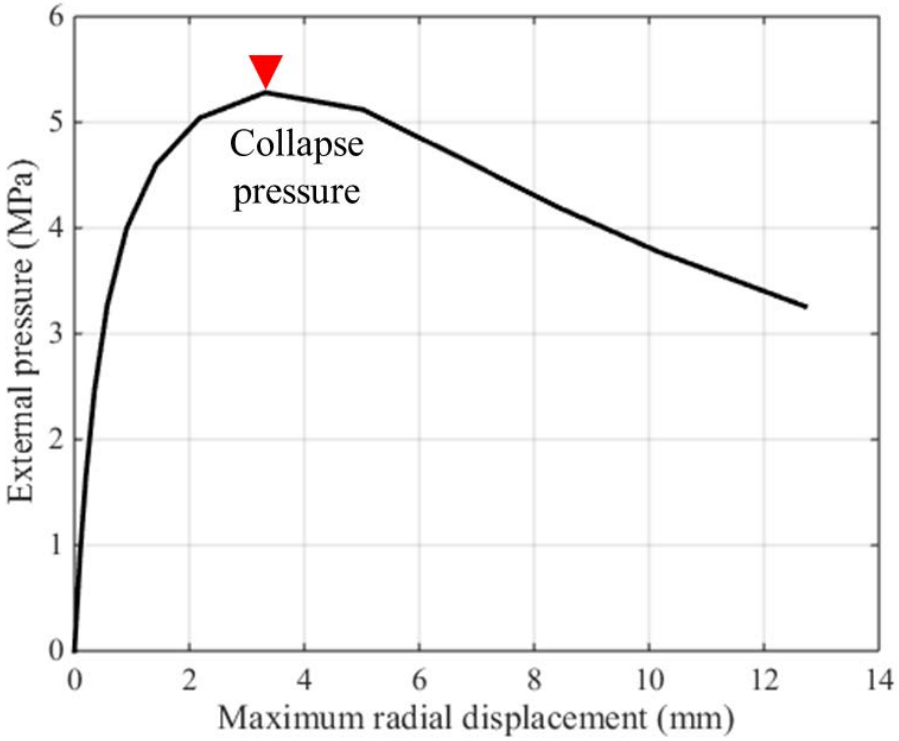

Figure 3.29 Result for Riks analysis on externally pressurized pipe

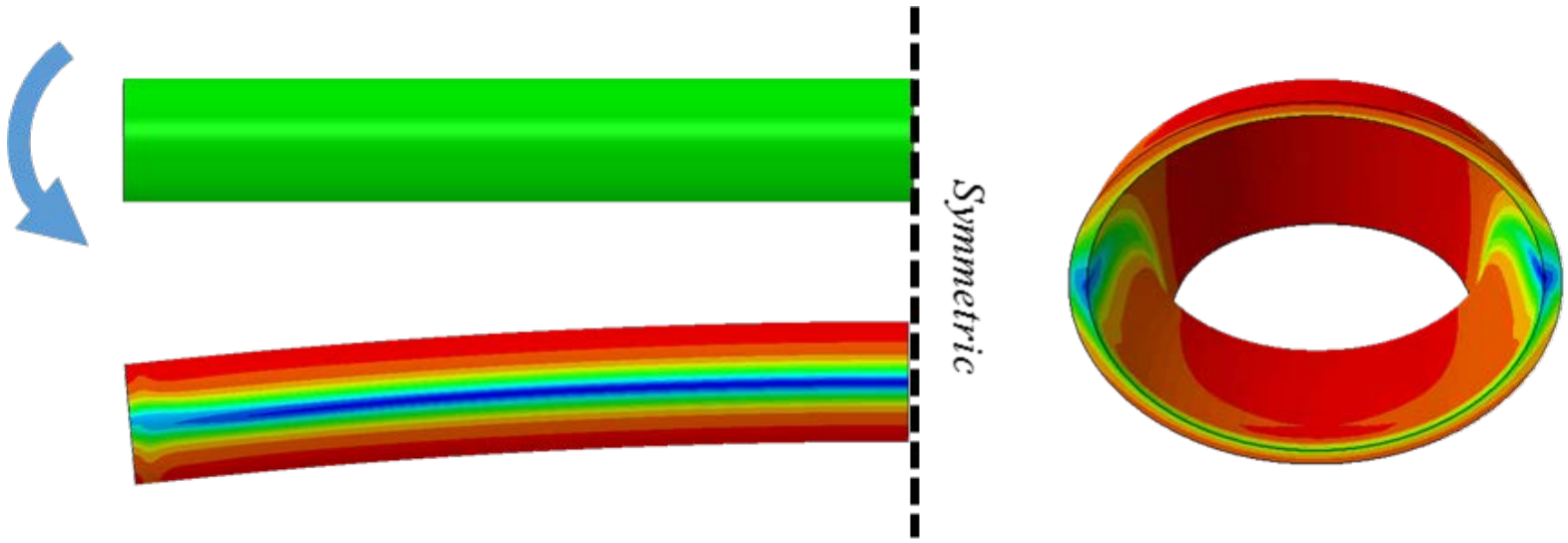

Figure 3.30 Loading condition and deformed shape of bending analysis

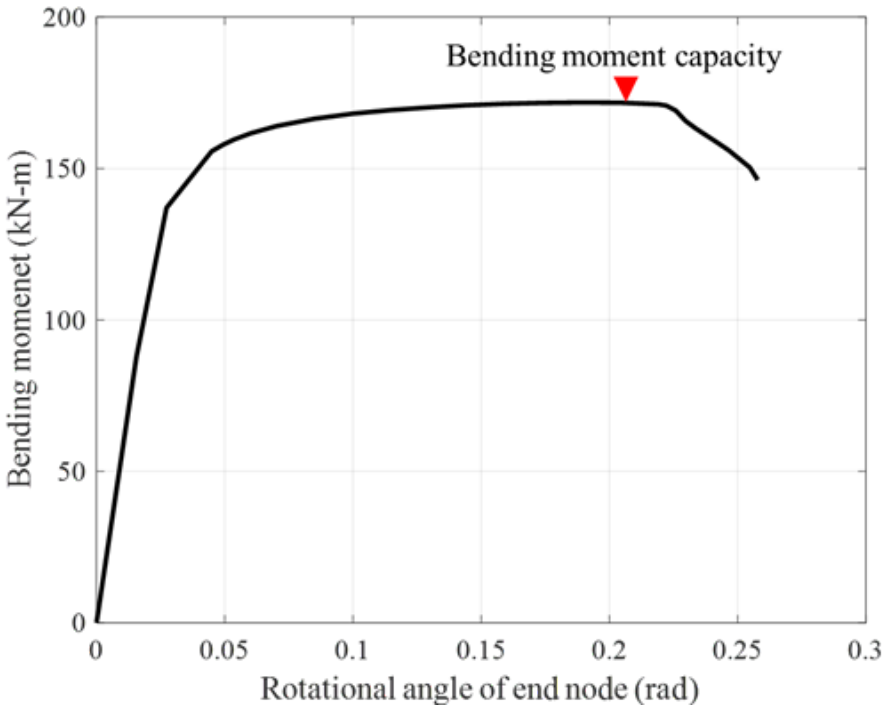

Figure 3.31 Response of the pipe under pure bending

3.3.4 Verification of the Model

Numerical model for structural analysis of steel pipe also requires experimental verification as simulation model did. However, corresponding experiments are with large scale and need complex equipment, which leads to the high cost. Thus the model was verified through comparison with various experimental results performed by previous researchers. Considering the practical use of offshore steel pipes in selecting cases, scrutinized attention was paid to ensure that the

verification model had sufficient representation.

First, five experiments conducted by Kyriakides and Corona (2007) were referred to verify the model for collapse analysis. The diameter-thickness ratio, ovality, and yield strength of the material of each case are summarized in the Table 3.10. Based on the given data, we introduced a material model using the Ramberg-Osgood model as in the original text. Roundness was assumed to be a full elliptical shape. Experimental measurements and analysis results of collapse pressure for all cases are also listed in the Table. The verification results are shown in Figure 3.32. Despite the insufficiency of the simulations of the experimental conditions, the overall accuracy is less than 10%, and the developed model is believed to be reliable.

In order to verify the bending analysis model, this thesis refers to the results of bending tests on six steel pipes performed by DNV (1993). The moment capacity of 6 mild steel pipes under pure bending were measured in the report. Diameter and yield strength, which are the dominant factors of bending strength as well as diameter-to-thickness ratio, are summarized in Table 3.11. As adopted for the verification of the collapse analysis model, the material model using the Ramberg-osgood model was introduced here. As a result of comparing the experimental data with the calculation results, high accuracy was confirmed as shown in Figure 3.33.

Table 3.10 Geometric and material parameters of the pipes used for model verifications of collapse analysis

Case no.	D/t	Ovality (%)	Yield Strength (MPa)	P_c (MPa)	
				Test	FEA
1	17.75	0.37	414.37	43.5	44.1
2	17.92	0.34	477.46	46.0	47.4
3	17.64	0.22	375.76	39.0	41.6
4	17.79	0.59	421.61	41.5	43.4
5	16	0.4	435.75	49.3	53.7

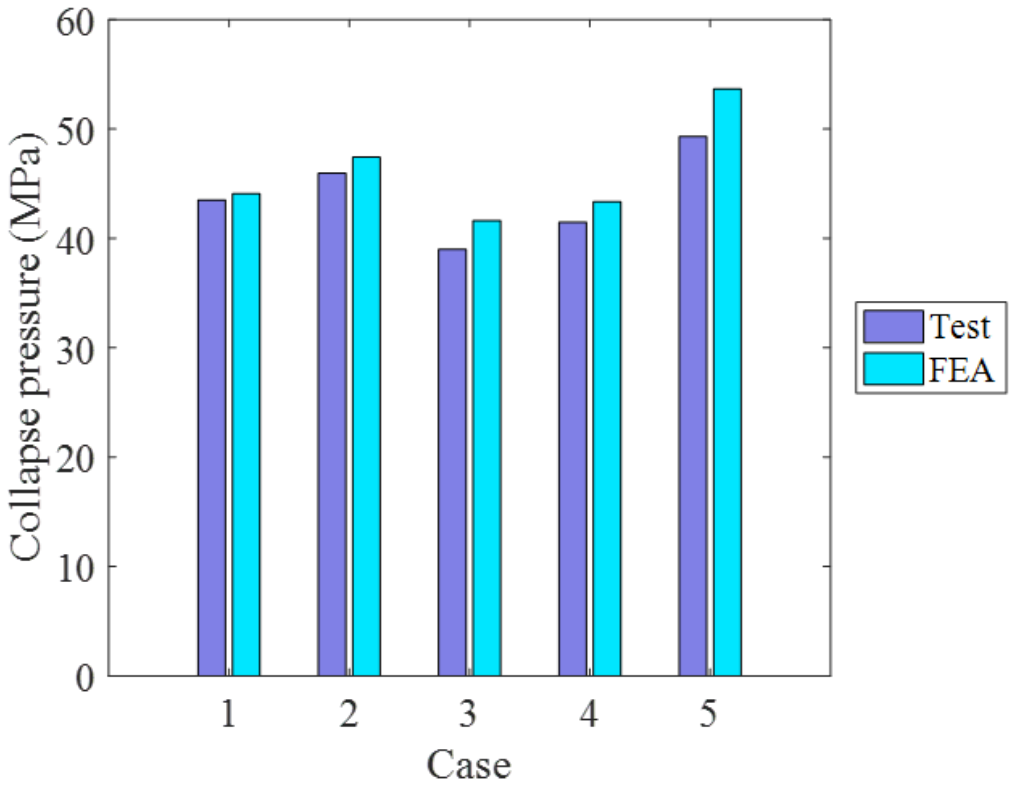

Figure 3.32 Comparison of predicted and measured collapse pressure for selected cases

Table 3.11 Geometric and material parameters of the pipes used for model verifications of bending analysis

Case no.	D/t	Ovality (%)	Yield Strength (MPa)	P_c (MPa)	
				Test	FEA
1	17.3	273	241	300.4	283
2	29.7	273	290	222.5	218
3	34.1	273	290	166.1	172
4	34.2	168	290	41.6	39.9
5	27.9	114	207	11.5	10.8
6	33	100	290	9.1	9.4

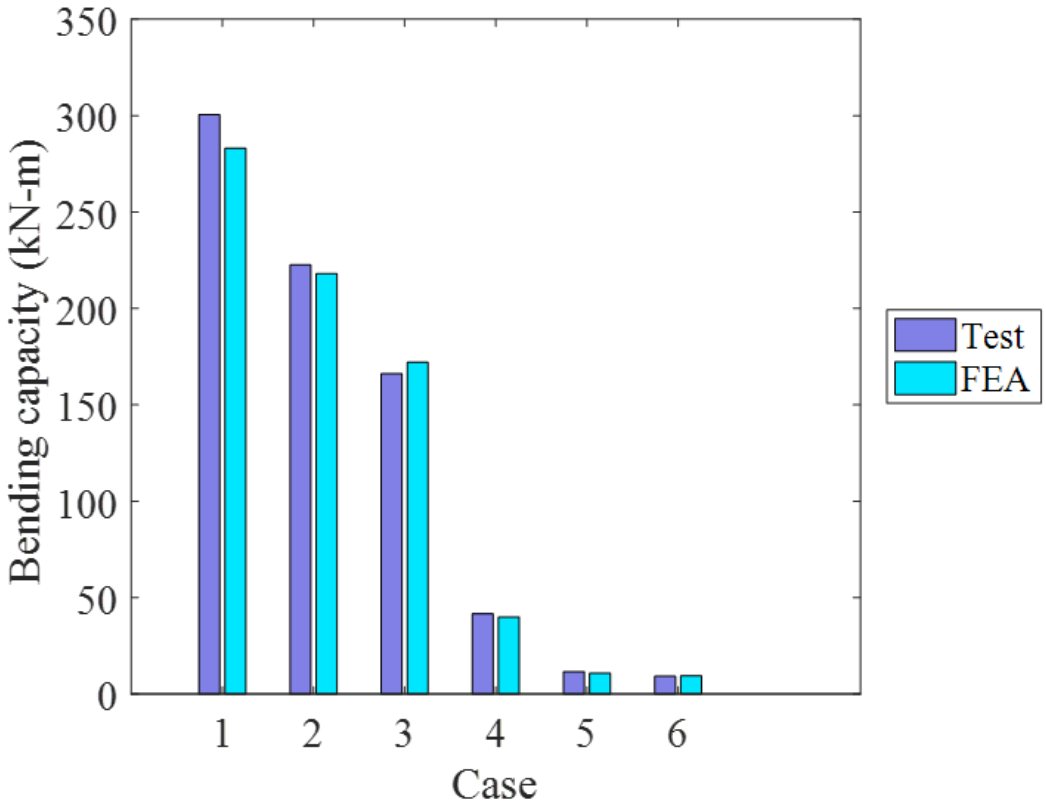

Figure 3.33 Comparison of predicted and measured bending capacity for selected cases

4 Investigation of the Influence of Design Variables through Parametric Study

4.1 Key Parameter Selection

In an attempt to quantify the effects of key design variables on yield strength and structural performances, parametric study is performed. As mentioned before, diameter, thickness, expansion ratio and compression ratio are highly influential factors among all the relevant design variables. Therefore they are varied individually as listed in Table 4.1, adjusting all other related parameters using automated input generation program developed in this study. Expansion ratio and compression ratio are defined as the relative change of the outer diameters before and after the calibration. They can be regarded to be equal to the circumferential strain increasing and decreasing, respectively. Values for diameter and thickness are selected embracing current practical usage and additional challenging scales for overall comprehension. Expansion ratio and compression ratio, which are defined as Eq. (4.1) and Figure 4.1, are also varied discretely within a range of values that is considered to be practical for offshore application. An example problem for design optimization of UOE pipe will be presented thereafter, in reference to results and findings on the parametric study.

$$\boldsymbol{\delta_e = \Delta r_e / R_e \times 100} \qquad \textbf{(4.1)}$$

Table 4.1 Selection of parameters and their values

	Values
Diameter ($\boldsymbol{D}$) (inch)	20, 24, 30, 32, 36, 40, 42, 48
Thickness ($\boldsymbol{t}$) (inch)	0.5, 0.625, 0.75, 0.875, 1, 1.25
Expansion ratio ($\boldsymbol{\delta_e}$) (%)	0, 0.25, 0.5, 0.75, 1, 1.25
Compression ratio ($\boldsymbol{\delta_c}$) (%)	0, 0.25, 0.5, 0.75, 1

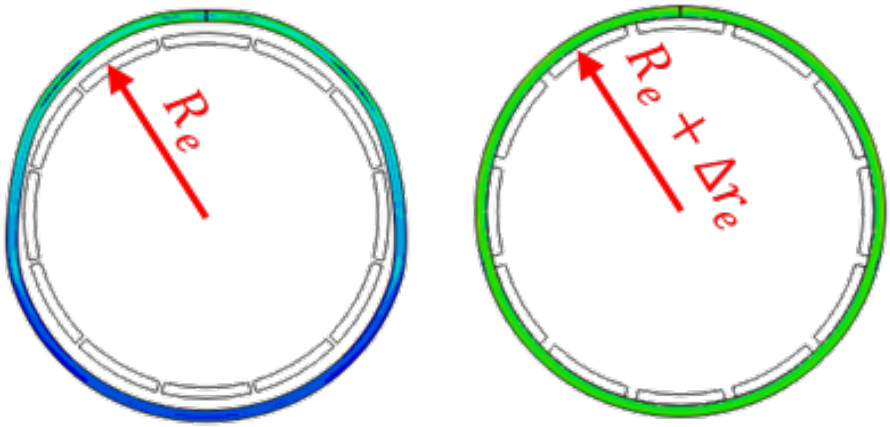

Figure 4.1 Geometric parameters used to define expansion ratio

4.2 Influence on the Yield Strengths

4.2.1 Compressive Yield Strength in hoop direction for Collapse analysis

As a most influential factor of collapse pressure, compressive yield strength in hoop direction was predicted firstly. The changes of yield strength with respect to $\boldsymbol{D/t}$ ratio and expansion ratio for UOE and JCOE pipes are illustrated in Figure 4.2 and Figure 4.3, respectively. Yield strength of virgin material (= 521 MPa) is depicted as a dotted line. It can be seen from the Figure 4.2 that the yield strength of the as-welded UO pipe is similar to or less than that of raw plate. In Figure 4.3, as-welded JCO pipe experiences reduction in yield strength for all $\boldsymbol{D/t}$ ratios, which is contrary to UO pipe. Because there is no circumferential compression in JCO forming, nothing can counterbalance a reduced compressive yield strength at punching forming stage. On the other hand, even though a compression ratio at O-forming stage is small, it can compensate the yield strength reduction of UO pipes.

Generally, large $\boldsymbol{D/t}$ ratio leads to greater decrease in yield strength due to stronger Bauschinger effect of thinner pipes. For all $\boldsymbol{D/t}$ ratio of UOE and JCOE pipes, the yield strength of the pipes drops significantly only with a little expansion of 0.25%. And the yield strength decreases with the increasing expansion ratio. The reason of these phenomena is that the circumferential tension dropped the yield strength in opposite (compressive) direction owing to Bauschinger effect. The maximum reductions of the yield strength due to expansion calibration are about 18% for UOE pipe and 15% for JCOE pipe.

The benefits of replacing the expansion calibration with compressive one can be found from Figure 4.4 and Figure 4.5. The figures show the effect of compression calibration on compressive yield strength with regard to UOC and JCOC pipes. Pipe compression definitely increases the compressive yield strength in hoop direction for all $\boldsymbol{D/t}$. The stronger compression is applied, the higher compressive yield strength is calculated. The largest increasing gap is more dramatic for JCOC pipe than UOC pipe. The compressive yield strength of UOC pipe is increased by only 8%, while that of JCOC pipe is increased by 12%. Their contribution for enhancing collapse pressure of the pipe will be presented in Section 4.3.1.

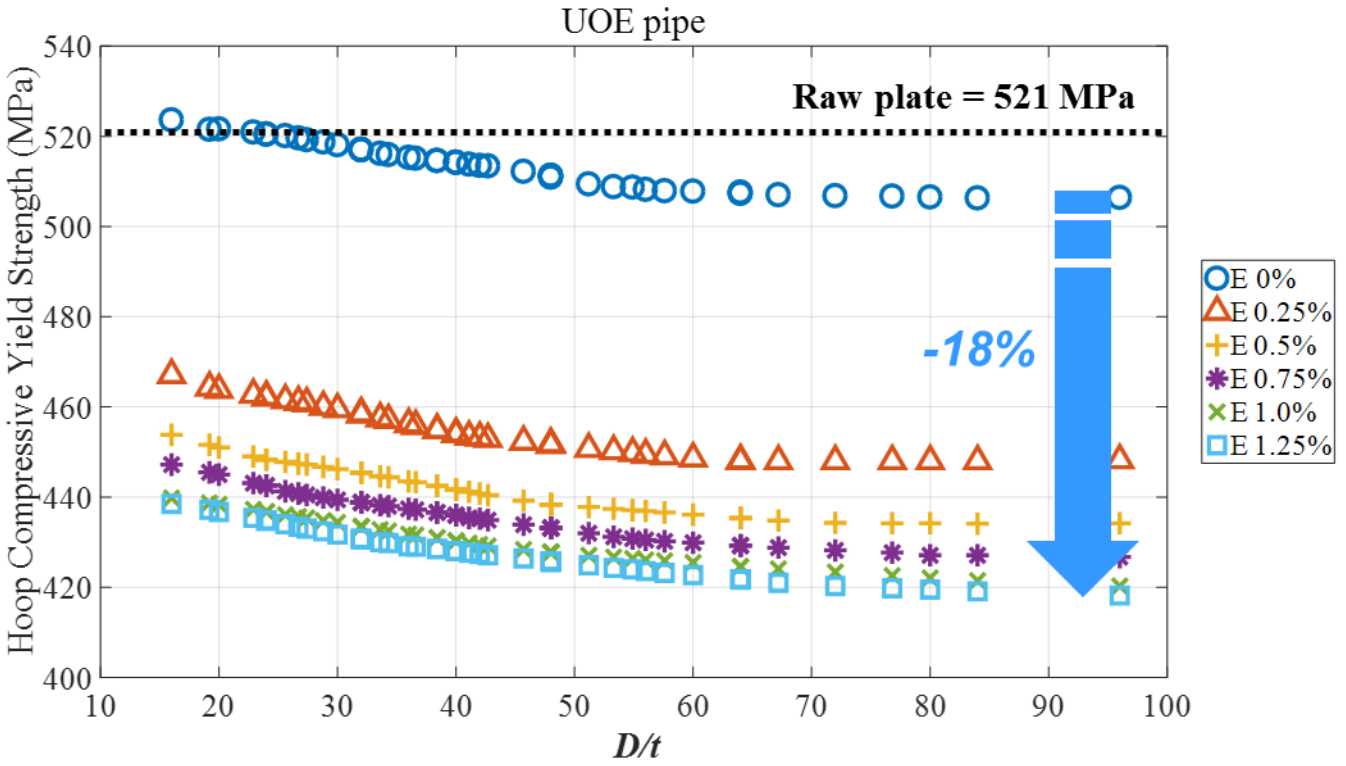

Figure 4.2 Effect of $\boldsymbol{D/t}$ ratio and expansion ratio on the compressive yield strength in hoop direction of UOE pipe

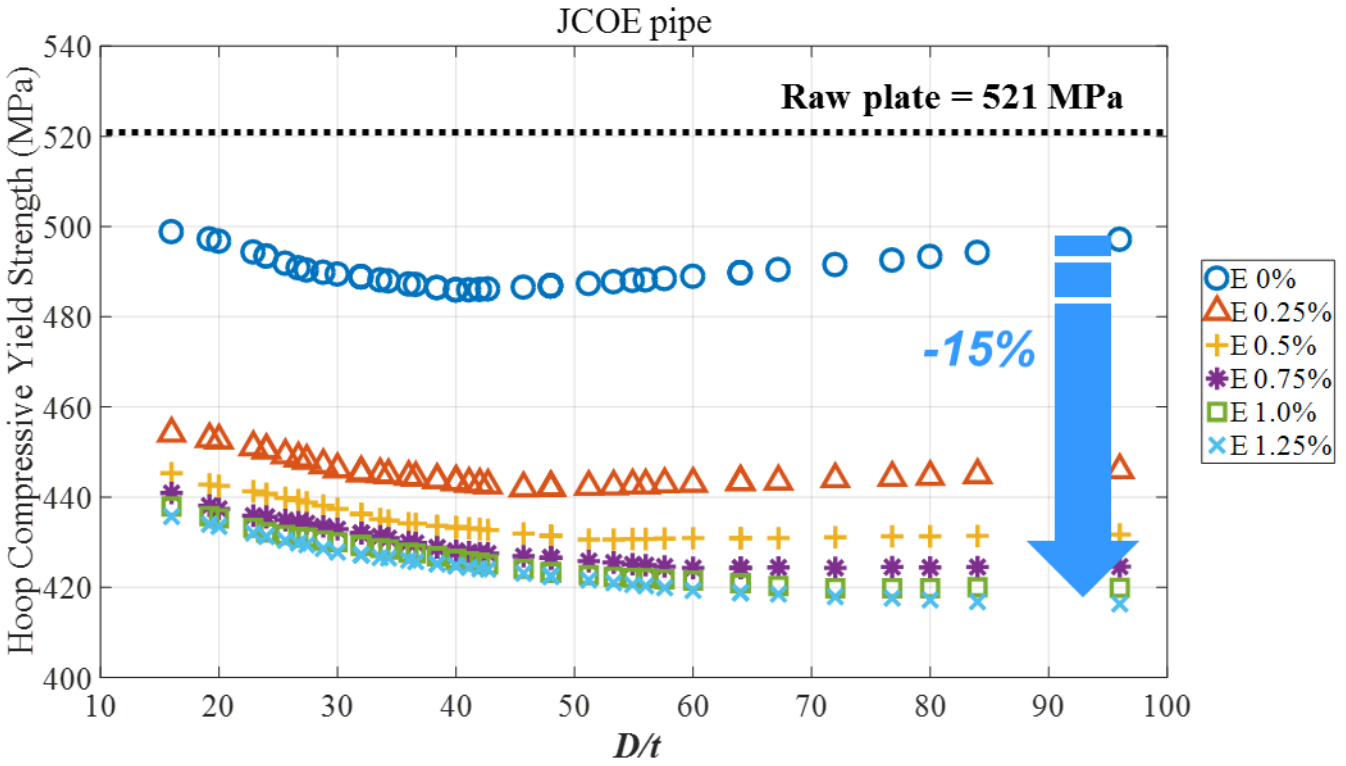

Figure 4.3 Effect of $\boldsymbol{D/t}$ ratio and expansion ratio on the compressive yield strength in hoop direction of JCOE pipe

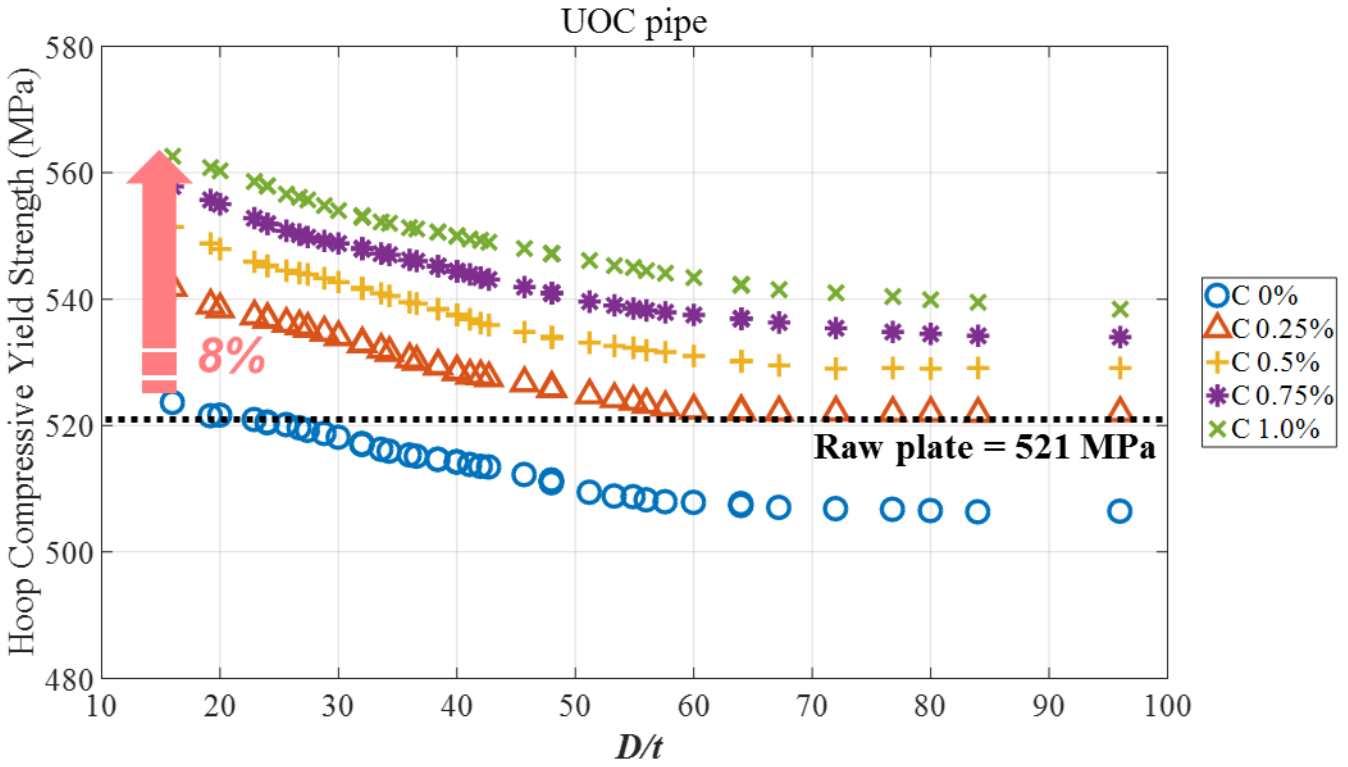

Figure 4.4 Effect of $\boldsymbol{D/t}$ ratio and compression ratio on the compressive yield strength in hoop direction of UOC pipe

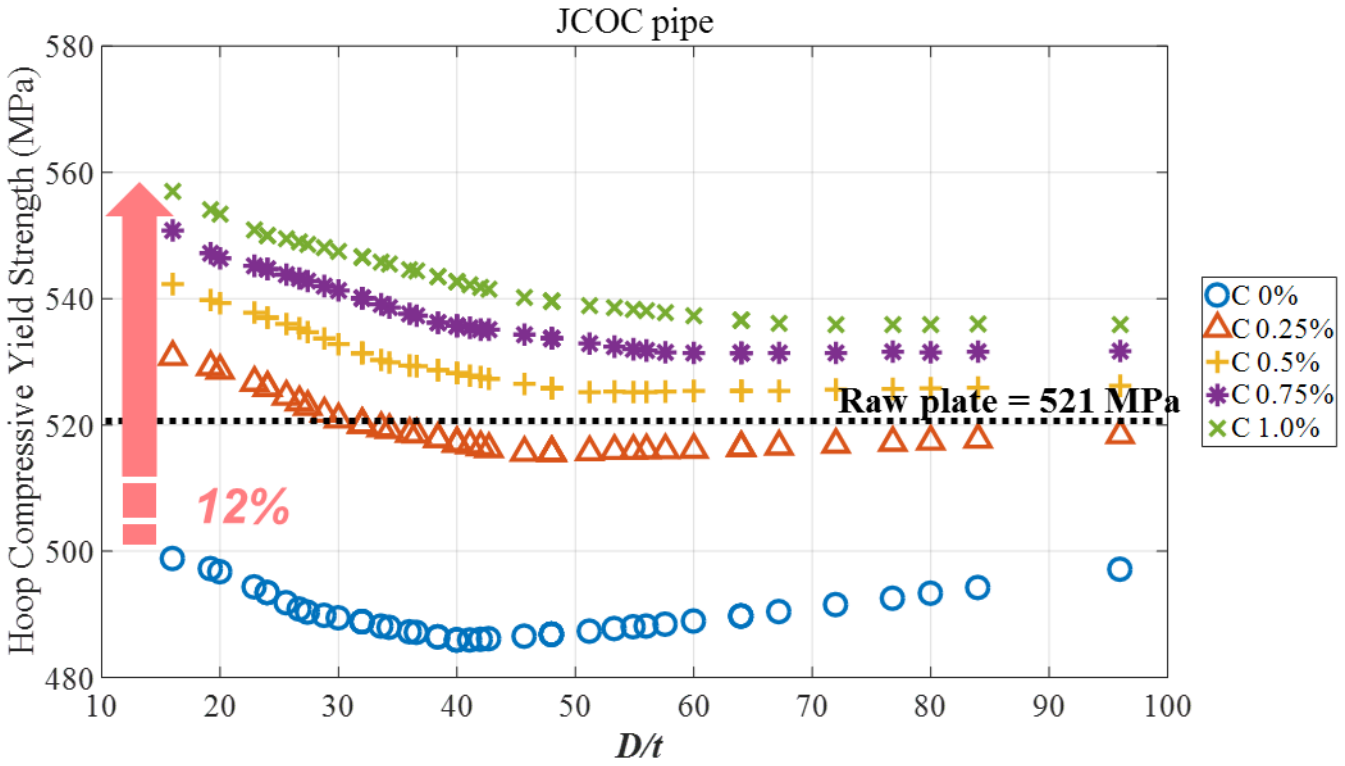

Figure 4.5 Effect of $\boldsymbol{D/t}$ ratio and compression ratio on the compressive yield strength in hoop direction of JCOC pipe

4.2.2 Tensile Yield Strength in longitudinal direction for Bending Analysis

Longitudinal tensile yield strength is a dominant factor of bending capacity of the pipe. Because *UOE and JCO* pipe forming processes are accomplished upon plane strain condition, material property changes independently in hoop direction and longitudinal direction. Figure 4.6 and Figure 4.7 show the calculated longitudinal yield strengths for UOE and JCOE pipes, respectively. Though no plastic forming occurs in longitudinal direction, there has been changes in yield strength on account of boundary effect and Poisson effect. Since longitudinal degree of freedom is fixed during whole forming process, the fiber undergoes slight longitudinal tension when stretched circumferentially while it experiences longitudinal compression when compressed circumferentially. Thus when comparing as-welded status of blue circles in figures, UOE pipes show lower values than JCOE pipes owing to the circumferential compression at O-forming stage. The effect of expansion ratio on the yield strength is more impressive for UOE pipes. Some UOE pipes finalized by expansion of 1.25% have 10% larger yield strength compared with as-welded status. For JCOE pipes, the maximum change in yield strength due to expansion calibration is calculated to be about 3%, which is not remarkable.

Figure 4.8 and Figure 4.9 illustrate the influences of compression calibration on longitudinal tensile yield strength. Despite a little reduction in calculated values, it seems that longitudinal tensile yield strength is not affected much from compression ratio, especially for pipes with low $\boldsymbol{D/t}$ ratios. The maximum change

due to compression calibration is only 6% for UOC pipes and 2% for JCOC pipes.

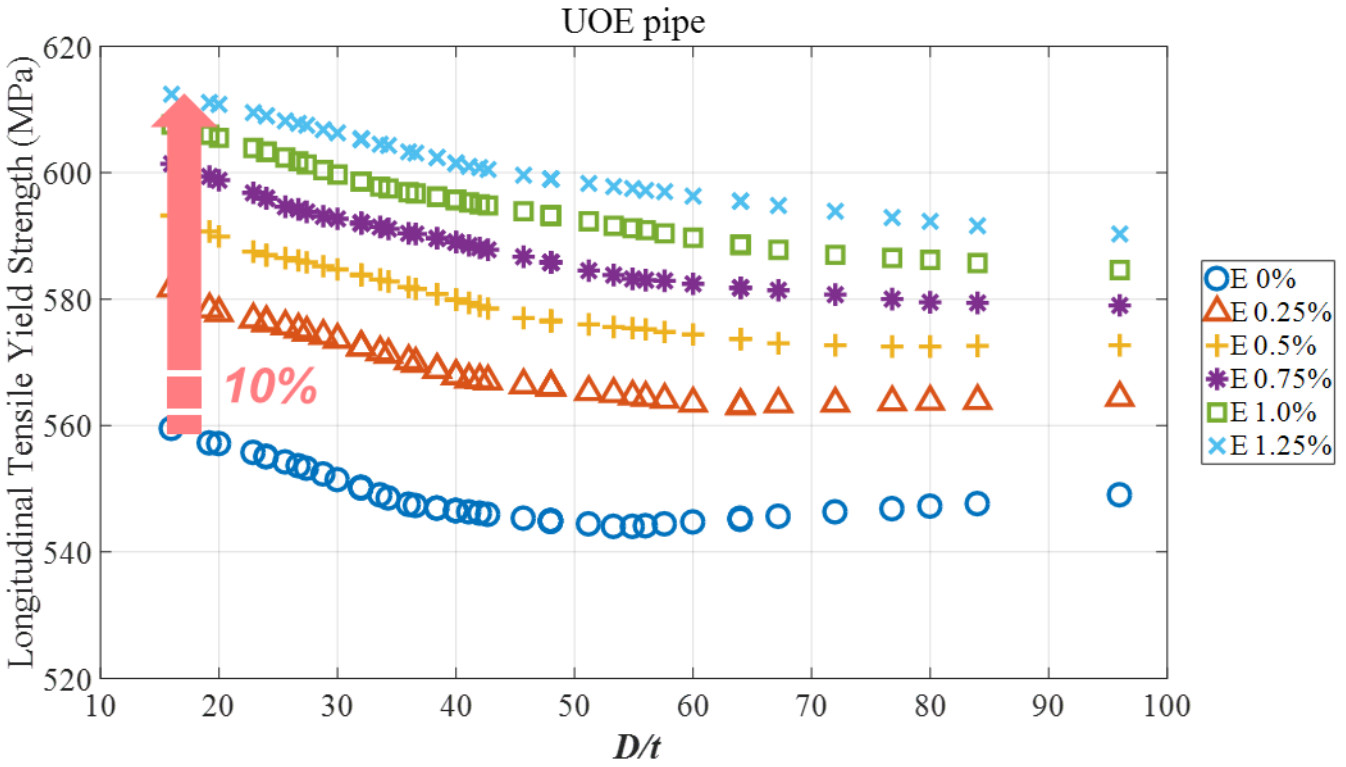

Figure 4.6 Effect of $\boldsymbol{D/t}$ ratio and expansion ratio on the tensile yield strength in longitudinal direction of UOE pipe

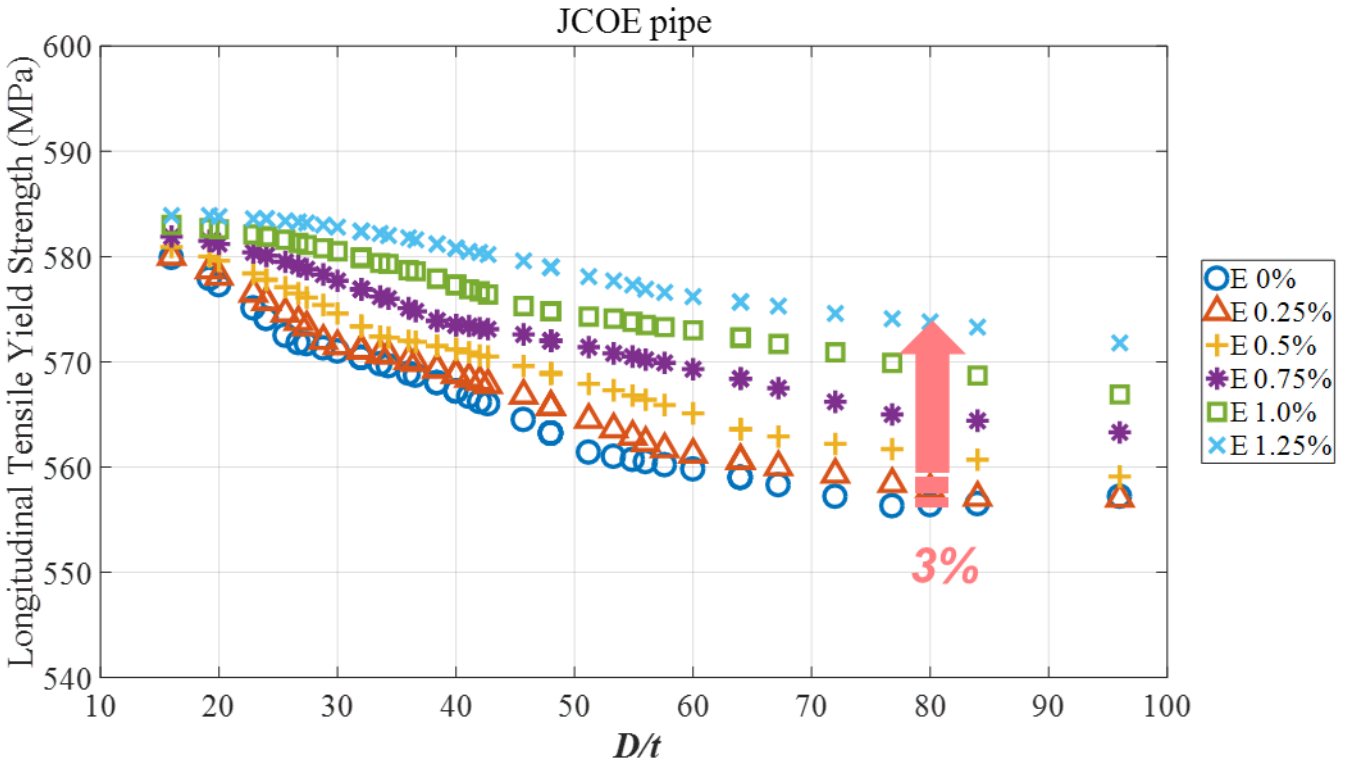

Figure 4.7 Effect of $\boldsymbol{D/t}$ ratio and expansion ratio on the tensile yield strength in longitudinal direction of JCOE pipe

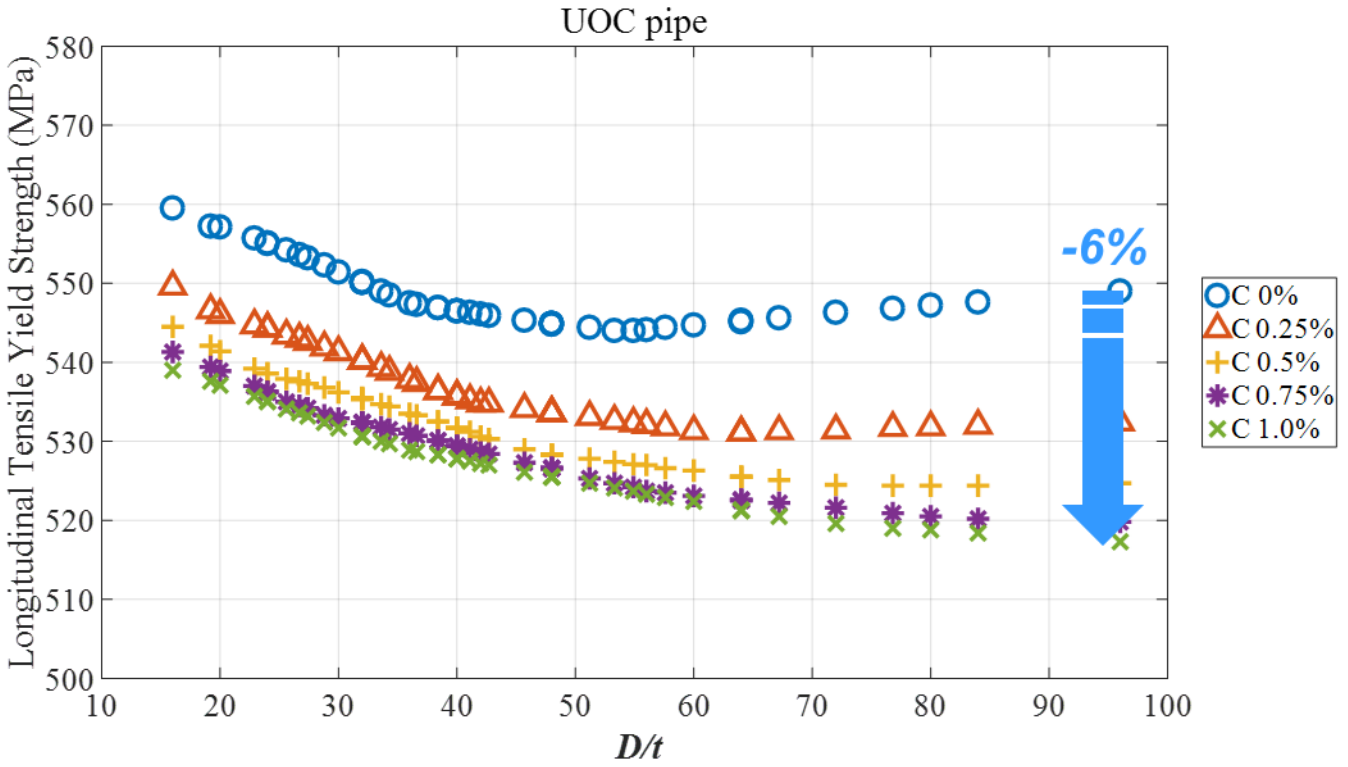

Figure 4.8 Effect of $\boldsymbol{D/t}$ ratio and compression ratio on the tensile yield strength in longitudinal direction of UOC pipe

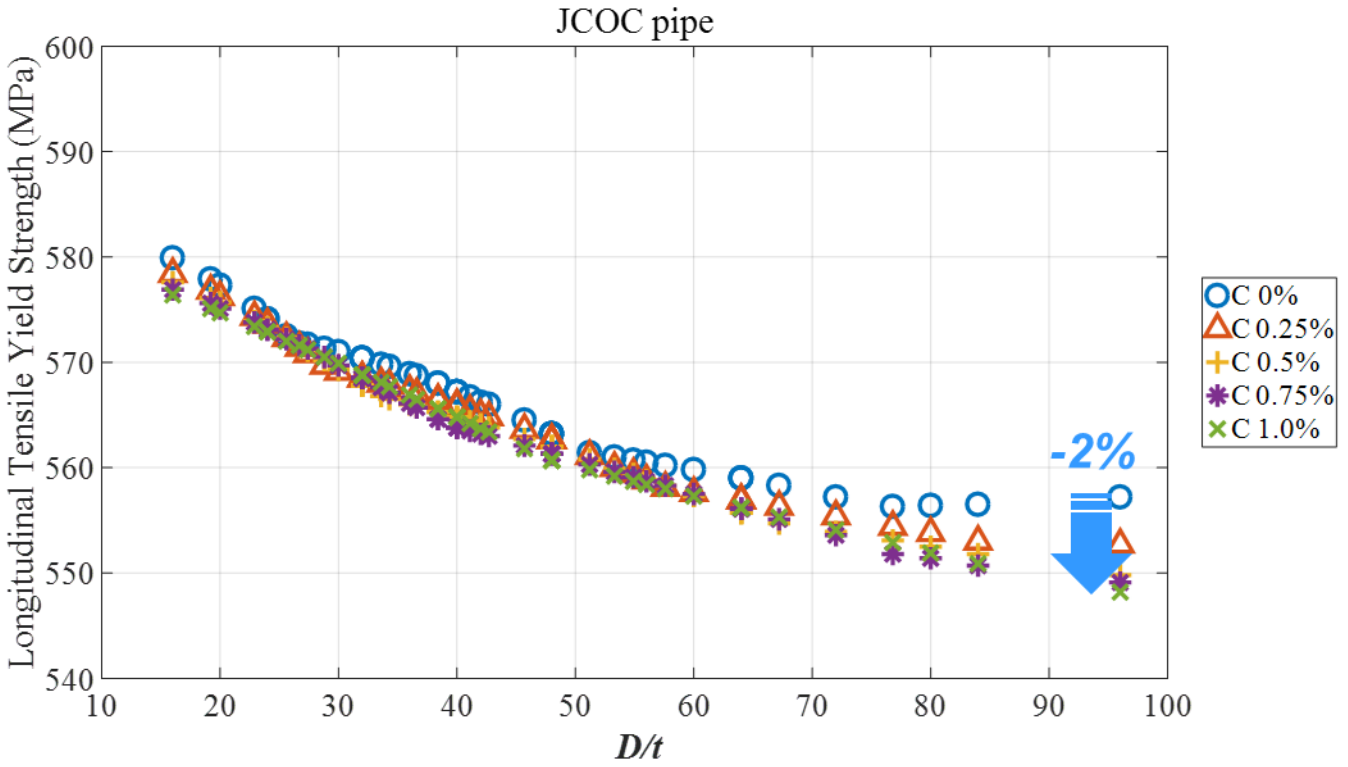

Figure 4.9 Effect of $\boldsymbol{D/t}$ ratio and compression ratio on the tensile yield strength in longitudinal direction of JCOC pipe

4.2.3 Tensile Yield Strength in hoop direction for Quality Control

For the purpose of quality control, tensile yield strength in hoop direction should be investigated. Figure 4.10 and Figure 4.11 show calculated yield strengths for UOE pipes and JCOE pipes respectively. As introduced in Section 3.2.2, the tensile yield strengths were estimated after specimen flattening. Likewise the results for compressive yield strength, as-welded pipes before expansion calibration have lower value than the yield strength of raw plate. As the pipes are expanded stronger, the tensile yield strengths definitely get higher almost proportionally to expansion ratio due to work hardening effect. The enhancement stands out for larger $\boldsymbol{D/t}$ ratios. UOE pipes expanded by 1.25% have approximately 14% higher tensile yield strength than as-welded status. With simpler forming stages, the yield strength reduction of JCO pipe is smaller than UO pipe. But that difference is vanished soon as a little expansion calibration of 0.25% or 0.5% is applied. Indeed, pipe expansion also plays a crucial role on tensile yield strength in hoop direction for JCOE pipes. They have experienced larger increasing effect with higher expansion ratio. The largest increase of all the pipes is as much as 13%. Interestingly, when the stronger expansion calibration is applied, the variance of the yield strength according to $\boldsymbol{D/t}$ ratio declines for both UOE and JCOE pipes. On the other hand, the tensile yield strengths tend to converge to similar values when the pipes are expanded hard enough by 1% or more. For example, when comparing as-welded status, the yield strengths for UOE pipes (470 MPa – 505 MPa) and JCOE pipes (490 MPa – 515 MPa) show obvious differences. If the pipes are expanded by

1.25%, however, the values are converged to between 535 MPa and 540 MPa for both UOE and JCOE pipes. These results can be interpreted that the influences of previously applied plastic forming on tensile yield strength would vanish gradually, as work hardening effect due to pipe expansion becomes governing.

On the other hand, it can be found in Figure 4.12 and Figure 4.13 that compression calibration has a detrimental effect on tensile yield strength for UOC and JCOC pipes. The biggest drop of the yield strength from as-welded pipes to UOC pipes is about 7%. JCOC pipe shows even larger reduction of 11% for large $\boldsymbol{D/t}$ ratio. As an intensity of compression goes stronger, the tensile yield strengths of the pipes tend to be scattered between similar ranges, from 435 MPa to 485 MPa. This fashion is analogous to those of UOE and JCOE pipes. This attributes to large amount of reverse loading occurred at compression stage. The influences of previous forming stages become faint due to a dominant action of Bauschinger effect by compression calibration.

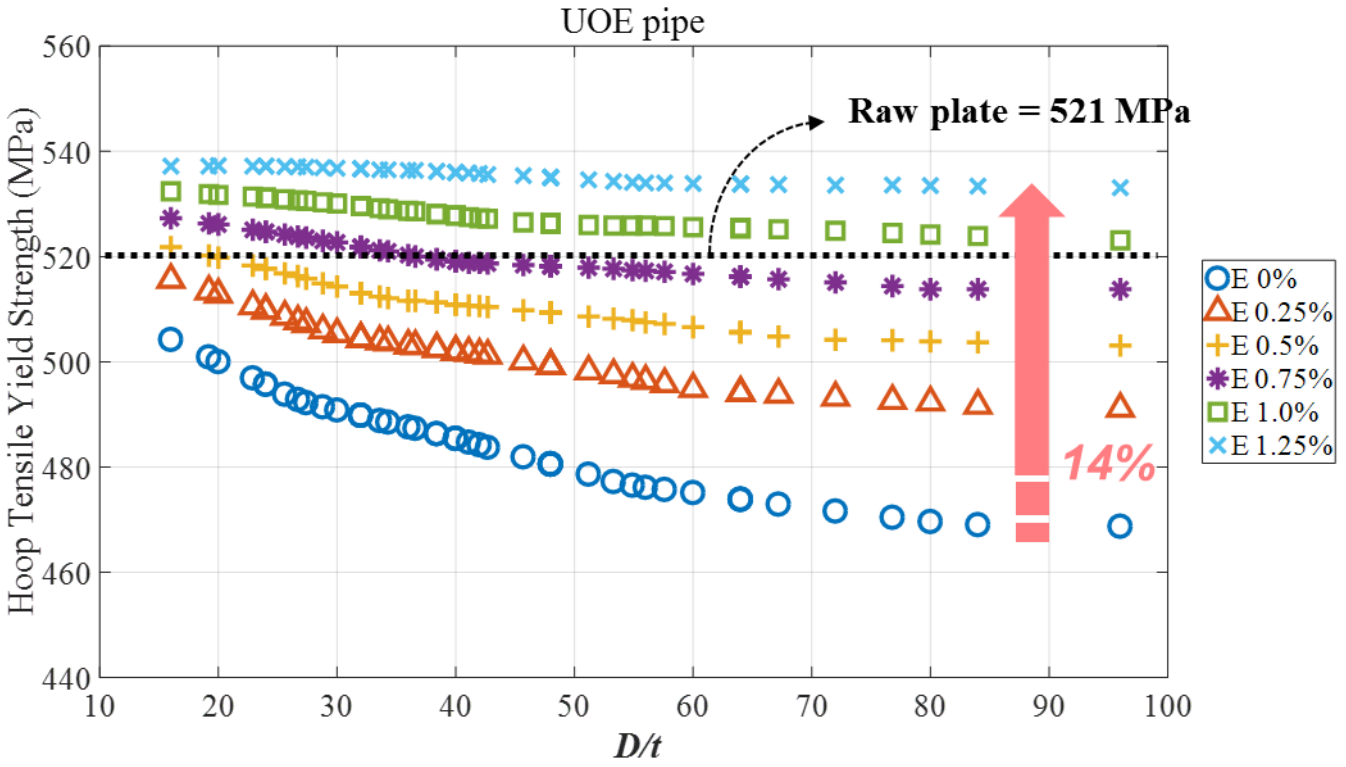

Figure 4.10 Effect of $\boldsymbol{D/t}$ ratio and expansion ratio on the tensile yield strength in hoop direction of UOE pipe

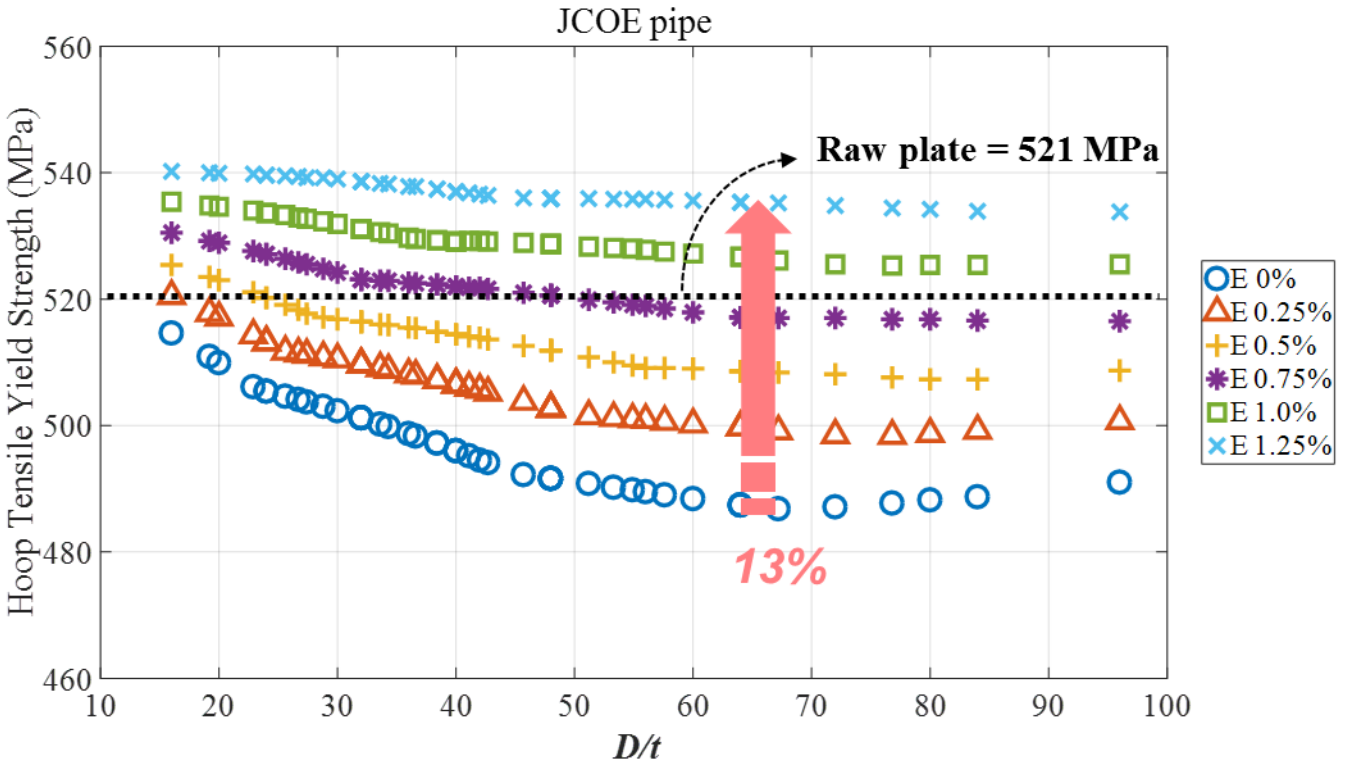

Figure 4.11 Effect of $\boldsymbol{D/t}$ ratio and expansion ratio on the tensile yield strength in hoop direction of JCOE pipe

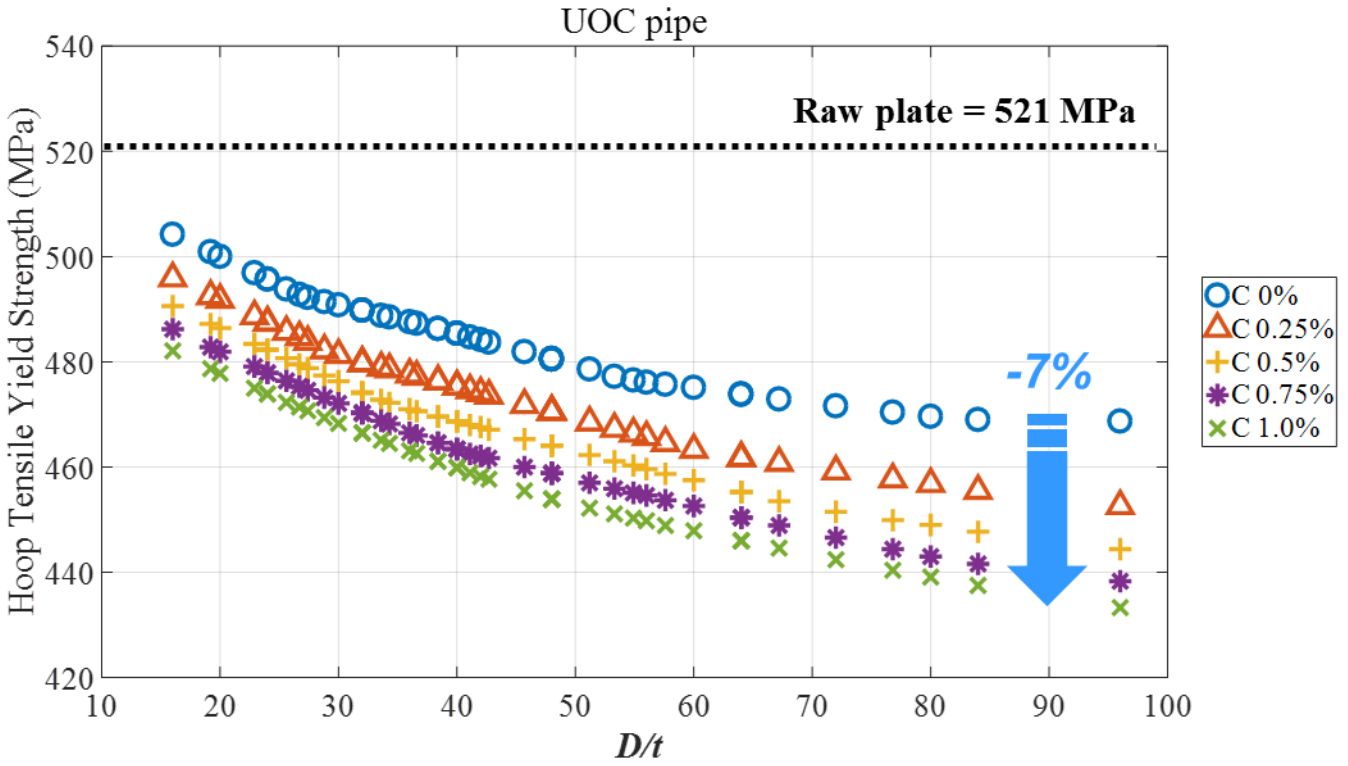

Figure 4.12 Effect of $\boldsymbol{D/t}$ ratio and compression ratio on the tensile yield strength in hoop direction of UOC pipe

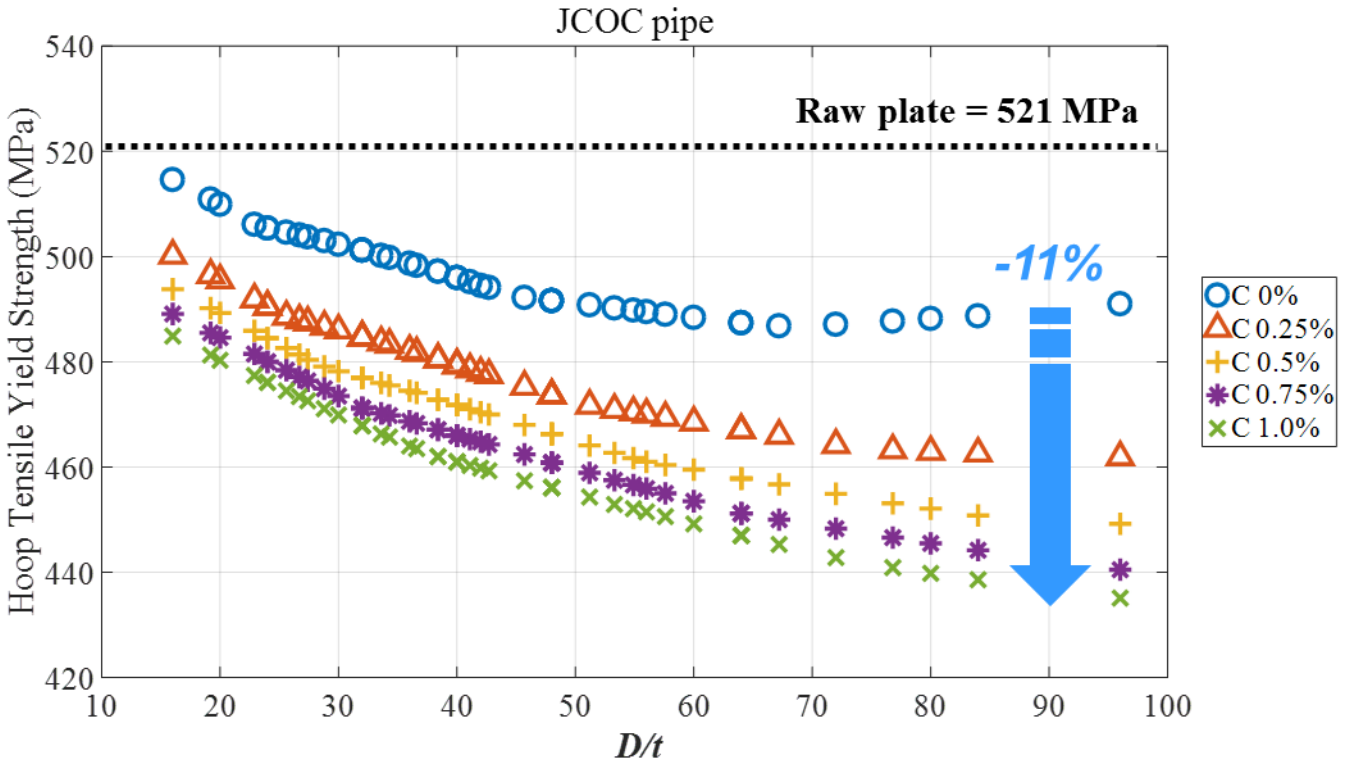

Figure 4.13 Effect of $\boldsymbol{D/t}$ ratio and compression ratio on the tensile yield strength in hoop direction of JCOC pipe

4.3 Influence on the Structural Performance

4.3.1 Collapse pressure

The way the expansion and compression calibration affect to the collapse pressures of the pipe is introduced in this section. First, the effects of expansion and $\boldsymbol{D/t}$ ratio on UOE and JCOE pipes are illustrated in Figure 4.14 and Figure 4.15. With the increasing $\boldsymbol{D/t}$ ratio, the collapse pressure drops rapidly and gains quite small values when $\boldsymbol{D/t}$ ratio is larger than 40. Additional increase of $\boldsymbol{D/t}$ ratio brings further reduction in collapse pressure as pipe's failure mode turns to elastic buckling from this point, due to relatively slender geometry of the pipe.

For all $\boldsymbol{D/t}$ values considered, collapse pressure is essentially influenced by pipe expansion since expansion calibration causes significant change of compressive yield strength in hoop direction as described in Section 4.2.1. The decreasing effect is larger for JCOE pipes than for UOE pipes. It comes from smaller reduction in compressive yield strength of JCOE pipes, especially with low $\boldsymbol{D/t}$ ratios as shown in Figure 4.14 and Figure 4.15. For lower $\boldsymbol{D/t}$ pipes, collapse pressure drops much only with a little expansion of 0.25% and the drop continues gradually when expansion ratio goes larger. But the effect of pipe expansion on collapse pressure is more considerable for lower $\boldsymbol{D/t}$ pipes since they buckle in the plastic range. Pipes with higher $\boldsymbol{D/t,}$ which buckle elastically is hardly affected by material property. Instead, they would be governed by geometric property.

On the contrary, the compression calibration generally improves ultimate strength of the pipe against external pressure. Figure 4.16 and Figure 4.17 exhibit calculated collapse pressures of UOC and JCOC pipes with varied values of $\boldsymbol{D/t}$ ratio and compression ratio. Here the advantages of altering expansion with compression can be inferred. The collapse pressures of UOC and JCOC pipes are mostly higher than that of as-welded pipes without calibration treatment. Indeed, the collapse pressure can be increased further if the pipe is compressed by larger extent. When comparing same amount of expansion and compression, the differences of corresponding results are very striking. For example, if we confront the UOE pipe with $\boldsymbol{D/t}$ = 16 and 1% expansion ratio, the collapse pressure is 34.9 MPa. But the UOC pipe with same geometry and compression ratio of same amount results in 48.3 MPa that is 38% higher than UOE pipe.

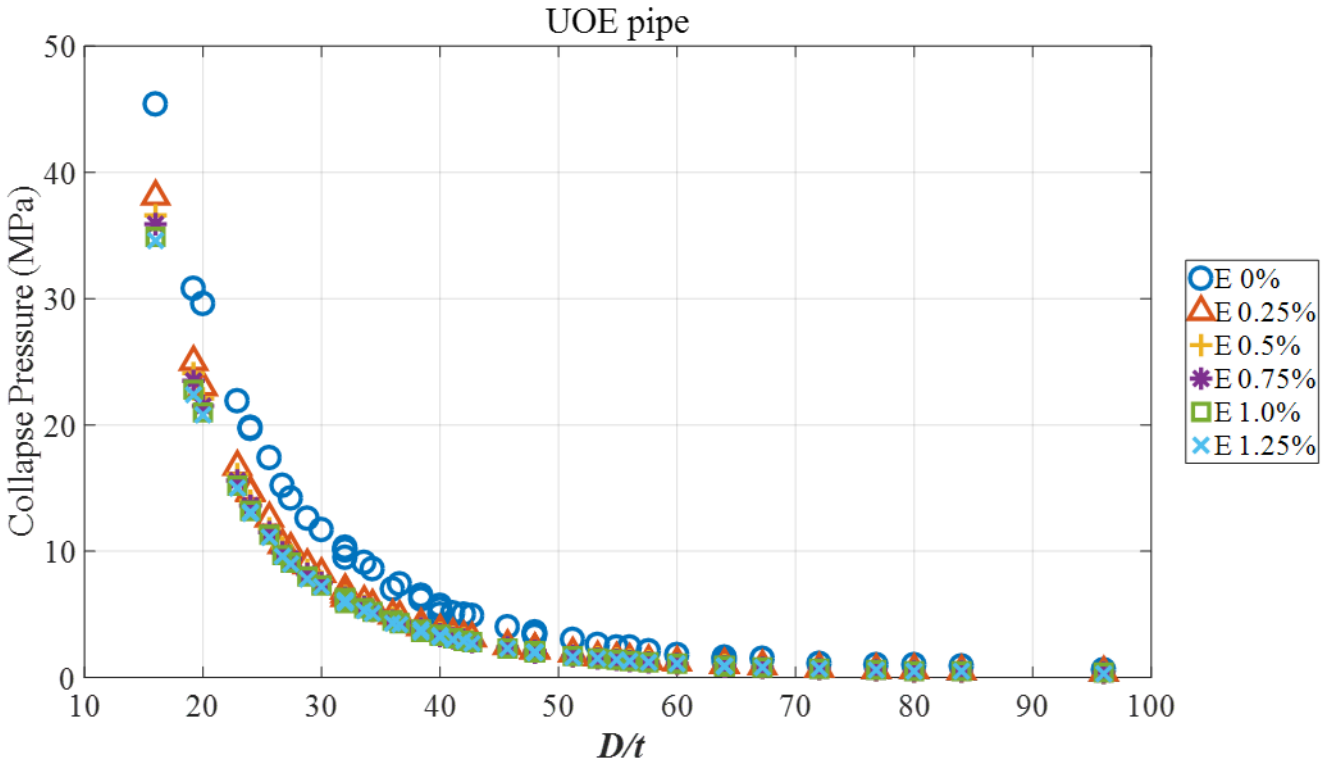

Figure 4.14 Effect of $\boldsymbol{D/t}$ ratio and expansion ratio on the collapse pressure of UOE pipe

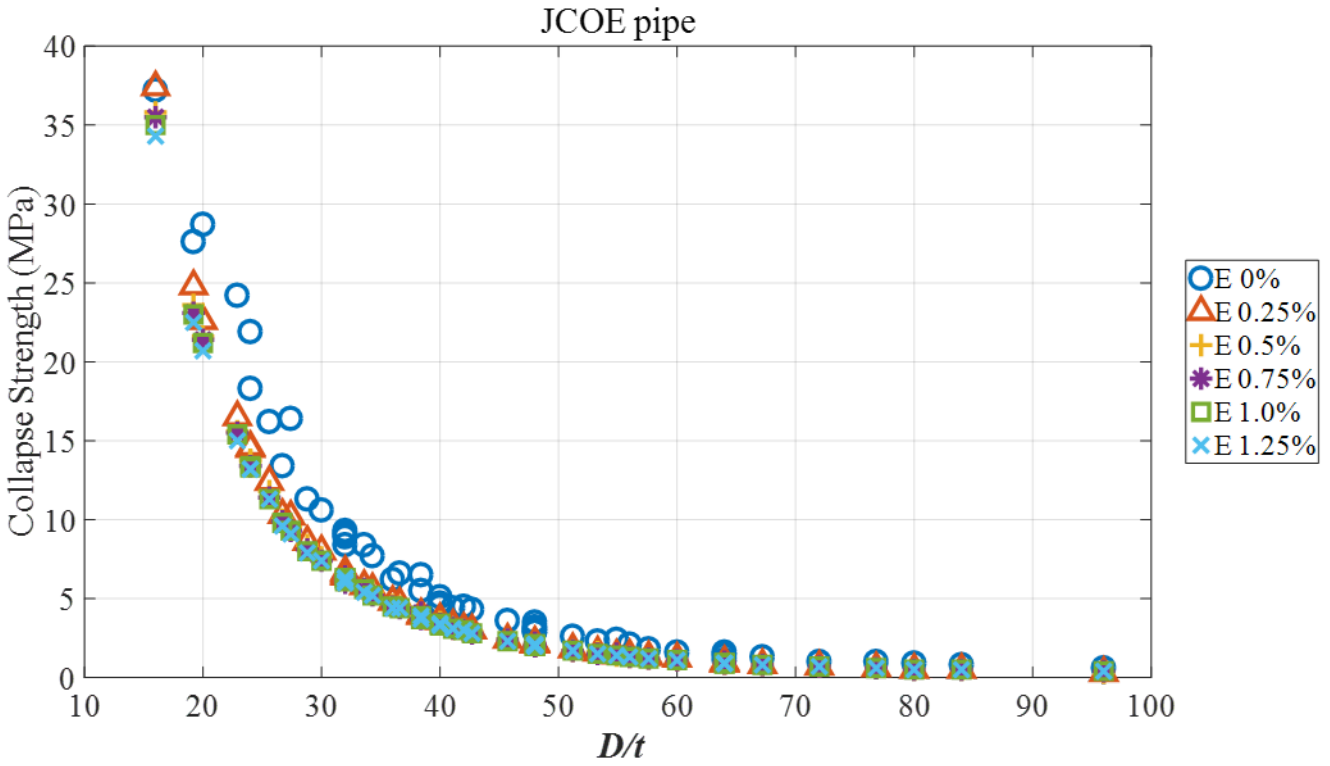

Figure 4.15 Effect of $\boldsymbol{D/t}$ ratio and expansion ratio on the collapse pressure of JCOE pipe

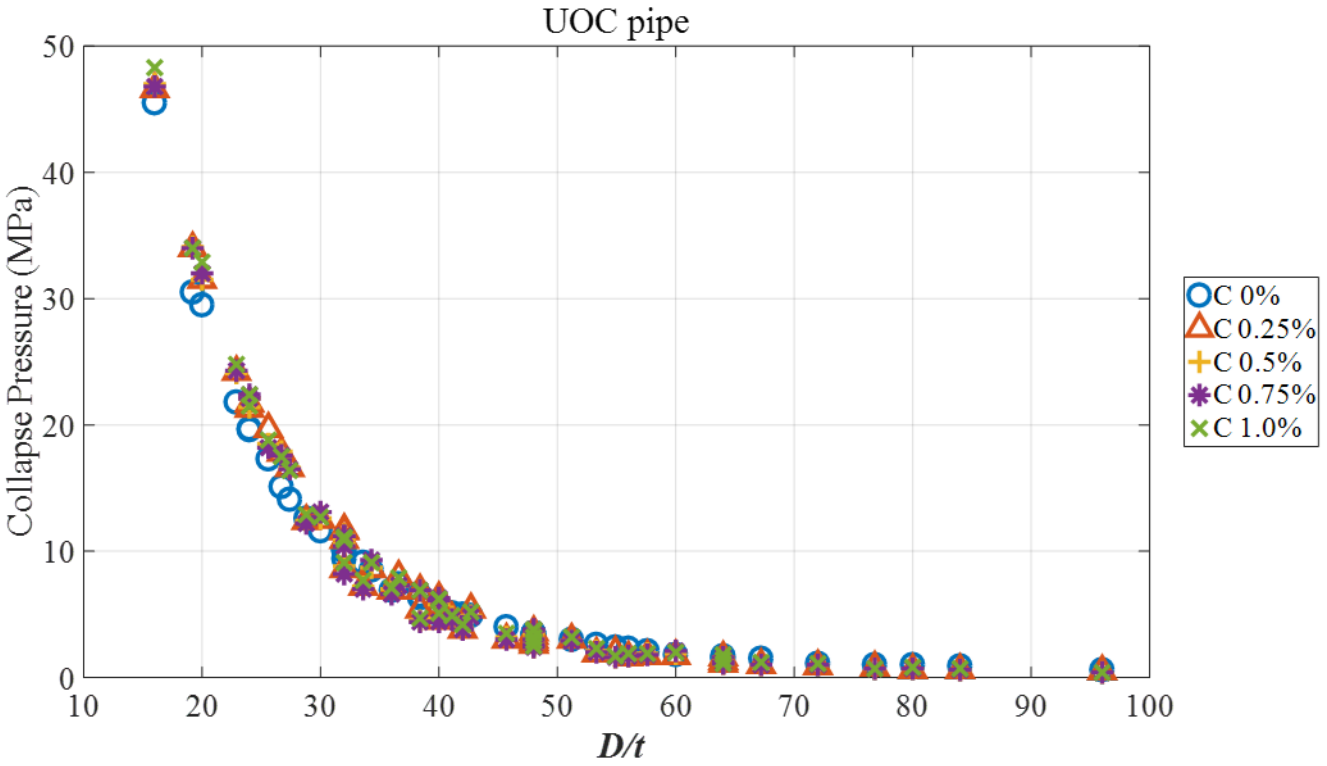

Figure 4.16 Effect of $\boldsymbol{D/t}$ ratio and compression ratio on the collapse pressure of UOC pipe

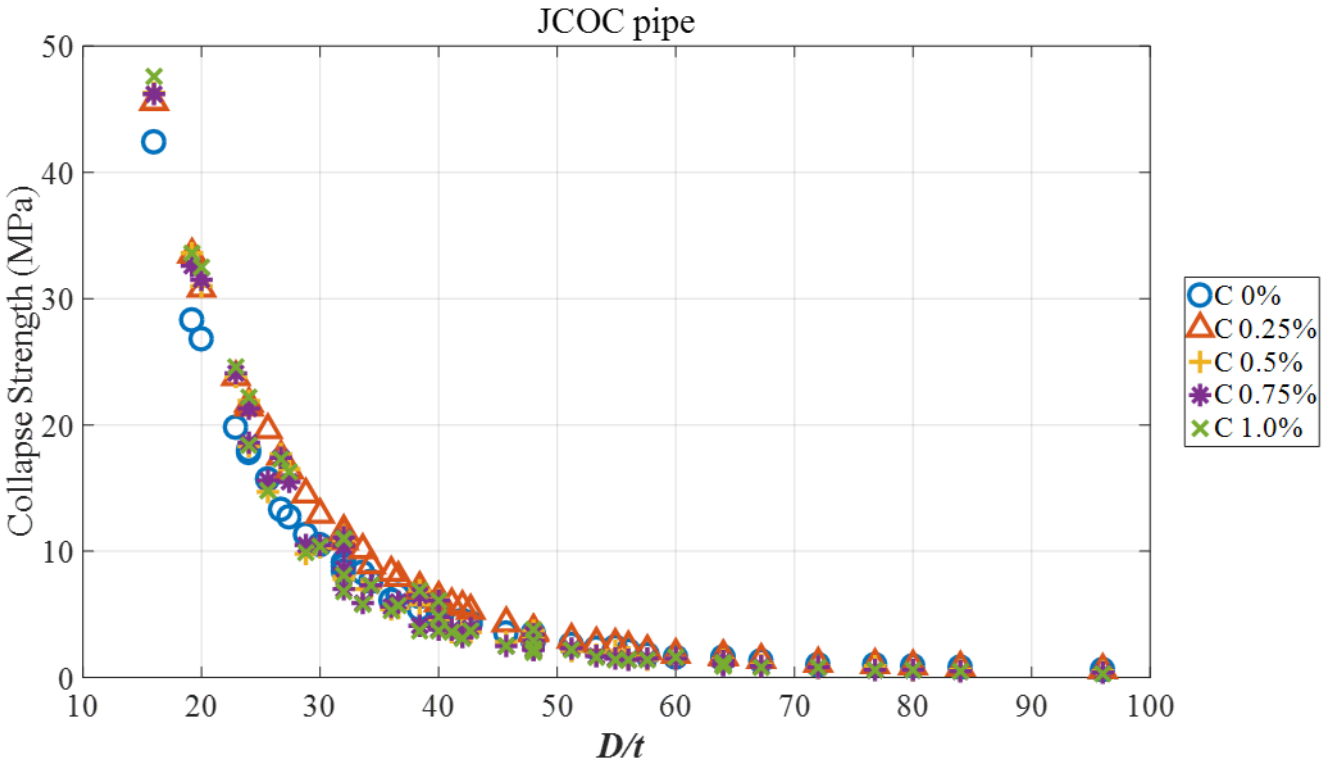

Figure 4.17 Effect of $\boldsymbol{D/t}$ ratio and compression ratio on the collapse pressure of JCOC pipe

4.3.2 Bending capacity

We now investigate the results of structural analysis on the pipe under pure bending. Figure 4.18 and Figure 4.19 show calculated bending capacities for UOE pipes and JCOE pipes of interest. For clear visualization, each figure includes a set of solid line that groups the pipes with same wall thickness. First of all, neither expansion nor compression has a noticeable influence on bending capacity of the pipe. Instead, the differences due to geometric factors such as diameter and thickness seem to be rather dominant. In Figure 4.18 and Figure 4.19, the maximum and minimum values of each solid line show great differences by over 5 times. For example, looking at the solid line of $\boldsymbol{t}$ = 1.125 inch in Figure 4.18, the bending capacity increases by 5.7 times from 4.9 MN-m to 27.9 MN-m when the diameter increases by 2.4 times from 20 inch to 48 inch. For 0.5 inch-thick pipe, the maximum value of 10.2 MN-m is 5.4 times larger than the minimum value of 1.9 MN-m. In the meantime, the bending capacity is also affected by wall thickness of the pipe. When thickness is increased by 2.25 times from 0.5 inch to 1.125 inch, the bending capacities of UOE pipes are strengthened by 2.6 times in average. On the other hand, the influence of pipe expansion seems not to be significant in comparison with that of geometric parameters. Though it brings increase by around 4% for the UOE pipes with large diameter over 30 inch, there is no remarkable change for other cases. The results for JCOE pipe are even undisturbed with expansion ratio, because the maximum increase of longitudinal yield strength by pipe expansion was only 3%, which was much less than 10% for UOE pipes.

In Figure 4.20 and Figure 4.21, the influences of diameter, thickness and

compression ratio on the bending capacity of UOC and JCOC pipes can be examined. The results show similar tendencies and even predicted capacities are comparable as well. The bending capacity of the pipes seems to be much more robust with the variance of compression ratio. It seems to be natural when recalling little variance in longitudinal yield strength due to pipe compression. In Section 4.2.2, it was verified that compression calibration can brings reduction in longitudinal yield strength by maximum of 6% and 2% to each of UOC and JCOC pipes. Considering dominant role of geometric parameters on bending capacity investigated for UOE pipes, this robust results does not require further explanation.

From the parametric study, it has been proven that adequate pipe expansion after welding is beneficial to achieve a high level of tensile yield strength for quality control and helpful for enhancing bending capacity to some degree. In the same time, however, the pipe becomes vulnerable to circumferential compressive loading as the pipe expansion can brings significant reduction in yield strength in that direction. On the contrary, if an expansion calibration is replaced with a compression calibration, collapse pressure of the pipe can be improved while bending capacity is not disturbed much. But as a trade-off effect, there would be important concern about quality control in terms of low tensile yield strength. In these context, strong attention should be paid in determining expansion or compression ratio for the design of *UOE and JCO* pipes.

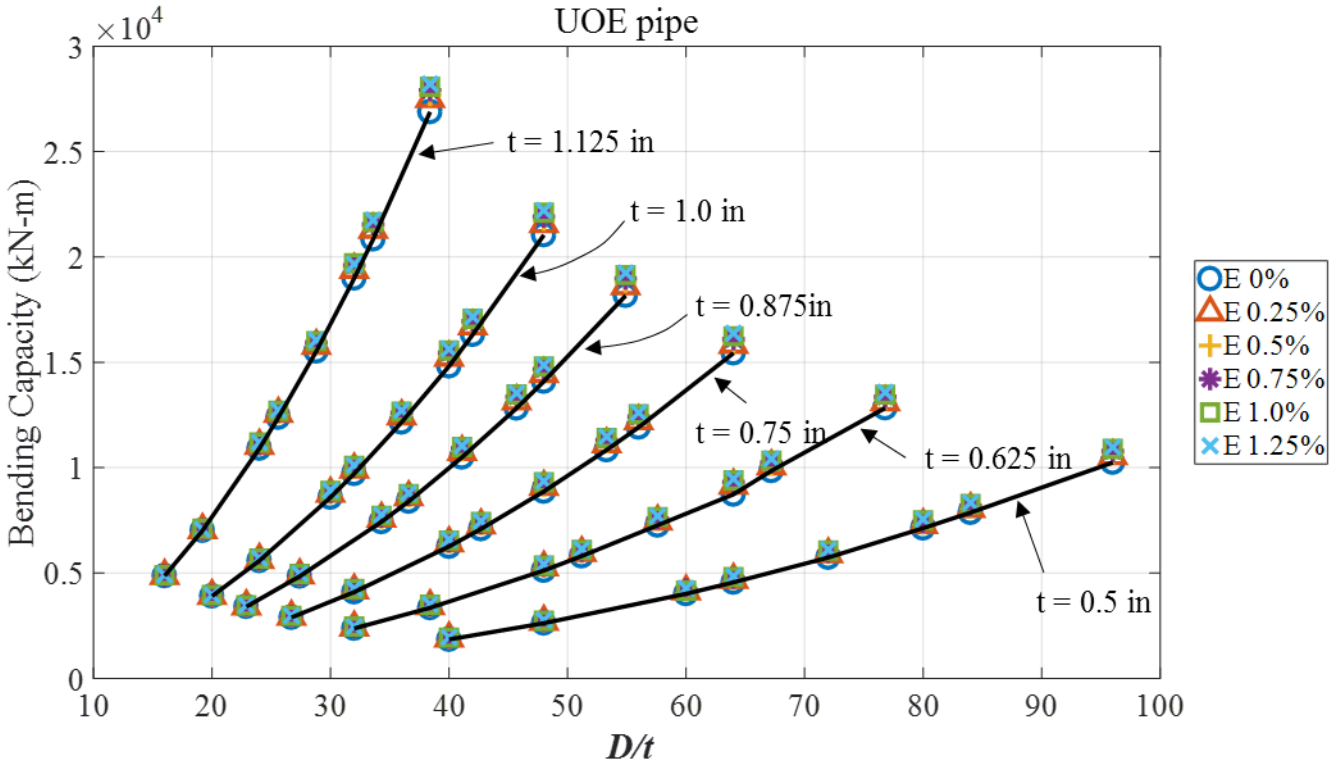

Figure 4.18 Effect of $\boldsymbol{D/t}$ ratio and expansion ratio on the bending capacity of UOE pipe

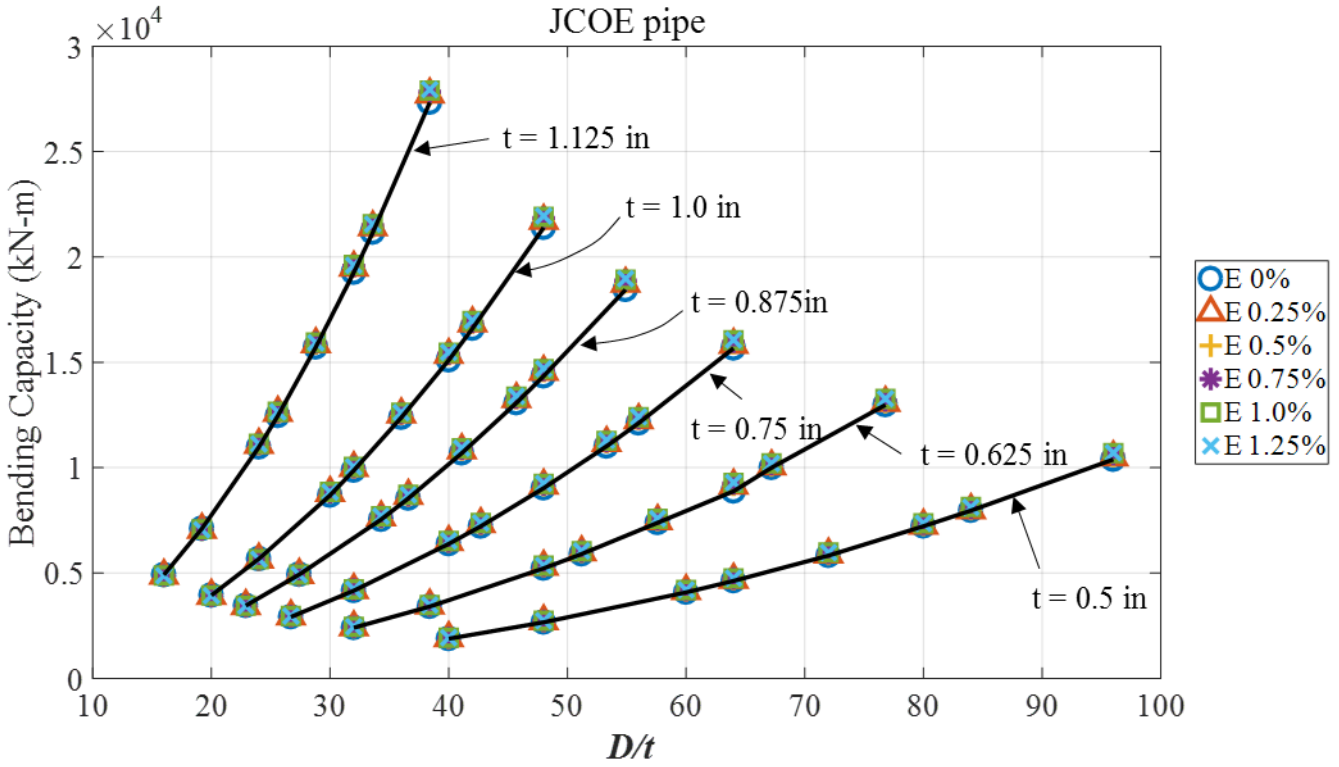

Figure 4.19 Effect of $\boldsymbol{D/t}$ ratio and expansion ratio on the bending capacity of JCOE pipe

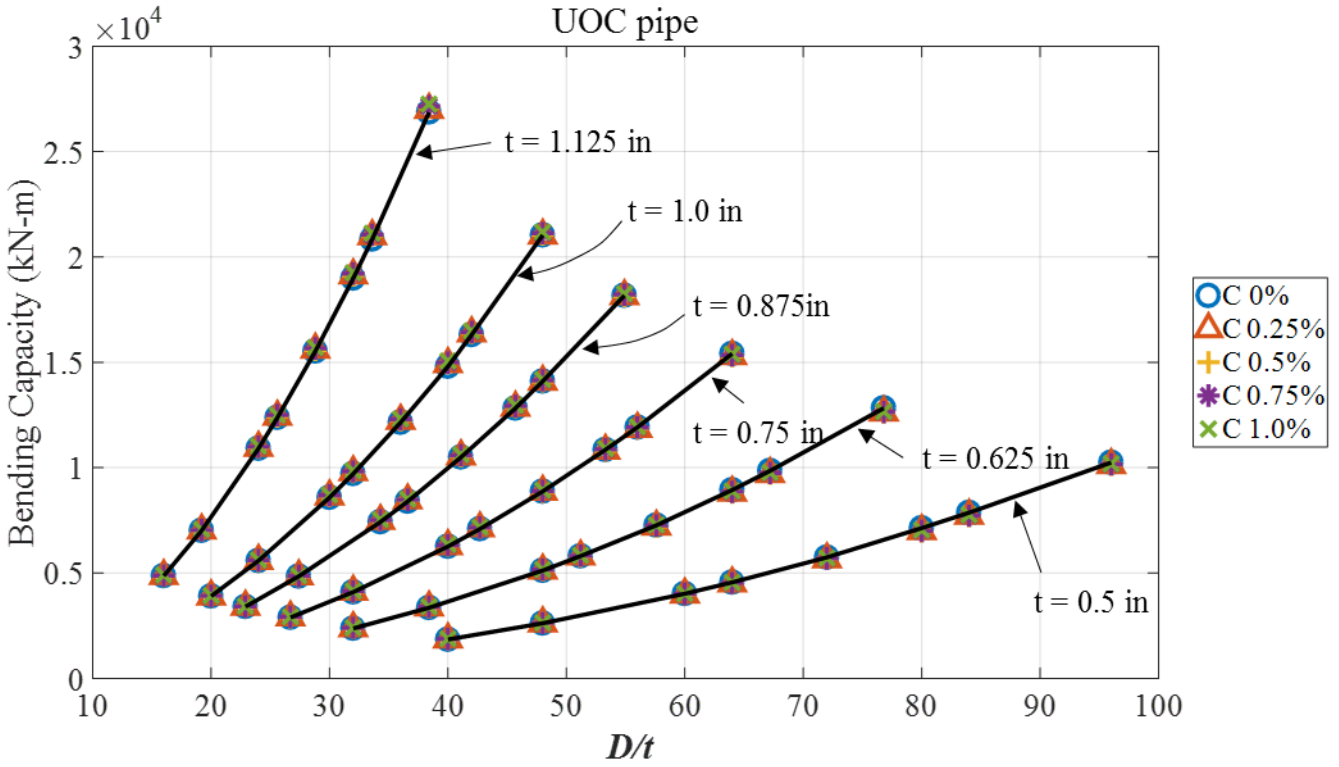

Figure 4.20 Effect of $\boldsymbol{D/t}$ ratio and compression ratio on the bending capacity of UOC pipe

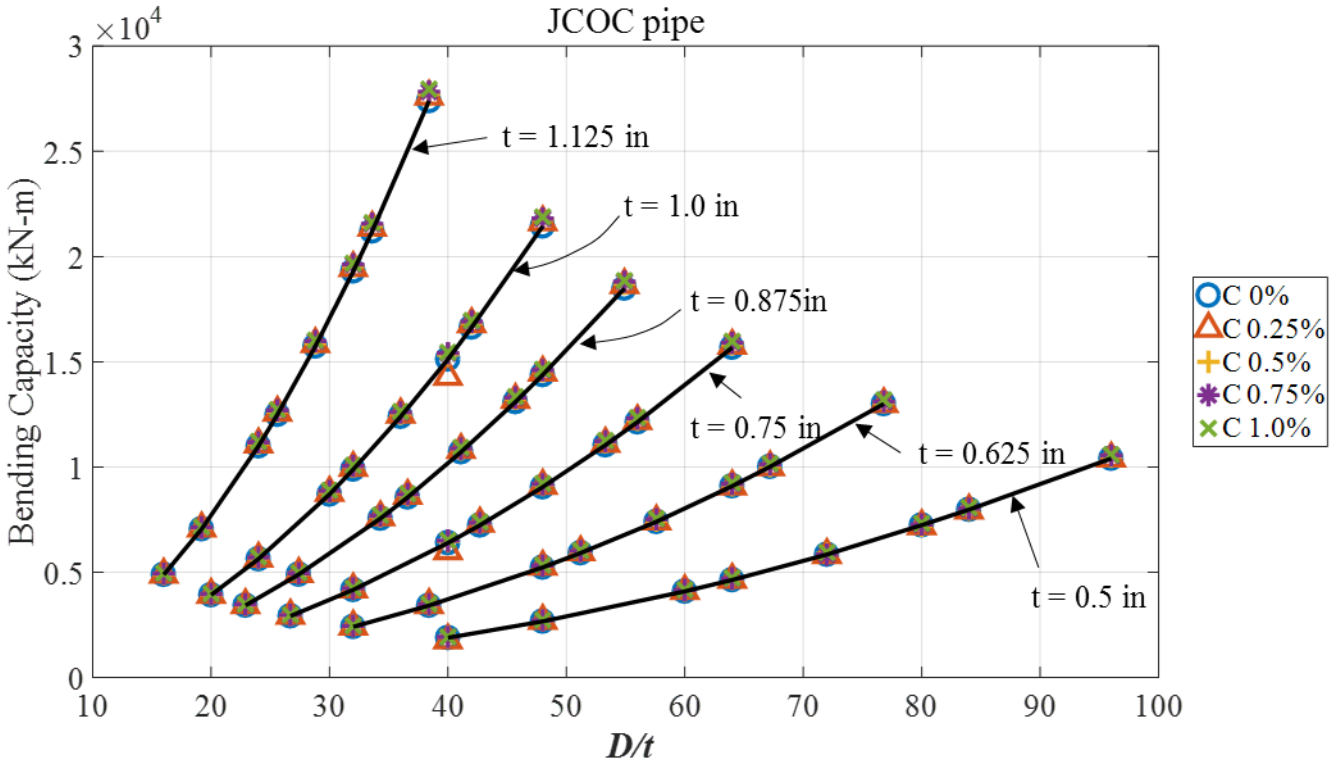

Figure 4.21 Effect of $\boldsymbol{D/t}$ ratio and compression ratio on the bending capacity of JCOC pipe

5 Optimal design procedure for Offshore Steel Pipes

5.1 Definition of the Optimization Problem

The purpose of this optimization is to obtain a set of design parameters for UOE pipe such as wall thickness and forming process parameters. In this optimization problem, structural performance is defined as an object value. Structure performance here means collapse pressure which is a fundamental limit state of offshore pipelines especially for deep water application. Constraints are specified in terms of circumferential tensile yield strength of the pipe, maximum tool forces and welding gap. The former is related to quality check of the pipe while the latter two determines producibility. With these design goal and constraint conditions, design variables are to be determined following optimal design procedure. For UOE and UOC pipe design, compression ratio at O-forming stage (C_r), radius of U-forming tool (R_u), wall thickness (t), expansion (compression) ratio (δ_e / δ_c), and pipe calibration method would be determined. For JCOE and JCOC pipe design, punching depth, distance between supporting dies and number of punching would replace C_r, R_u, δ_e / δ_c of UOE and UOC pipe design.

As a primary constraint condition, tensile yield strength of the pipe is required to be larger than specified minimum yield strength (SMYS) of the raw material given in design standards. Since SMYS has a flexible range with minimum and maximum value considering the uncertainty, yield strength criterion is up to client's

decision.

In practice, the demand for O-forming gap is ordinarily 2 - 3% of the nominal outer diameter of pipe. Too narrow gap makes it hard to clean the both edges of the plate before welding, which results in poor welding quality. On the other hand, wide gap causes excessive residual stress after hard joining and welding, and even makes the welding impossible sometimes. It is a matter of course that the maximum tool force plays a crucial role in the way that it must not exceed force capacity of the actuator. Because the force on the tool is known to be much larger for O-forming and pipe calibration than U-forming and crimping, force conditions are assessed only for those two stages. The process would be invalid unless the force conditions and O-forming gap condition meet corresponding requirements. Thus they need to be assessed first prior to yield strength of the pipe. In other words, the constraints are to be assessed in serial order unlike other ordinary optimization problems.

5.2 Flow for Optimal Pipe Design

For the design of *UOE and JCO* pipes, the outer diameter of the pipe and material are preferentially given on account of the amount of oil and gas transport. Thereafter the initial wall thickness is determined considering the environment where the pipe is installed and operates. Then the forming parameters are to be determined by using prevalidation program developed in this thesis. This step is referred to as a *variable setting step*. In order to examine the validity of the determined design parameters, it is possible to monitor the reaction force applied to forming tools and the geometric configuration change of the plate by inputting the parameters to *pipe forming simulation* program. In case of *UOE* steel pipe, if the appropriateness of the design parameter cannot be guaranteed at this stage, go back to the *variable setting step* and try to modify compression ratio at O-forming stage, C_r first. When it is difficult to obtain the proper producibility by only the modification of C_r, radius of U-forming tool, R_u and wall thickness are changed in order. In the case of *JCO* steel pipe, try to modify the design parameters in order of punching depth, die width, number of punching, and wall thickness.

If production possibilities are judged to be satisfactory, a quality specification step is to be carried out to examine whether the tensile yield strength of the steel pipe in the hoop direction predicted from the forming simulation is higher than the minimum reference value. At this time, if the yield strength is not high enough, we can try to increase the expansion ratio according to the results of the parametric study in this paper. Although the expansion ratio is increased, it will be advantageous in terms of strength quality, but collapse pressure can be significantly

lowered. Conversely, if the yield strength is sufficiently high compared to the required standard, a compression calibration may be introduced to increase the additional collapse pressure instead of lowering the yield strength. Again, care must be taken because extreme parameter adjustments may not meet the strength quality level. Since the influence of design variables on yield strength and collapse pressure is dependent on other variables, it is desirable to precede parametric study of various design parameters as performed in this study for precise design. Also, adjusting the calibration ratio or method may not be sufficient to meet the desired level. In this case, resize the cross-section and follow the design procedure again from the beginning.

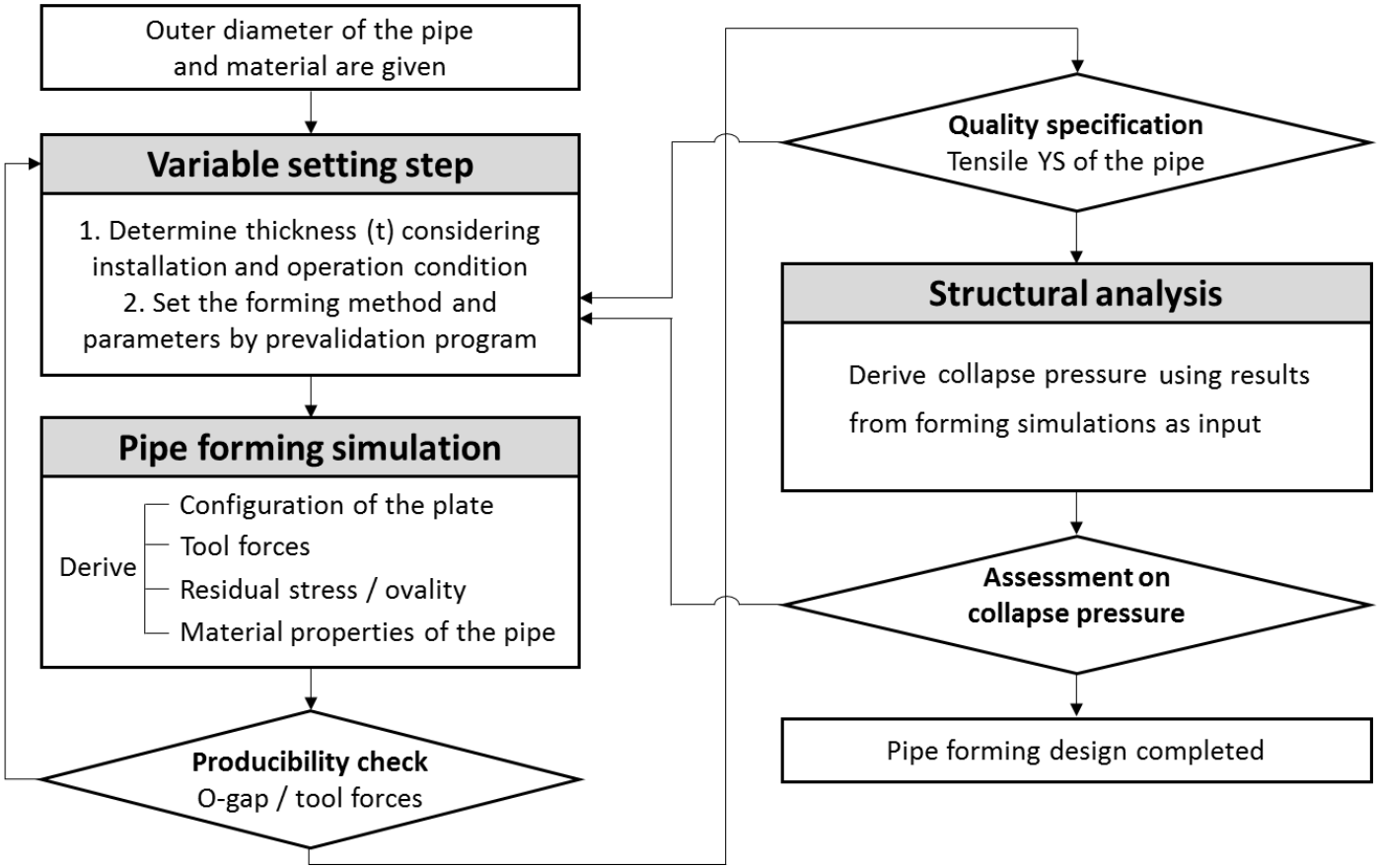

Figure 5.1 Flow chart of optimal design procedure for *UOE and JCO* pipes

5.3 Illustrative Example of UOE Pipe Design

Following the suggested optimal design procedure, a design example of typical offshore UOE pipe is now introduced for a specific comprehension. The effectiveness of the implemented numerical analysis program on pipe design will also be shown through the example.

The example problem considers a UOE pipe made of API X70 steel which specifications are listed in Table 5.1. In this problem, design parameters are to be determined towards the maximization of collapse pressure of the pipe under uniform external pressure. Although there can be an optimum solution that has many significant figures like 1.234%, this example would only consider the ratio discretely by 0.1%, considering practical application. One of the essential constraint, the O-forming gap should be in range between 2% to 3% of nominal outer diameter, i.e. 15 mm to 23 mm. The force capacities are 25,000 kN for O-forming tool and 10,000 kN for expanding tool. The minimum requirement on tensile yield strength in hoop direction of the pipe is given to be 520 MPa. The process initially adopts expansion calibration of 1% while the other 12 input variables can be derived through prevalidation program as listed in Table 5.2.

Table 5.1 Specification of the pipe

Symbol	Description	Value
OD	Target outer diameter (in)	30
t	Target thickness (mm)	21.5
σ_o	Yield strength of the raw plate (MPa)	540
E_o	Initial Young's modulus (MPa)	207,000

Table 5.2 Design variables to be determined for UOE pipe manufacturing and corresponding initial values

Category	Symbol	Description	Initial value (mm)
Crimping	$\boldsymbol{R_c}$	Involute radius	260
	$\boldsymbol{L_c}$	Length of crimped part	270
U-forming	$\boldsymbol{R_{u1}}$	Radius of U-forming tool	288
	$\boldsymbol{R_{u2}}$	Small radius of U-forming tool	144
	$\boldsymbol{L_p}$	Horizontal position of pusher	493.5
	$\boldsymbol{TD_u}$	Travel distance of U-forming tool	850
	$\boldsymbol{TD_p}$	Travel distance of pusher	140
	$\boldsymbol{R_p}$	Radius of pusher	90
O-forming	$\boldsymbol{R_o}$	Radius of O-forming tool	380
	$\boldsymbol{D_c}$	Maximum distance between upper and lower O-forming tool	760
Expansion	$\boldsymbol{\delta_e}$	Expansion ratio	0.01%
	$\boldsymbol{R_e}$	Radius of the tool	359.1

First trial with initial values results in maximum force of 20,052 kN on O-forming tool, which is less than the capacity of 25,000 kN. Now the constraint of O-forming gap should be assessed. It is calculated as 25 mm that is beyond the upper bound of 23 mm. To make close the distance between both edges, the compression ratio at the O-forming stage can be adjusted as it is most important factor of O-forming gap (Zou *et al*, 2015). Meanwhile, designer should note that the O-forming gap might become larger because suppression of spring back occurs in complicated manner. In this example, O-forming compression ratio was modified from 0 to 0.2%. Accordingly, adjusted design variable set is inputted again to get the forces, O-forming gap and yield strength of the pipe. The maximum forces on O-forming tool and expansion tool are 20,052 kN and 5,826 kN that are less than allowable values. O-forming gap of 18 mm is also within the tolerable range. In the next quality check step, the tensile yield strength of the pipe is calculated to be 515 MPa. This is less than criteria by 5 MPa, which is not acceptable. So expansion ratio is increased to be 1.1% with the expectation of further hardening of material. On third trial with modified expansion ratio, all constraints are judged to be agreeable as listed in Table 5.3.

The collapse pressure of the manufactured pipe is then calculated with developed analysis program in this study. The pipe is expected to endure the uniform external pressure of 8.3 MPa by maximum. We recognize that the additional expansion strain, say, expansion ratio of 1.2% could have been applied for confident tensile yield strength in hoop direction. However, it not only causes more burdens on forming tool but also drops the collapse pressure obviously. Actually, the collapse pressure is computed to be 7.4 MPa when the expansion ratio

becomes 1.2% from 1.1%. This indicates 1.1% expansion ratio and other corresponding design variables deserve optimum solution set for maximization of pipe's collapse pressure.

Table 5.3 Assessment of constraints of the problem with final solution

Constraint	**Criteria**	**Calculated value**
Maximum force on O-forming tool	< 25,000 kN	21,958 kN
Maximum force on expansion tool	< 25,000 kN	7,186 kN
O-forming gap	> 15 mm, < 23 mm	16 mm
Tensile yield strength of the pipe	> 520 MPa	523 MPa

6 Conclusion

An optimal design procedure for *UOE and JCO* steel pipes for offshore application was proposed in this study. A finite element analysis-based virtual factory program was developed to simulate the pipe forming processes and track the change in material properties, geometric imperfection and residual stress throughout the *UOE and JCO* forming processes. Using the results of the simulation, collapse and bending analysis on the pipe were conducted for assessing the structural performance of the pipe. The influence of the key design variables on the yield strength and structural performance of the pipe was verified through parametric study and a new design procedure was suggested to achieve maximum collapse strength of the pipe satisfying constraint conditions such as yield strength criterion and O-forming gap.

For the computational simulation, a combined hardening model describing the repeated loading and unloading cycles executed throughout the forming process was adopted. Cyclic stress-strain response of API X70 steel was fitted with the material model. It was shown that work hardening, Bauschinger effect, yield plateau and evolution of Young's modulus developed during the *UOE and JCO* forming processes can be taken into account in the model adequately. Using this model, the UOE, UOC, JCOE and JCOC pipe forming processes were simulated by finite element analysis. The simulation enabled to predict the yield strength directly and to check the possibility of steel pipe production by monitoring the shape change of the plate and the reaction force applied to the forming tool. In addition, the simulation could provide large amount of useful and efficient

information for pipe design such as quantitative influence of friction force and defect detection that were unavailable with conventional trial-and-error based empirical design method. The forming simulation showed substantial feasibility through an experimental verification of UOE pipe manufacturing and tensile test of a specimen sampled from the pipe. Collapse and bending analyses were then performed with refined 3-dimensional finite element analysis using the results from the forming process as inputs.

Extensive parametric study was conducted to examine the influence of the design variables on the material property and structural performance of the formed pipe. Diameter to thickness ratio, expansion ratio and compression ratio were selected as key parameters. The following findings could be drawn from the study.

For UOE and UOC pipes, expansion reduces the geometric imperfection and enhances the tensile yield strength in hoop direction by as much as 10%. However expansion has detrimental effect on the compressive material properties especially for thicker pipe with $\boldsymbol{D/t}$ < 45. In practice, common expansion ratio of 1% degrades the collapse performance. This indicates the existence of an optimum expansion ratio that balances quality level of tensile yield strength and collapse strength maximization.

Executing expansion instead of compression (UOC and JCOC pipes) can result in significantly higher collapse performance. This is particularly true for pipes with $\boldsymbol{D/t}$ <30, which are suitable size for ultra-deep water application. However compression exerts a reducing effect on the tensile yield strength due to Bauschinger effect for all the examined cases. Therefore compression calibration

has to be treated carefully when it comes to quality control of the pipe.

Expansion increases the longitudinal tensile yield strength, and the effect is more remarkable for pipes with $\boldsymbol{D/t}$ < 45. The resulting bending capacity is strengthened to some degree but in a lesser extent than the collapse strength. On the contrary, compression reduces the longitudinal yield strength by about 6%. This change affects merely the bending capacity due to the counterbalance brought by the improved ovality.

An optimal design procedure for *UOE and JCO* pipes was developed based upon these findings. Design procedure and specific guideline for maximum collapse pressure of the pipe satisfying quality specification and adequate producibility were introduced and illustrated by an example of UOE pipe design. The proposed design proved to be capable of controlling the design variables while monitoring the geometric configuration of the skelp, yield strength quality, and structural performance of the pipe. Besides, it leads to high flexibility and versatility in design especially when applying newly developed material of which mechanical behavior is hard to predict.

Though this study is based on deterministic design, reliability-based design approach is preferable for practical pipe design since various kind of uncertainties exist throughout the whole pipe production such as material properties of the raw plate, O-compression ratio and calibration ratio, size and travel distance of forming tools, and other minor factors. Taking into account those uncertainties, product supplier should guarantee a certain level of quality with quantitative index. Therefore reliability-based design optimization for pipe forming is recommended

as a further study by using simulation program and design procedure suggested in this study.

References

Aiman Al-Showaiter, F.T., Shawn Kenny, 2008. Influence of pipeline misalignment on the local buckling response. *7th International Pipeline Conference*, Calgary, Alberta, Canada.

Ajit Bastola, J.W., Ali Mirzaee-Sisan, James Njuguna, 2014. Predicting hydrostatic collapse of pipes using finite element analysis. *33rd International Conference on Ocean, Offshore and Arctic Engineeing*, San Francisco, CA, US.

American Petroleum Institute, 2012. Specification for line pipe. US: American Petroleum Institute.

Andrii Kostryzhev, M.S., Claire L. Davis, 2010. Mechanical property development during uoe forming of large diameter pipeline steels. *Materials and Manufacturing Processes,* 25 (1-3), 41-47.

Chaboche, J.L., 1986. Time-independent constitutive theories for cyclic plasticity. *International Journal of Plasticity,* 2 (2), 149-188.

Chandel, J.D. & Singh, N.L., 2011. Formation of X-120 m line pipe through J-C-O-E technique. *Engineering,* 03 (04), 400-410.

Chatzopoulou, G., Karamanos, S.A. & Varelis, G.E., 2016. Finite element analysis of UOE manufacturing process and its effect on mechanical behavior of offshore pipes. *International Journal of Solids and Structures*, 83, 13-27.

Dave G. Crone, L.E.C., Yankui Bian, Paul Weber, 2010. The effect of sample flattening on yield strength measurement in line pipe. *8th International Pipeline Conference*, Calgary, Alberta, Canada.

DET NORSKE VERITAS, 2013. OFFSHORE STANDARD DNV-OS-F101. Norway: DET NORSKE VERITAS.

E. Tsuru, H.A., 2003. Collapse pressure prediction and measurement methodology of uoe pipe. *13th International Offshore and Polar Engineering Conference*, Honolulu, Hawaii, US.

Erica Marley, O.A., Leif Collberg, 2012. Assessment of recent experimental data on collapse capacity of uoe pipeline. *9th International Pipeline Conference*, Calgary, Alberta, Canada.

Fan, L., Gao, Y., Li, Q. & Xu, H., 2012. Quality control on crimping of large diameter welding pipe. *Chinese Journal of Mechanical Engineering,* 25 (6), 1264-1273.

Fatt, M.S.H., 1999. Elastic-plastic collapse of non-uniform cylindrical shells subjected to uniform external pressure. *Thin-Walled Structures,* 35, 117-137.

Fraldi M., Guarracino F., 2011. An improved formulation for the assessment of the capacity load of circular rings and cylindrical shells under external pressure. Part 1 Analytical derivation. *Thin-Walled Structures,* 49, 1054-1061.

Fraldi M., Guarracino F., 2013. Towards an accurate assessment of UOE pipes under external pressure: Effects of geometric imperfection and material inhomogeneity. *Thin-Walled Structures,* 63, 147-162.

Fusahito Yoshida, T.U., Kenji Fujiwara, 2002. Elastic-plastic behavior of steel sheets under in-plane cyclic tension-compression at large strain. *International Journal of Plasticity,* 18, 633-659.

Gao, Y., Li, Q. & Xiao, L., 2009. Numerical simulation of JCO/JCOE pipe forming. *2009 World Congress on Computer Science and Information Engineering,* Los Angeles, CA, US.

Garret Meijer, T.K., 2012. Circumferential compression material characterization for pipe collapse load prediction. *9th International Pipeline Conference,* Calgary, Alberta, Canada.

Giannoula Chatzopoulou, G.E.V., Spyros A. Karamanos, 2014. Finite element analysis of UOE pipes under external pressure and bending. *24th International Ocean and Polar Engineering Conference*, Busan, Korea.

Gresnigt A.M., Van Foeken J.J., Chen S., 2000. Collapse of UOE manufactured steel pipes. *10th International Offshore and Polar Engineering Conference*, Seattle, Washington, 170-181.

Gresnigt A.M., Van Foeken J.J., 2001. Local buckling of UOE and seamless steel pipes. *11th International Offshore and Polar Engineering Conference*, Stavanger, Norway, 131-142.

Haagsma Sc, S.D., 1981. Collapse resistance of submarine lines studied. *Oil & Gas Journal*, 79.

He, T., Duan, M. & An, C., 2014. Prediction of the collapse pressure for thick-walled pipes under external pressure. *Applied Ocean Research,* 47, 199-203.

Herynk, M.D., Kyriakides, S., Onoufriou, A. & Yun, H.D., 2007. Effects of the UOE/UOC pipe manufacturing processes on pipe collapse pressure. *International Journal of Mechanical Sciences,* 49 (5), 533-553.

Hiroshi Muruyama, M.K., Masafumi Shoji, 1993. Developement of as rolled type HF-ERW casings with high resistance to collapse. *13rd International Offshore and Polar Engineering Conference*, Singapore.

J. L. Chaboche, G.R., 1983a. On the plastic and viscoplastic constitutive equations - part I: Rules developed with internal variable concept. *Journal of Pressure Vessel Technology*, 105, 153-158.

J. L. Chaboche, G.R., 1983b. On the plastic and viscoplastic constitutive equations - part II: Application of internal variable concepts to the 316 stainless steel. *Journal of Pressure Vessel Technology*, 105, 159-164.

J. Wolodko, D.D., 2006. Critical local buckling conditions for deepwater pipelines. *25th International Conference on Offshore Mechanics and Arctic Engineering*, Hamburg, Germany.

Javier Raffo, R.G.T., Luciano Mantovano, Eduardo N. Dvorkin, 2007. Numerical model of UOE steel pipes forming process and structural behavior. *Mechanica Computacional*, 26, 317-333.

Jeom Kee Paik, Jeong Hwan Kim, Bong Ju Kim, Chang Hyo Tak, 2013. Nonlinear finite element analysis of spring-back characteristics in the cold-forming process of three-dimensionally curved thick metal plates. *Journal of Offshore Mechanics and Arctic Engineering*, 135.

Jia, L.-J. & Kuwamura, H., 2014. Prediction of cyclic behaviors of mild steel at large plastic strain using coupon test results. *Journal of Structural Engineering*, 140 (2).

Jin B.-H., 2016. *Collapse strength of thick-walled steel pipe considering post-buckling behavior*. (Master). Seoul National University.

Juliana E. Roza, G.M., Marcelo C. Fritz, Gianluca Mannucci, Luis Chad, Jan Ferino, Ronaldo C. Silva, 2008. Numerical simulation analysis of high strength uoe steel pipes. *7th International Pipeline Conference*, Calgary, Alberta, Canada.

J. Cheng and N. Kikuchi, 1985. An analysis of metal forming processes using large deformation elastic-plastic formulations. *Computer Methods in Applied Mechanics and Engineering*, 49, 71-108.

Katsumi Kawada, H.K., 1989. Recent developments of bending in japan. *International Journal of Machine Tools and Manufacture*, 29 (1), 55-62.

Louis, J.G., 2010. *Collapse of thick walled uoe pipes corrosive resistant cladding*. (Master). University of Oslo.

M. Elchalakani, X.L.Z., R. H. Grzebieta, 2002. Plastic mechanism analysis of circular tubes under pure bending. *International Journal of Mechanical Sciences*, 44, 1117-1143.

M. K. Yeh, S.K., 1986. On the collapse of inelastic thick walled tubes under external pressure. *Journal of Energy Resources Technology,* 108, 35-47.

Murphey C.E., Langner C.G., 1985. Ultimate pipe strength under bending, collapse and fatigue, *4th International Conference on Offshore Mechanics and Arctic Engineering,* Dallas, Texas, US, 467-477.

Moen C.D., Igusa T, Schafer B.W., 2008. Prediction of residual stresses and strains in cold-formed steel members. *Thin-Walled Structures,* 46(11), 1274-1289.

M. Thome, J.V., 2011. High-speed calculation tool for design of the JCO pipe forming process. *The 10th International Conference on Technology of Plasticity.* Aachen, Germany, 331-336.

Ming Liu, Y.-Y.W., 2007. Modeling of anisotropy of tmcp and UOE linepipes. *International Journal of Offshore and Polar Engineering,* 17 (4), 288-293.

N. Suzuki, J.K., S. Endo, N. Ishikawa, M. Okatsu, J. Shimamura, 2006. Effects of geometric imperfection on bending capacity of X80 linepipe. *6th International Pipeline Conference,* Calgary, Alberta, Canada.

Palumbo G. & Tricarico L., 2005. Effect of forming and calibration operations on the final shape of large diameter welded tubes. *Journal of Materials Processing Technology,* 164-165, 1089-1098.

Qiang Bai, Y.B., 2014. *Subsea pipeline design, analysis, and installation* MA, US: GPP.

Ren Q., Zou T., Li D., Tang D. & Peng Y., 2015. Numerical study on the X80 UOE pipe forming process. *Journal of Materials Processing Technology,* 215, 264-277.

Rita G. Toscano, J.R., Marcelo Fritz, Ronaldo C. Silva, Joshua Hines, Chris Timms, 2008. Modeling the UOE pipe manufacturing process. *27th International Conference on Offshore Mechanics and Arctic Engineering*, Estoril, Portugal.

Stark P.R., M. D. S., 1995. Hydrostatic Collapse Research in Support of the Oman-India Gas Pipeline. *Offshore Technology Conference*, Houston, US.

SUPERB Project, 1996. Buckling and collapse limit state.

S. Kyriakides, E. Corona, 1991. On the effect of the UOE manufacturing process on the collapse pressure of long tubes. *Offshore Technology Conference.* Houston, Texas, 531-543.

Shinkin V.N. & Kolikov A.P., 2011. Simulation of the shaping of blanks for large-diameter pipe. *Steel in Translation,* 41 (1), 61-66.

Stark P.R., McKeehan D.S., 1995. Hydrostatic collapse research in support of the Oman-India gas pipeline. *Offshore Technology Conference*. Houston, Texas.

Stelios Kyriakides, E.C., 2007. *Mechanics of offshore pipeline* Oxford, U.K.: Elsevier.

Stephen P. Timoshenko, J.M.G., 1989. *Theory of elastic stability* NY, US: McGraw-Hill Book.

T. Reichel, V.P., J. Beissel, Eisenbau Kramer, S. Kyriakides, W.-Y. Jang, 2011. New impander technology for improved collapse resistance of large diameter pipe for deepwater applications. *Offshore Technology Conference*. Houston, Texas.

Thilo Reichel, V.P., Jochem Beissel, Ivan Aretov, Stelios Kyriakides, 2010. On the collapse pressure of impanded large diameter pipe (JCO-C). *9th International Pipeline Conference*, Calgary, Alberta, Canada.

Thilo Reichel, V.P., Jochem Beissel, Stelios Kyriakides, Wen-Yea Jang, 2012. Improved collapse resistance of large diameter pipe for deepwater applications using a new impander technology. *8th International Pipeline Conference*, Calgary, Alberta, Canada.

Wang J., Saraswat R., Mirzaee-Sisan, A., 2013. Influence of residual stresses on pipeline integrity: A state-of-the-art review. *Rio Pipeline Conference and Exposition*, Rio de Janeiro, Brazil.

William J. Walsh, D.P., 2010. Yield strength of line pipe - Analysis of forming operations and flattened straps. *8th International Pipeline Conference*, Calgary, Alberta, Canada.

X Huang, M.M., 2000. Finite element prediction of the ultimate collapse strength of casings. *Proceedings of the Institution of Mechanical Engineers, Part C*, 214, 1515-1527.

You-Min Huang, D.-K.L., 1995. An elasto-plastic finite-element simulation of successive UO-bending processes of sheet metal. *Journal of Materials Processing Technology*, 53, 643-661.

Yu WW., 2000. *Cold-formed steel design*. NY, US:Wiley.

Z. Marciniak, J.L.D., S. J. Hu, 2002. *Mechanics of sheet metal forming* Oxford, U.K.: Butterworth-Heinemann.

Zhang, W., Ding, D. & Gu, M., 2012. A model for predicting the yield strength difference between pipe and plate of low-carbon microalloyed steel. *Metallurgical and Materials Transactions A*.

Zhu, H.X., 2007. Large deformation pure bending of an elastic plastic power-law-hardening wide plate: Analysis and application. *International Journal of Mechanical Sciences,* 49 (4), 500-514.

Zou, T.-X., Xin, J.-Y., Li, D.-Y. & Ren, Q., 2014. Analytical approach of springback of arced thin plates bending. *Procedia Engineering,* 81, 993-998.

Zou, T., Li, D., Wu, G. & Peng, Y., 2016. Yield strength development from high strength steel plate to UOE pipe. *Materials & Design,* 89, 1107-1122.

Zou, T., Wu, G., Li, D., Ren, Q., Xin, J. & Peng, Y., 2015. A numerical method for predicting o-forming gap in UOE pipe manufacturing. *International Journal of Mechanical Sciences*, 98, 39-58.

초 록

파이프라인은 유정, 플랫폼, 저장소 등 사이의 긴 거리를 잇는 연속적인 강관 시스템으로서 자원을 이송하는 효율적인 방식 중 하나이다. 파이프라인은 주로 분절적인 강관으로 구성되는데, 그 중 16인치 이상의 직경을 가지는 강관의 제조에는 여러 조관 방식 중 *UOE* 조관과 *JCO* 조관이 특히 효율적인 것으로 알려져 있다. 이들 조관 공정은 단계적인 소성 가공을 통해 후판을 둥그런 형태로 변형시킨 후 용접을 통해 강관을 제작한다. 이들은 특히 비교적 두꺼운 두께가 요구되는 해저 파이프라인의 생산에 있어서 기존의 보편적인 SEAMLESS 강관에 비해 생산 가능한 직경의 폭이 넓고 가격이 저렴하기 때문에 지난 수십 년에 걸쳐 사용이 증가되어왔다.

하지만 *UOE, JCO* 조관은 복잡한 이력을 동반하는 소성 가공 공정으로서 다음과 같은 문제점을 내포한다. 첫 번째로 조관 후 강관의 항복강도, 항복비 등 재료 물성이 초기 소재의 물성과 차이를 보인다. 이는 공정 전반에 걸쳐서 소성 변형과 탄성 회복이 반복되면서 가공 경화, Bauschinger 효과 등이 재료 물성에 변화를 가져오기 때문이다. 강관의 재료 물성은 강관의 구조적 성능에 민감한 영향을 미치는 변수일 뿐만 아니라 강관 품질 평가의 대표적 항목이다. 그렇기 때문에 물성 예측이 정확하게 되지 않는다면 조관 후 강도 및 구조 성능이 예상보다 낮게 발현되어 원인 규명, 설계, 생산의 반복으로 인한 비용 및 시간적 소모가 크게 발생하게 된다. 두 번째로 소성 가공으로 인해 복잡하게 발생하는 기하학적 결함과 잔류응력 또한 강관의 구조적 성능에 영향을 크게 미치는 변수이다. 이들은 좌굴 강도 및 휨 강도 등의 성능 예측을 어렵게 하여 설계의 불확실성을 높인다. 위와 같은 현상들은 소재의 기하학적 형상, 물성, 조관 계수들에 의해 복합적인 영향을 받음과 동시에 높은 재료적, 기하학적 비선형성을 동반하므로 기존에는 설계 단계에서 정확하게 예측하기 어려운 한계가 있었다. 이는 곧 과도한 보수성을 띠는 재료

생산 및 단면 설계로 이어져 시간과 비용의 증가를 초래한다. 또한 강관 설계 시 구조 성능을 비롯한 품질에 대해 만족할만한 수준을 일관되게 보장할 수 없게 된다. 이와 같은 비효율성 때문에 강관의 물성과 구조 성능을 정밀하게 예측할 수 있는 방법에 대해 지속적인 요구가 있어왔다.

이 연구에서는 유한요소해석을 이용한 조관 시뮬레이션을 통해 *UOE, JCO* 조관 공정을 모사함으로써 강관의 물성과 기하학적 결함, 잔류 응력 등을 정밀하게 예측하고, 그 결과를 이용하여 강관의 구조 성능을 평가할 수 있는 프로그램을 개발하였다. 또한 개발된 프로그램을 이용하여 강관의 생산 가능성과 물성 품질을 보장하면서도 주요 구조 성능인 붕괴압력을 극대화시킬 수 있는 최적 설계 절차를 제안하였다.

먼저 수치 해석의 정확도를 높이기 위해서 기존의 Chaboche 모델을 개선한 복합 소성 재료 모델을 도입하여 유한요소해석에 적용했다. 개선된 모델은 조관 중 나타나는 재료의 주요 소성 거동 특징인 가공경화, Bauschinger 효과뿐 아니라 항복참(Yield plateau), 탄성계수변화까지 모사할 수 있다. 소재에 대한 인장-압축 반복 시험으로 변형률-응력 응답을 얻고 유전자 알고리즘과 RMS 기법을 혼용하여 15가지 재료 계수를 도출했다.

유한요소해석을 이용한 조관 시뮬레이션에서는 UOE, UOC, JCOE, JCOC 조관공정을 각각 모사하고 각 공정에 대해 판재의 형상 변화, 재료 물성 변화, 기하학적 결함, 잔류응력 등을 도출한다. 이 결과로부터 직접적으로 재료 물성 품질을 예측할 수 있을 뿐만 아니라, 판재의 형상 변화 및 조관 툴에 가해지는 반력 등을 모니터링하면서 강관의 생산가능 여부를 판단할 수 있다. 개발된 모델을 검증하기 위해 UOE강관을 제작한 후 시편을 절단하여 인장시험을 수행하였다. 각 조관 단계별 강판의 기하학적 형상 및 인장항복응력에 대한 비교 검증을 한 결과 조관 시뮬레이션의 정확성을 입증할 수 있었다. 이어서 조관 시뮬레이션에서 도출된 강관의 재료 물성, 기하학적 결함, 잔류 응력에 근거하여 3차원 정밀 유한요소해석을 수행함으로써 강관의 붕괴압력과 휨강도를 산정할 수 있

다.

개발된 프로그램을 이용해 주요 설계변수인 직경, 두께, 확관율 및 축관율이 강관의 재료 물성, 붕괴 압력, 휨강도에 미치는 영향을 규명하기 위한 매개변수 해석을 수행하였다. 대부분의 강관에 대해, 확관율이 높을수록 강관 품질의 주요 지표로 사용되는 원주방향 인장항복응력이 높아졌지만 구조 성능인 붕괴압력은 크게 낮아졌다. 반면 축관율은 원주방향 인장항복응력을 낮추는 대신 붕괴압력을 증가시키는 효과를 보였다. 휨강도는 확관율 및 축관율의 변화에 큰 영향을 받지 않았다. 이와 같이 주요 변수들이 재료 물성 품질과 구조 성능에 미치는 trade-off 관계 영향을 고려하여 강관의 최적 설계 절차를 제시하였다. 제안된 설계 방식은 강관의 생산 가능성과 품질을 확보하는 동시에 붕괴압력을 극대화하는 강관 생산을 가능하게 함으로써 기존의 방식에 비해 설계의 일관성을 확보하고 효율성을 증진시킬 수 있다.

주요어 : 해저용강관, 재료물성, 붕괴압력, 수치해석, 최적설계절차

학 번 : 2012-30247